The role of KRT5+ progenitors in chronic otitis media

Deepak P. Chandrasekharan

Lungs for Living Research Centre, UCL Respiratory

Genetics and Pathobiology of Deafness, MRC Harwell

University College London

A thesis presented for the degree of Doctor of Philosophy

October 2020

Declaration

I, Deepak Chandrasekharan, confirm that the work presented in this thesis is my own. Where information has been derived from other sources, I confirm that this has been indicated in the thesis.

Deepak P Chandrasekharan

Abstract

Background: Chronic inflammation of the middle ear, known as chronic otitis media, is a debilitating condition of unknown aetiology that causes hearing loss in children and adults. Recent work suggests the epithelial lining of the middle ear cavity may play a role in the disease process. The hypothesis is that abnormal proliferation and differentiation of keratin-5(KRT5)-positive progenitor cells results in a maladaptive epithelial remodelling. The work here characterises KRT5+ progenitor cells and explores their contribution to middle ear epithelial homeostasis in health and chronic otitis media with effusion (COME).

Methods: Murine middle ear epithelial cells from the *Fbxo11*$^{Jf/+}$ model of COME and healthy controls were isolated by enzymatic dissociation and used for colony forming assays, immunocytochemistry and flow cytometry. Cells were grown at air-liquid interface to analyse differentiation potential and a 3D-spheroid assay was used to analyse single cell differentiation. KRT5-Cre-ER^{T2};R26R-Confetti multicolour reporter mice were generated to perform lineage tracing to visualise middle ear epithelial homeostasis in vivo.

Results: Middle ear epithelium has cells with progenitor cell capacity that are KRT5+. These make up approximately 7% of the epithelial compartment and may have a dorso-ventral asymmetry of distribution that reverses in *Fbxo11*$^{Jf/+}$ mice. Differentiation assays show middle ear progenitors from *Fbxo11*$^{Jf/+}$ mice have aberrant differentiation potential with reduced bipotent differentiation ability. 3D whole-mount visualisation of the middle ear from multicolour reporter mice shows the presence of distinct KRT5+ progenitor derived clones in multiple regions of the middle ear.

Conclusion: This work provides further support that KRT5+ cells are progenitor cells of the middle ear epithelium with bipotent differentiation capacity and thus may maintain the epithelium in health. These progenitor characteristics seem to be perturbed in the *Fbxo11*$^{Jf/+}$ mouse model of COME. Understanding the mechanism underlying these changes offers the potential to identify new therapeutic targets.

Impact Statement

There is increasing interest in the cell biology of the middle ear to understand how the middle ear epithelium is maintained in health by progenitor cells and how problems with this process may contribute to chronic inflammatory disease.

This work describes a platform of assays which are adapted from established techniques from the fields of skin and airway epithelial biology. This has allowed characterisation of the KRT5+ progenitor cell compartment of the middle ear and study of how their function and capabilities are affected in mouse models of chronic disease.

Colony forming ability, flow cytometric analysis, and 3D spheroid assays of murine middle ear epithelium have not been described before. Likewise, the ability to perform multicolour lineage tracing using reporter mouse lines with 3D whole mount visualisation affords a high level of analysis of middle ear epithelium clonal dynamics.

These in vitro and in vivo assays allow effective phenotyping of middle ear epithelial proliferation and differentiation. It is hoped that these can be used by other researchers to help better understand middle ear epithelial homeostasis and to identify novel therapeutic targets for chronic middle ear disease.

Acknowledgements

One of the most enjoyable aspects of scientific research is the inherent collaborative nature and the work in this thesis is no exception. I owe thanks and acknowledgement to a great number of people without whom this work would not have been possible. In particular, I would like to thank my supervisors Sam Janes at UCL, Steve Brown at MRC Harwell and Kate Gowers at UCL for their guidance and support of this work. Their enthusiasm for science and dedication to research training, together with their kindness and generosity of spirit has been constant and unwavering throughout this process. Sandra Gómez López, Rob Hynds, Hilda Tateossian, Mood Bhutta, Colin Butler, Derek Hood and Mike Bowl have been instrumental in their input and I am indebted for their time and efforts in training me, discussing science, and providing guidance and trenchant criticism to help with my development as a scientist. The expertise and training from Lucie Vizor, Michelle Stewart and Anju Paudyal in the design of animal experiments was invaluable. Many thanks also to the rest of the Ward 4 team for their help with animal care. Jeremy Sanderson is a wonderful microscopist and teacher and I am very grateful for his efforts in helping obtain imaging data of the mouse middle ear. Many thanks also to Marianne Yon for training in mouse dissections. I have been lucky to work in a wonderful and professionally and personally supportive environment made possible by all the members of Lungs for Living, the wider UCL Respiratory team, and the Deafness group and all the team at MRC Harwell. Particular thanks to Krish Kolluri for being a source of calmness, scientific wisdom and good humour at all times. I am also grateful to the core facilities staff for advice and training especially at the UCL Biological Services Unit, Flow Cytometry and UCL and ICH Confocal facilities, the MRC Harwell Mary Lyon Centre, Histology, Pathology, Genotyping, Imaging, and the mouse import and rederivation teams who obtained the lines for experiments at Harwell. Thank you also to the Harwell leadership team who have been exceptional and Nanda Rodrigues and Sara Wells in particular.

Finally, this work was funded and supported by the excellent training offered by the Wellcome Trust PhD Programme at UCL and the Medical Research Council at Harwell.

Statement of contribution of others

This thesis describes original, unpublished research performed primarily by the author, D. Chandrasekharan. However, this thesis could not have been completed without the contributions of others. All in vitro and in vivo assays were initially performed and, where needed, devised and optimised by the author. Animal care and basic husbandry was supported at UCL by BSU staff. Subsequently, the Mary Lyon Centre provided all animal care at MRC Harwell, and basic husbandry was completed by Ward 4 animal technicians who also provided support for tamoxifen induction. Genotyping at MRC Harwell was performed by the genotyping core facility.

Abbreviations

2D	2 dimensional
3D	3 dimensional
3T3-J2	3-day transfer, inoculum 3×105 cells - a cell line of mouse embryonic fibroblasts
ACT	Acetylated tubulin
ALI	Air-liquid interface
AOM	Acute otitis media
BCL6	B-cell lymphoma 6 protein
BrdU	Bromodeoxyuridine / 5-bromo-2'-deoxyuridine
BSA	Bovine serum albumin
Cas-9	CRISPR associated protein 9
CD	Cluster of differentiation
Cdt2	Cell division cycle protein cdt2
CFE	Colony forming efficiency
CFP	Cyan fluorescent protein
CK5	Cytokeratin 5
COM	Chronic otitis media
COME	Chronic otitis media with effusion
Cre	Cause recombination

CRISPR	Clustered regularly interspaced short palindromic repeats
CSOM	Chronic suppurative otitis media
ddH2O	Distilled and deionised water
DNA	Deoxyribonucleic acid
EDTA	Ethylenediaminetetraacetic acid
EdU	5-ethynyl-2´-deoxyuridine
ENU	N-ethyl-N-nitrosourea
EpCAM	Epithelial cell adhesion molecule
ERT2	Estrogen receptor T2
EVI1	Ecotropic virus integration site 1 protein homolog
FACS	Fluorescence activated cell sorting
FBS	Fetal Bovine Serum
FBXO11	F-Box Protein 11
FMO	Fluorescence minus one
G1	First generation progeny
G1 phase	Gap 1 phase
G2	Second generation progeny
G2M phase	Gap 2 phase preceding mitosis
GaAsP	Gallium arsenide phosphide
GFP	Green fluorescent protein

GMP	Good manufacturing practice
GS-IB4	Isolectin B4 from *Griffonia Simplicifolia*
GWAS	Genome wide association studies
HIF	Hypoxia inducible factor
ITGA6	Integrin alpha 6
KRT5	Keratin 5
MGI	Mouse genome informatics
MHC	Major Histocompatibility Complex
MMEC	Mouse middle ear epithelial cells
MMEC-Basic	Mouse middle ear epithelial cell-basic medium
MMEC-plus	Mouse middle ear epithelial cell-plus medium
MMEC-SF	Mouse middle ear epithelial cell-serum free medium
MOM block	Mouse on mouse block
MRC	Medical Research Council
mT/mG	Cell membrane-localized tdTomato/cell membrane-localised green fluorescent protein
MUC5AC	Mucin 5AC, Oligomeric Mucus/Gel-Forming
NGFR	Nerve Growth Factor Receptor
NIH-3T3	National Institute of Health 3-day transfer, inoculum 3×105 cells - a cell line of mouse embryonic fibroblasts

OM	Otitis media
p53	Cellular tumour antigen p53
p63	Tumour protein 63
PBS	Phosphate buffered saline
PBST	Phosphate buffered saline with triton
PCR	Polymerase chain reaction
PFA	Paraformaldehyde
PMT	Photomultiplier tube
Qdot	Quantum dot
R26R-Confetti	Rosa26
rcf	Relative Centrifugal Force
RFP	Red fluorescent protein
RIPA	Radioimmunoprecipitation assay
RNA	Ribonucleic acid
rtTA/tetO-Cre/LoxP	Reverse tetracycline-controlled transactivator/tetracycline-responsive promoter element/locus of X-over P1
S phase	Synthesis phase
SEM	Standard error of mean
SMAD2	Mothers against decapentaplegic homolog 2
SPF	Specific pathogen free
T-tube	Tympanostomy tube

TBX1	T-box transcription factor 1
TGF-ß	Transforming growth factor beta
TGIF1	TGF-ß Induced Factor Homeobox 1
U	Units
UCL	University College London
YFP	Yellow fluorescent protein

Table of contents

Table of Tables

Table of figures

Chapter 1 Introduction

1.1 Background

The ability of tissues and organs to maintain a dynamic stability of structure and function in response to perturbations is termed homeostasis. An understanding of disease pathogenesis is therefore a case of identifying the underlying mechanisms of homeostasis, and how these processes succumb to insults put upon them to result in a disease state. This thesis serves to explore these processes for the mammalian middle ear.

Our modern world has an *embarrassment of riches* of visual stimuli and it is clear that we are reliant on vision for our primary sensory interaction with our surrounding environment. Nevertheless, our auditory system still remains our primary sense for peer-to-peer communication via speech, as well as the dominant modality for 360° environmental monitoring, even without a need for actively attending to stimuli. Alarms to wake us and warn us are still primarily auditory in their nature. A healthy and functioning organ of hearing is of relevance not only for function in everyday life, but also for adequate quality of life too - think of the joy derived from communicating with others or from listening to a favourite song. The importance of the auditory system can be seen throughout our lives from birth to older age. For example, whilst the ability to read requires active teaching to children, the ability to hear, understand and speak is a more naturally acquired skill during critical periods of neurodevelopment primed for hearing and language acquisition. Furthermore, hearing loss has been identified as the single biggest modifiable risk factor for dementia[1]. Maintaining an effective auditory system with functioning hearing during childhood and throughout adulthood is thus an important health consideration.

1.2 Conduction of airborne sound waves requires impedance matching in land mammals

The auditory system begins with the ear which can be divided into the outer ear (pinna and ear canal), middle ear and inner ear (cochlea and semi-circular canals). The middle ear is an air-filled cavity between the tympanic membrane and the inner ear. It houses the three connected bones of hearing (ossicles). The three ossicles are the smallest bones in the human body. The lever mechanism of the ossicles together with the change in surface area from the large tympanic membrane to the small stapes footplate are together responsible for the process of impedance matching.

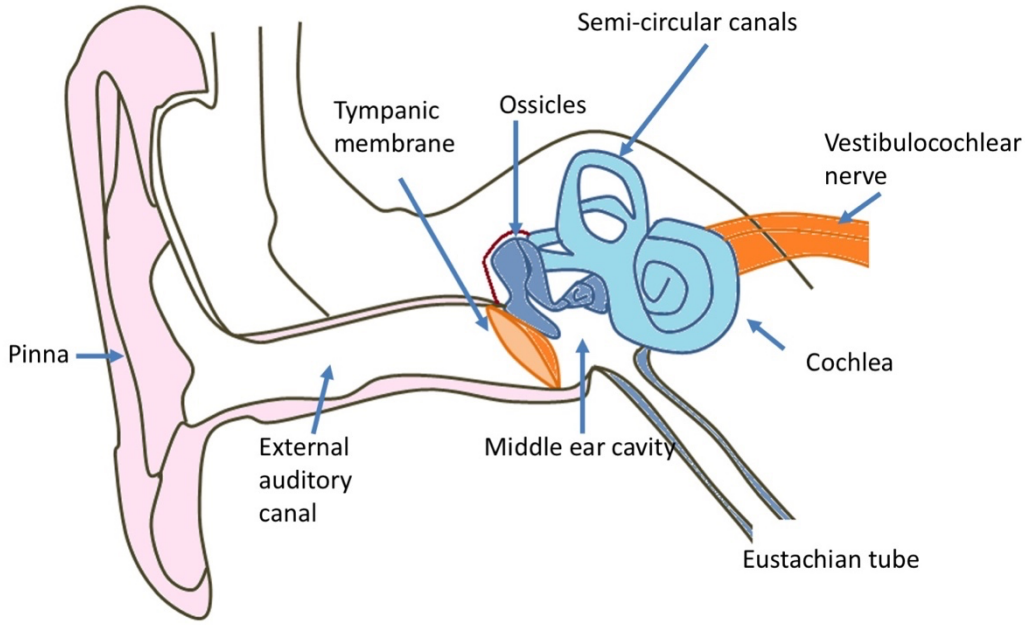

Figure 1 Schematic representation of anatomy of a human right ear.

Sound is a longitudinal wave and is conducted by the molecules of the medium it travels in, be this air or liquid. Conduction in a liquid medium requires more energy as there are more molecules in a given volume and thus there is more impedance and dissipation of sound energy. Impedance matching in the ossicular chain helps overcome this. Much like a drawing pin, the pressure of the incident sound wave on the larger surface area of the tympanic membrane is focussed into the small area of the stapes footplate to enable effective movement of the fluid within the cochlea where sensory transduction can take place. Without this, conduction of sound waves from the medium of air into the fluid filled endolymph of the cochlea would still be possible but reduced. The importance of the ossicular chain to mammalian hearing is reflected in its evolutionary origin. Anthwal and colleagues highlight how possessing three ossicles is one of the defining features of mammals[2]. The stapes bone is similar to the single ossicle architecture of the middle ear found in reptiles and birds. Human hearing is therefore generally more sensitive to specific frequencies than birds[3] and humans can hear over a broader range of frequencies too. However, birds, especially songbirds can process sounds quicker both peripherally and in the auditory cortex hence allowing the complexity of birdsongs. In triple ossicle ears the malleus and incus are evolutionarily derived from the quadrate and articular which are akin to the upper and lower jaw of non-mammalian vertebrates. Evolution of a novel jaw joint articulation i.e. the temporomandibular joint, is therefore thought to have been required for the formation of the three component ossicular chain.

The effective functioning of the mechanics of the ossicular chain requires an air-filled middle ear cavity maintained at a pressure equivalent to that of the external atmosphere. This allows free movement and vibration of the ossicles and the tympanic membrane to which the malleus is attached[4,5]. Much of this pressure equalisation is performed by the Eustachian tube. This is a hollow tube that connects the middle ear to the nasopharynx. The Eustachian tube is normally closed, but opens during swallowing and yawning and enables pressure equalisation by ‘popping our ears’. Working together with the mucosal lining of the middle ear which have a small gas exchange role[6], it is responsible for pressure regulation and effective ventilation of the middle ear

cavity. It also serves as a drainage pathway for middle ear contents[7]. Effective pressure maintenance of the middle ear allows effective conduction of sound waves by permitting free vibrations and movement of the eardrum and ossicles. Conversely, anything that compromises the movement of these structures results in impaired hearing, termed 'conductive hearing loss'. One of the most frequent causes of such conductive hearing problems is a build-up of fluid in the middle ear secondary to tissue inflammation.

1.3 Otitis media is the commonest cause of hearing loss worldwide

Inflammatory disorders of the middle ear encompass a spectrum of interlinked and overlapping pathologies known collectively as otitis media (OM) characterised by the presence of fluid in the middle ear (termed an effusion) with potential for a concomitant conductive hearing loss[8]. Otitis media poses a significant burden of disease in terms of healthcare needs, particularly regarding antimicrobial use and surgical intervention. Without appropriate treatment when required, immediate complications, although uncommon are potentially very serious. These include local spread of middle ear infection causing, for example, mastoid abscess, meningitis and intracranial collections. The most common consequence however is a hearing loss that persists for the duration of fluid in the middle ear.

Acute otitis media (AOM) is one of the most common childhood diseases worldwide with 709 million cases per year[9]. Caused by an acute infective process that can be viral or bacterial in origin, AOM is usually self-resolving but some children will go on to have *recurrent* acute otitis media with cycles of infection and resolution. It is not yet clear what are the underlying factors that predispose a child to recurrent episodes of disease.

In other instances, middle ear inflammation can persist over a longer period and this chronic otitis media (COM) manifests in two main types, differing in the nature of the middle ear fluid effusion, and whether the tympanic membrane is intact or perforated[10-12]. When the fluid in the middle ear is purulent and associated with a perforated tympanic membrane, this is known

as chronic otitis media mucosal type. This is termed active if the ear is discharging with middle ear infection/inflammation and inactive if the middle ear is dry. When the fluid in the middle ear is non-purulent but sero-mucinous this is termed chronic otitis media with effusion (COME). In COME, there is no obvious sign of infection and the tympanic membrane is usually intact, albeit sometimes thinned and scarred. There is middle ear mucosal hyperplasia with an increase in the goblet cell population[13]. COME is most common in high income countries and affects up to 80% of children at some point during childhood and there are 2.2 million new cases per year in the USA alone. This high incidence makes COME one of the most common causes of paediatric hearing loss[14]. Although COME may be spontaneous, it usually follows an episode of AOM with a persistent non-purulent effusion and is most commonly seen in high income countries[15,16]. On the other hand, chronic otitis media – mucosal type, is a burgeoning global health problem and is predominantly seen in low and middle-income countries. It has a global prevalence of up to 350 million and a disease burden of 2 million disability-adjusted life years[17].

Both of the chronic subtypes pose a major clinical problem as they can lead to permanent hearing loss. COME can result in tympanic membrane changes such as atelectasis and tympanosclerosis, even with tympanostomy tube insertion, in 1-73% of patients[18]. As these most commonly affect children, even a temporary hearing loss can cause affected individuals to struggle at school and at home leading to poor educational and behavioural outcomes[19,20]. COM leads to high levels of medical consultation in both low and high-income countries for adults and children. There is significant use of antimicrobial therapy with concomitant risks of antimicrobial resistance[21]. COME is also the most common indication for surgery in children in high-income countries at a cost of over $1billion per year in the USA alone[8] and tympanostomy tube insertion is one of the most common paediatric surgical procedures performed in the UK[22]. Despite this high prevalence of COME and COM and high intervention rate, current treatment strategies are of limited effectiveness, particular in the long term, and consist mainly of repeated attempts at surgical interventions under general anaesthesia[23]. These surgical treatments are variably effective, and it is unclear how, when, or why they

work. In addition, a subset of patients with COM, be it suppurative or effusion based, will see spontaneous resolution and again it is unclear why this occurs[12,24]. Further research is therefore needed to understand the natural history and pathogenesis of chronic otitis media and the mechanism of action of interventions such as tympanostomy tubes.

1.4 Chronic otitis media with effusion is challenging to treat and the pathogenesis is poorly understood

The earliest reported treatment for COME was in 1649 when Jean Riolan the Younger was cleaning the ear of a patient with an ear spoon and accidentally pierced the eardrum and found the patient reported hearing improvement[25]. This is the first recorded case of a tympanotomy being performed. Modern day treatment for COME is derived from this, with the patient undergoing a surgical procedure under general anaesthetic in which a hole (myringotomy or tympanotomy) is made in the tympanic membrane and a temporary ventilation tube known colloquially as a 'grommet' is inserted to keep the opening patent for a period of approximately 9 months. In recurrent or persistent disease, the treatment is the same with repeated ventilation tube placement or insertion of a longer term 'T-tube.' For COM mucosal type, treatment is a surgical procedure known as a tympanoplasty to reconstruct the ear drum and any ossicles damaged by disease and diseased tissue, including middle ear mucosa, is removed. As in COME, in recurrent or persistent cases of COM mucosal type, the main treatment option is repeated surgical intervention[26]. It is currently challenging to predict which patients will improve with treatment and which require multiple interventions suggesting a heterogeneity of disease and treatment response.

There is thus a need to better understand COME and identify better therapeutic strategies. However, our limited understanding of the pathogenesis of COME has prevented significant progress from being made[27]. Epidemiological studies have identified numerous risk factors for the various types of OM including tobacco smoke exposure, pacifier use, nursery attendance, enlarged adenoid tissue, reflux, and younger age[8]. The exact

mechanism of how these factors are causative for otitis media is still an area of active research. In addition, it is unclear which of these factors, if any, result in a chronic inflammatory picture and the underlying mechanisms therein. One approach that has helped provide useful research targets builds on the proven heritability of OM. Genetic epidemiological studies such as with twins suggest a heritability of OM of 0.73 [28,29] and lend weight to the argument that there is a genetic contribution to COME that results in the chronic disease phenotype[28].

1.5 Mouse models provide insights into the genetics and pathogenesis of otitis media

It has been posited since 1938 that heritability plays a significant role in chronic otitis media[30]. Epidemiological twin studies and recent advances in sequencing capability support this theory[28,29,31,32] but studying potential genes from primary human tissue is challenging and limited by difficulties in obtaining middle ear biopsies. The use of mouse models in studying human diseases in general and otitis media in particular is now well established and provides a viable model system to probe the disease[12]. The low cost, short breeding time and analogous biology of mice to humans makes mouse models highly suited to studying human disease. The relatively recent sequencing of the mouse genome[33] and the human genome[34] has also enabled deciphering the genetic basis of human disease at a hitherto unapproachable level. This intricate knowledge of the mouse and human genome can be combined with the ability to breed mice into congenic inbred strains (using brother x sister or parent x offspring matings) to tease out the effects of only the gene of interest whilst minimising other genetic sources of variation. The judicious use of littermate and cage mate controls allows further reduction of other background sources of variation such as environmental factors. Other animal models of otitis media also exist such as the rat and chinchilla[35], but none offer the low cost or versatility of mice.

The ability to mutate the mouse genome has permitted the development of mouse models of human disease. This manipulation of the genome can be

performed using targeted strategies e.g. using CRISPR Cas-9[36], or via phenotype driven mutagenesis[37]. The latter strategy in some ways provides a more unbiased approach as any mutations are generated at random, secondary to mutagen exposure. Offspring post-mutagenesis can be screened for any resulting phenotypes that are then characterised using standardised pipelines[38]. The causative genetic mutation, be this dominant, recessive or modifying can then be identified. One such chemical mutagen is N-ethyl-N-nitrosourea (ENU). ENU is used to cause single base-pair changes in male mouse sperm stem cells in an unbiased manner. It works by alkylation and results in mouse mutants with single gene change driven phenotypes that are independent of position effects[39].

To generate such mice, male mice are exposed to ENU to trigger mutagenesis. They are then crossed with untreated females to generate first generation progeny (G1) with potential dominant mutations that can be screened using a phenotyping pipeline. Potential recessive mutations are identified by crossing second generation (G2) progeny females with first generation (G1) progeny males. Any identified mutants can then have the causative gene identified and cloned.

Such an unbiased dominant genome-wide mutagenesis screen performed at MRC Harwell has thus far identified three mice with a conductive hearing loss secondary to a COM phenotype[40-45]. Known as Jeff, Junbo and Edison, these mice have point mutations in the genes for *Fbxo11, Evi1 and Nischarin* respectively, all of which are linked to the TGF-β signalling pathway[46-56]. By weaning age, these mice spontaneously develop a middle ear effusion that persists throughout adulthood, even when the mice are grown in germ-free conditions where infective causes have been removed. Jeff has a chronic otitis media with effusion whilst Junbo has a suppurative otitis media albeit without a perforation. Histopathological analysis of middle ear sections from these mice shows a hyperplasia in the mucosal lining of diseased mice when compared with control mice and tissue hypoxia in the mucosa that is rescued by myringotomy[57,58]. Other mouse models also exist but are mainly of syndromic causes of otitis media such as Down syndrome, 22q12 deletion and mucopolysaccharidosis (reviewed by[12]).

A phenotyping-based approach however is not without limitations. The major limitations are monetary cost and time-cost as well as the necessity to identify phenotypes effectively and reliably. In terms of phenotyping OM, the use of middle ear histological sections and auditory brain stem response testing means that the tests are robust and comparable to those used in human assessment of hearing. Of note, tympanometry is not performed as part of the standard phenotyping. Another potential limitation specific to ENU mutagenesis is that up to 30% of mice born are embryonic lethal meaning ENU may predispose to particularly severe mutations. However, the relatively mild non-syndromic COME phenotype of the *Fbxo11* mutant Jeff makes it an appealing mouse model as there are no significant craniofacial or ciliary problems as seen in other mouse models of otitis media. In addition, of the genes identified from the mouse mutagenesis screen, *Fbxo11* has been validated in human genome wide association studies (GWAS) of otitis media[50,59,60] and is therefore a useful first model to characterise and explore further.

1.6 *Fbxo11* mutant mice are a validated single gene model of chronic otitis media with effusion

The Jeff mouse was initially identified from a UK national ENU mutagenesis screen performed at MRC Harwell[41]. Mice with a heterozygous mutation were found to have raised hearing thresholds, middle ear effusion and mucosal proliferation[47]. The mutation was mapped using backcrosses to mouse chromosome 17. Bilateral otitis media with effusion occurred in all mice by 21 days after birth and persisted throughout adulthood, even when mice were grown in specific pathogen free conditions meaning no infection source is present. This was further corroborated by the low levels of MHC Class II expression on immune cells in mice with otitis media suggesting the absence of any antigen trigger. Whilst Jeff mice are up to 21% smaller than wild-type littermates they have only very mild craniofacial abnormalities. This includes a narrower Eustachian tube in keeping with the 21% smaller size, but the extent of narrowing is variable[47]. The limited syndromic phenotype of the Jeff mouse

is helpful in studying middle ear biology when compared with other mouse models which are more suited to syndromic causes of otitis media such as models of Downs or Di George syndrome[50,61,62].

The middle ear cavity of Jeff mice is fluid filled with a chronic proliferative otitis media. The mucosa is hyperplastic with polyp formation and a mix of cuboidal epithelium, flat epithelium and ciliated cells without the normal regional demarcation between cell types. There is also stromal/fibroblast infiltration, angiogenesis with immune cell infiltration and bone osteosclerosis[47].

The mutation in Jeff is an A-T transversion at base 1472 leading to a non-conservative glutamine to leucine change (Q491L) in a highly conserved region in exon 13 of the *fbxo11* gene[48]. This encodes an F-box protein involved in protein degradation. *Fbxo11* is expressed in the mouse middle ear from embryonic day 18.5 (E18.5) until 13 days after birth (P13) after which it has declined by P21. Homozygotes for the Jeff mutation are embryonic lethal with cleft lip and palate and eyes open at birth. Heterozygotes are viable and apart from chronic otitis media have no other obvious health problems.

Fbxo11 is a gene located on mouse chromosome 17 and human chromosome 2. The FBXO11 protein is a component of a ubiquitin protein ligase complex. FBXO11 has multiple actions as part of this complex. It neddylates p53 to suppress its function[63]; works in the ubiquitination and degradation of Cdt2 (a cell cycle regulator)[64], DTL (which regulates TGF-ß signalling)[65] and BCL6[66]. It also is involved in the hypoxia pathway and regulates HIF-1α via demethylation via arginine methyltransferase activity[67]. The effects on TGF-ß signalling is evidenced by increased nuclear localisation of phospho-Smad2[53,54] and hypoxia is also seen in the middle ear of Jeff mice with otitis media. The role of TGF-ß is also supported by the *Tgif1-/-* (TGF-ß induced factor homeobox 1)mutant mouse also having otitis media [53,54] and levels of TGF-ß being associated with middle ear effusion in children[68,69]. These pathways all present druggable targets and have also been identified to some degree in the pathogenesis of otitis media in the Jeff mutant model. Studying these pathways further is thus appealing, despite the complexities and challenges this poses.

Mutations in *Fbxo11* have also been shown to be associated with chronic otitis media in three independent cohorts in Australia, USA and UK[51,52,70]. However, of note the polymorphisms in these associations are different between each cohort. Whilst this does not allow clear identification of a unifying mechanism by which the protein is affected and downstream pathways are disrupted, the multiple polymorphisms that have been associated with COM suggests that *fbxo11* may play a significant permissive or causative role in COM pathogenesis. One explanation for how any of a variety of polymorphisms could result in the common end pathology of chronic otitis media is that *fbxo11* is expressed primarily during development in the middle ear. Recent work has shown that Jeff mice seem to have a cavitation defect in the middle ear. That is, when the middle ear cavity usually forms from a solid structure by becoming hollow – known as cavitation – there is persisting mesenchyme in the middle ear [71] intermixed with normal regions of epithelium, whereas normally the mesenchyme would have disappeared after development and become fully epithelial in adulthood[72]. Over time this remnant mesenchyme becomes fibrous and adherent to the tympanic membrane. The authors suggest that this cavitation defect may be an initiating factor in otitis media in the Jeff mouse. However, such persisting mesenchyme is not seen in other mouse models of otitis media such as the Junbo mouse. As such, cavitation defects may indeed be causative as an initiating event for chronic otitis media in Jeff mice, but this does not explain how this causes the ubiquitous epithelial remodelling with changes in ciliation and goblet cell architecture and resultant middle ear effusion formation that is seen in all forms of chronic otitis media. This question of how remodelling occurs is not simply of intellectual interest alone. Cavitation defects during development cannot be targeted for therapeutic gain, however downstream signalling mechanisms, potentially triggered by the presence of this persisting mesenchyme, do offer this potential. Therefore, investigating how the common end state pathology of epithelial remodelling occurs, regardless of the initiating factor, is warranted.

1.7 Mucosal and epithelial remodelling is seen in human and mouse models of chronic otitis media

Anatomically, the mucosal lining of the middle ear is continuous with the upper respiratory tract, consisting of distinct regions of flat squamous cells, ciliated cells, goblet cells and basal cells[73-75]. The mucosa serves a homeostatic function. It performs gas exchange with the mastoid air cells, and functions as a mucociliary escalator to maintain a fluid-free and ventilated middle ear to allow effective sound conduction.

When mucosal surfaces are affected by infection or injury, self-limiting acute inflammation activates regenerative processes via the innate immune system to enable a return to normal structure[76]. This is part of the normal and necessary response to maintain tissue homeostasis[77]. However, inappropriate or persistent inflammation can also trigger aberrant tissue repair processes causing abnormal remodelling leading to serious pathologies such as fibrosis and malignancy[78-80]. In the middle ear, inflammation results in the production of an effusion by the mucosa and changes to the mucosal lining. Histological analysis of human biopsies shows mucosal remodelling in COM in particular with an increase in the thickness of the lining, a change in some regions from simple squamous to pseudostratified and an increase in the number of basal cells[81]. There is also a reduction in cilia and increase in secretory cells[82]. Such remodelling in the ear results in changes in mucosal function resulting in fluid build-up, poor aeration and hearing loss[83-85]. Characterising how cellular level tissue homeostasis is maintained and how it is perturbed in remodelling is the first necessary step in identifying therapeutic targets.

1.8 Adult tissue resident stem/progenitor cells play a role in tissue remodelling

It is now accepted that resident adult stem cells (i.e. non-embryonic) are responsible for the steady-state maintenance and repair of tissues. Adult stem cells are defined by pluripotency and limitless divisional capability[86]. Their presence has been confirmed in numerous organs including skin, respiratory

system, retina, gut and nervous system. Quantitative lineage tracing experiments has shown the dynamics of how stem cells function in homeostasis. At resting state, turnover of cells in organs is low with division only to maintain the organ and preserve stem cell population. When tissue injury occurs, adult stem cells increase their proliferation and their progeny commence differentiation for repair[87-92]. However, in chronic inflammatory conditions, abnormal proliferation and differentiation of stem cells is proposed to be responsible for pathological remodelling that occurs[93]. An understanding of the pathogenesis of COM may thus be helped by better understanding the stem cell biology of the middle ear.

Therefore, a systematic literature review was performed to explore the existing evidence for the potential role of middle ear stem/progenitor cells in chronic otitis media and inform this thesis. A search of PubMED and EMBASE was performed based on the following search strategy:

(((((progenitor cell) OR stem cell) OR keratin 5) OR cytokeratin 5)) AND (((chronic otitis media) OR otitis media*) OR middle ear)

382 non-duplicate results were returned and the titles and abstracts screened for relevant studies. Studies were included regardless of whether performed in human or model organisms. Studies about middle ear disease alone without reference to stem/progenitor cells were excluded. The reference lists of relevant studies and citing literature were hand searched for further relevant studies. Below is a brief summary of the findings.

In the upper airway of both humans and mice, there exists a population of cells close to the basal lamina hence known as basal cells. Classically described in the skin, basal cells are identified by expression of the transcription factor Trp-63 (p63) and cytokeratin-5 (Krt5) and are thought to be a multipotent stem cell responsible for maintaining and repairing all epithelial surfaces in health and disease[93-96]. This has been supported by lineage tracing experiments in which putative stem/progenitor cells are marked with a fluorescent protein linked to the KRT5 promoter, such that all daughter cells will also express the same fluorescent protein. This allows tracking of proliferation and differentiation over

time and mathematical modelling of these processes[97].

Early evidence of the presence of similar basal cells in the middle ear has been shown from human histological sections of normal and COME[13]. These sections showed a comparable architecture to that of the epithelium of the airway and similar changes in inflammatory conditions with basal cell hyper-proliferation[80,81]. However, the exact characteristics, phenotype and role of these basal cells in the middle ear is still debated.

The murine middle ear epithelium has similarities to the respiratory epithelium of the airway with a pseudostratified epithelial architecture consisting of basal cells (thought to be epithelial progenitors), ciliated cells and secretory cells. However, this type of epithelium is generally seen only in the ventral aspect of the murine middle ear and around the Eustachian tube. It is thought to provide mucociliary clearance via the Eustachian tube orifice. Studying middle ear development using lineage tracing has shown the middle ear has a dual embryological origin. The lower/ventral region consisting of pseudostratified ciliated and secretory epithelium is of endodermal origin[72]. The dorsal attic epithelium is more simple in architecture with few, if any, ciliated and secretory cells and is of neural crest origin – these cells undergo a mesenchymal to epithelial transition during development and become epithelial in nature[72].

Luo and colleagues performed lineage tracing in adult mice using a transgenic K5-Cre^{ERT};mT/mG reporter mouse to explore how ciliated cells are generated. In this reporter, KRT5+ cell can be seen red under confocal microscopy as they expressing the tdTomato fluorophore. Exposure to tamoxifen induces expression of green fluorescent protein instead. Red KRT5+ cells were found in both dorsal and ventral regions and green KRT5+ derived progeny developed into both ciliated and non-ciliated cells in both regions[98]. Further work by the Tucker group shows that some KRT5+ cells also stain with 5-bromo-2'-deoxyuridine (BrdU) and retain this label over a long period of time without dilution as would be expected if they were dividing. This suggests some KRT5+ cells are of low turnover and potentially thus a good candidate progenitor cell[99]. Interestingly, unlike the Luo data, this study does not show ubiquitous KRT5+ expression in both dorsal and ventral regions but reports

KRT5+ cells predominantly in the ventral endoderm-derived pseudostratified epithelium with minimal expression in the neural crest derived epithelium.

Studies on the development and mechanism of middle ear bulla cavitation have identified cavitation defects in Jeff mice and has also identified the presence of KRT5+ cells in the epithelium[71]. These are found particularly in the epithelium in regions adjacent to embryonic mesenchyme in both wild type and Jeff mice. The authors suggest that this mesenchyme-associated epithelium with KRT5+ cells may eventually develop and give rise to the final epithelium that is seen around the cochlear promontory in adult mice. KRT5+ cells have also been found to be present in the tympanic membrane and are thought to be progenitor cells that contribute to healing in perforations[100].

There is now also the ability to isolate and culture murine middle ear epithelial cells at air-liquid interface[101] to model the middle ear epithelium. In this technique, cells are grown in a semi-permeable membrane and medium supplied underneath and the cells exposed to air from above to model a respiratory epithelial surface. Submerged culture in tissue culture plastic of airway and skin cells is also possible to culture undifferentiated basal stem/progenitor cell colonies. However, heterogeneity is seen between tightly packed pure progenitor colonies and some with senescent and partially differentiated cells[102]; whether such cellular heterogeneity exists in the middle ear epithelium is unknown.

Various strategies can also be used to enhance progenitor cell expansion in culture and minimise differentiation. This is helpful both in enhancing progenitor cell survival in vitro but also as a method of ex-vivo expansion of progenitor cells for subsequent transplantation or therapy. Such strategies include co-culture with a lethally irradiated mouse embryonic fibroblast layer (NIH/3T3 or 3T3-J2 fibroblasts, also known as feeders) and TGF-ß inhibition[103]. Whilst feeder co-culture based methods have been used successfully for therapeutic transplantation in human disease, the ability to culture cells in feeder-free conditions is attractive. Although challenging, this is potentially more scalable into human therapeutics without the need for good manufacturing practice (GMP) quality feeder cells[104].

Taken together, there is increasing interest in the hypothesis that KRT5+ cells are a progenitor cell of the mouse middle ear mucosa, and as such abnormal functioning of these cells may be responsible for at least some of the mucosal remodelling seen in chronic inflammation. There is still debate about KRT5+ cell characteristics in the middle ear such as number, regional distribution, proliferative capacity and differentiation ability. Delineating these processes and exploring how inflammation affects these in vitro, and using mouse models of otitis media to study this in vivo, may help our understanding of how chronic otitis media occurs and thus identify new treatment targets. In addition, if it is found that there is an intrinsic abnormality of stem/progenitor cells in chronic otitis media, understanding the nature of these potential progenitor cells is an important first step in regenerative medical therapies where ex-vivo expansion and subsequent transplantation is performed[104-106].

1.9 Hypothesis

The hypothesis of this thesis is that abnormal proliferation and differentiation of KRT5+ progenitors underlies the pathogenesis of chronic otitis media. The first step in testing this hypothesis is establishing how KRT5+ cells maintain the middle ear epithelium in health, before exploring how these processes are perturbed in chronic otitis media with effusion. It is hoped that the understanding generated will help identify new therapeutic strategies to target potential aberrant regenerative processes and help preserve a healthy middle ear epithelial lining.

1.10 Research Questions and Aims

1. How do KRT5+ derived cells contribute to maintenance in the healthy mouse middle ear?

Aim 1. Isolate and expand KRT5+ cells in vitro and establish assays of proliferation and differentiation.

2. Does the function of KRT5+ cells change in *Fbxo11*$^{Jf/+}$ mutant (Jeff) mice with chronic otitis media?

Aim 2: Use the *Fbxo11*$^{Jf/+}$ mutant mouse model of otitis media to assay proliferation and differentiation of KRT5+ cells.

3. How can the contribution of KRT5+ derived cells to epithelial homeostasis in vivo be visualised?

Aim 3: Establish in vivo lineage tracing model of KRT5+ derived cells using an inducible multicolour reporter line.

Chapter 2 Materials and methods

2.1 Chemicals, solvents and plasticware

All chemicals were of analytical grade or above and were purchased from Sigma Aldrich, unless otherwise stated. Distilled and deionised water (ddH2O) from a Millipore Q Plus water purification system was used to prepare all buffers. Laboratory plasticware was purchased from BD Biosciences.

2.2 Animal husbandry

Mice were housed in specific pathogen free (SPF) conditions in individually ventilated cages (Techniplast UK Ltd) containing grade 6 sawdust bedding (Datesand Ltd, UK), under a controlled 12 hour light/dark cycle at 21°C (±2) and 55% (±10) relative humidity. Mice were supplied with irradiated mouse diet (Special Diets Services, UK) and water (25 μL/L of chlorine) *ad libitum*. All animal procedures were conducted in accordance with the appropriate UK Home Office Project and Personal licences and procedural and ethical guidelines as well as under the guidelines issued by the Medical Research Council in "Responsibility in the use of animals in bioscience research: Expectations of the major research council and charitable funding bodies" (updated April 2019).

2.2.1 Mouse strains and crosses

Genetically modified mouse strains used were as shown in Table 1.

For initial lineage tracing optimisation work at UCL, the KRT5-Cre^{ERT2} transgene mice on a B6 background were a kind gift from Emma Rawlins (Cambridge). A heterozygous breeding pair of R26R-Confetti multicolour reporter mice were purchased from Jax (Stock number 013731)[107,108]. For initial optimisation work (working with Dr. Gomez Lopez at UCL), both strains were backcrossed onto an FVB/N background for 5 generations for subsequent experiments. R26R-Confetti mice were crossed with KRT5-Cre-ER^{T2} (transgene) to generate matched litters of KRT5-Cre^{ERT2};R26R-Confetti double transgenic mice on a congenic FVB/N background for lineage tracing experiments.

For work at the Mary Lyon Centre at MRC Harwell, *Fbxo11*$^{Jf/+}$ mice were being maintained on a mixed C57BL/6J x C3H background.

The KRT5-Cre^{ERT2} transgene mice on a B6 background were a kind gift from Emma Rawlins (Cambridge) and rederived and maintained on C57BL6/J background. The KRT5-Cre^{ERT2} knock-in mouse was purchased from Jax (Stock Number 029155)[109], rederived and maintained on a C57BL6/N background. The R26R-Confetti multicolour reporter mouse was purchased from Jax (Stock number 013731)[107,108], rederived and maintained on a C57BL6/J background. Breeding pairs or trios of KRT5-Cre^{ERT2} knock-in mice were set up with R26R-Confetti reporter mice to generate KRT5-Cre^{ERT2}; R26R-Confetti double transgenics to permit tamoxifen inducible lineage tracing.

MGI code	Strain	Description	Rederivation Background	Maintenance Background
4358332	Tg(KRT5-creERT2)1Blh	KRT5 transgene insertion	C57BL/6 x C3H	C57BL/6J
5767095	B6N.129S6(Cg)-Krt5<tm1.1(cre/ERT2)>Blh/J	KRT5 knock-in	C57BL/6N	C57BL/6N
4835542	STOCK Gt(ROSA)26Sor<tm1(CAG-Brainbow2.1)Cle>/J	Brainbow/Confetti reporter	C57BL/6J 129P2Ola	C57BL/6J
1862017	Fbxo11^{Jf}	Jeff heterozygous mutant model of COME	N/A	C57BL/6J x C3H

Table 1. Transgenic mouse strains.

Wild type mice strains used for cell culture were C57BL6/J sourced from Biological Services at UCL.

2.3 Middle ear epithelial cell isolation

The dissection was based on a protocol used by Mulay and colleagues[110]. 8 to 12-week-old mice were euthanised using a terminal dose of pentobarbital injected intraperitoneally. Mice were decapitated, the heads were skinned and the lower jaw, skull cap and brain removed. Samples were transported in mouse middle ear epithelial cells basic (MMEC-basic) medium (DMEM/F12 (Life Technology, 31330-038) with 100µg/ml Penicillin and 100µg/ml Streptomycin) and kept on ice. Under a dissection microscope, the mastoid bullae were surgically removed and cleared of surrounding tissue. The external auditory canal and tympanic membrane were cut away to remove potentially contaminating cells[110].

Middle ear epithelial cells were isolated based on a protocol for isolation of tracheal cells[111,112]. Briefly, the bullae were placed in 16 units dispase (Corning 354235) in 1ml MMEC-basic at room temperature for 30 minutes. The bullae were then transferred to DNase I (Sigma Aldrich DN25) for 20 minutes to prevent clumping of cells. Finally, the bullae were placed in TrypLE (Gibco 12604013) for 30minutes at 37°C and kept on a shaker at 300rpm. The three reactions were each quenched by dilution with MMEC-basic+10% Fetal Bovine Serum (FBS). The three suspensions were pooled and filtered through a 70µm cell strainer to remove any large debris. The effluent was centrifuged at 500 x g for 10minutes at 10°C before being resuspended in 1ml MMEC-plus ((mMEC basic with 5% FBS, 10 µg/ml of insulin (Sigma-Aldrich I1882), 25 ng/ml of mouse epidermal growth factor (BD Biosciences 354001), 5 µg/ml of transferrin (Sigma-Aldrich T1147), 30 µg/ml bovine pituitary extract (Life Technology 13028-014), 0.1 µg/ml of cholera toxin (Sigma-Aldrich C8052), 10µM Rho Kinase inhibitor Y-27632 dihydrochloride (Tocris Biosciences 1254) and 0.01 µM of freshly added retinoic acid (Sigma-Aldrich R2625)) and viable cell number counted using trypan blue staining and a haemocytometer.

The middle ear mucosa comprises epithelial and stroma (mainly fibroblasts) as seen on histological sections. To study the epithelial cells alone, it is necessary to isolate them from the stromal component. It has been shown that fibroblast cells adhere more rapidly than epithelial cells onto tissue culture

plastic over a time period of 3 to 4 hours. As such, one strategy is using this differential adherence to enrich for epithelial cells (which should remain unattached in the supernatant) whilst leaving the fibroblast component adherent to the plastic[101,110]. A single cell suspension of middle ear cells was obtained, resuspended in 8ml of 10% FBS and seeded in entirety onto a 10cm Primaria tissue culture dish. After incubation at 37°C in 5% CO2 for 3-4 hours, the supernatant was then gently aspirated, the plate washed once in 10%FBS and the combined supernatants from each plate centrifuged at 300 x g and 21°C for 5 minutes. The resulting cell pellet was resuspended in 1ml of MMEC-plus with freshly added 0.01μM retinoic acid and cell number and viability assessed again. The adherent cells on the dish were cultured in 10% FBS with media changes thrice a week to check for effective fibroblast isolation. After 3 days, colonies of fibroblast like cells were seen growing in the tissue culture. These increase in size and number over 2 weeks. Within any 10cm dish, there was occasional contamination with colonies of epithelial morphology cells. After 2 weeks of culture, cells were lysed using RIPA buffer and the protein fraction extracted and frozen.

2.4 Colony forming assay[113]

Viable middle ear cells were seeded at clonal density in each well of a 6-well dish in rat-tail collagen type I (Corning 354326) coated, and non-collagen coated 6-well plates. Cells were fed three times a week with 1.5ml of MMEC-plus with freshly added 0.01μM retinoic acid. After 14 days cells were fixed in freshly prepared 4% PFA for 15 minutes at room temperature. Cells were then covered in 1% Crystal Violet solution (Sigma-Aldrich V5265) for 30 minutes at room temperature before being washed in cold tap water until the solution ran clear. Plates were air dried overnight then sealed ready for scanning using an ImageQuant LAS 4000 system (GE Healthcare) and counting of colonies using Fiji software[114-116]. Colonies of more than 10 cells were counted and any

fibroblast contaminating colonies were discounted. Colony forming efficiency (CFE) was calculated as

CFE = Number of colonies/Number of cells seeded * 100

2.5 Immunocytochemistry

Cells were seeded at 50,000 cells per well in rat-tail collagen I coated 6-well plates with 22mm x 22mm coverslips in place. Cells were fed three times a week with 1.5ml of MMEC-plus with freshly added 0.01μM retinoic acid. After 21 days cells were fixed in freshly prepared 4% PFA for 10 minutes then ice-cold methanol for 5 minutes. Coverslips were drawn around with a wax pen. Non-specific binding was blocked with 5% serum/3%BSA/0.25%Triton X-100/PBS (serum from same species as secondary antibody) for 2 hours at room temperature. The blocking solution was removed and cells were incubated with the primary antibody diluted in blocking solution for 16 hours at 4°C in the dark. Cells were washed thrice with 0.1% PBST before incubating with secondary antibodies diluted in 5% serum/3% BSA/0.1% Triton X-100/PBS for 16 hours at 4°C in the dark. When mouse on mouse antibodies were used, a mouse on mouse blocking kit was used to prevent non-specific binding (MOM block, Vector labs, MKB2213). Controls included unstained, secondary only, and single stains. Cells were washed thrice with 0.1% PBST and then counterstained if needed with Hoechst-33342 (Invitrogen H3570) (1:5000). Cells were washed with PBS then distilled water to remove salts. Coverslips were then removed from wells before mounting onto Superfrost-plus slides (Thermo) cell side down with Fluoromount-G anti-fade medium (Thermo) and the edges sealed with nail varnish. Cells were imaged using a Zeiss LSM 880 Inverted Confocal Microscope. Antibodies used were against KRT5 1:300 (Biolegend 905901) and P63 1:100 (Abcam ab53039 or ab735). All secondary antibodies were AlexaFluor conjugates (ThermoFisher).

2.6 Fluorescent Immunohistochemistry

The same staining protocol as described above for immunocytochemistry was used. For paraffin embedded sections, an automated system (TissueTek) was used to dewax and rehydrate slides by immersion in xylene followed by a graded series of ethanol through to water. Antigen retrieval when needed was performed using 10mM sodium citrate buffer pH 6.0 and heat induced epitope retrieval in a microwave for 20 minutes. Subsequent staining was performed in a humidity chamber to keep the slides from drying out. Antibodies used were against acetylated tubulin (ACT) 1:100 (Sigma T7451) and MUC5AC 1:100 (SantaCruz Biotechnology sc-21701) to identify ciliated and mucus secretory cells.

2.7 Histology

8 to 12-week-old mice were harvested using a rising concentration of carbon dioxide. Mice were decapitated, the heads were skinned and the lower jaw, skull cap and brain removed. When mice were from reporter lines with endogenous fluorescence, subsequent steps were performed with the heads protected from light. Heads were fixed in freshly thawed 4% PFA for 16 hours at 4°C before rinsing thrice in PBS for 15 minutes. Heads were then decalcified for 14 days in 10% EDTA (Pioneer Research Chemicals PRC/R/118) at 4°C with fresh EDTA replacement every 48 hours. Decalcifying specimens were kept on a roller. Heads were then trimmed to remove the skullcap and brain, jaw, sinuses and posterior cranial fossa to reduce subsequent sectioning requirements. Heads were processed via a graded ethanol series into paraffin wax using an automated system (Leica TP1050) and then embedded in paraffin before sectioning into 8μm sections, mounted on Superfrost-plus slides and left to air dry overnight. Haematoxylin and eosin (H&E) staining was performed using an automated system (TissueTek) before automated coverslipping and scanning using a Nanozoomer (Hamamatsu).

2.8 Transwell cultures for air-liquid interface[110]

100,000 middle ear cells were seeded onto rat-tail collagen I coated 0.4µm PET transwell inserts (Corning 353095) in a 24-well plate format. The lower chamber was fed with 700µl and the upper chamber with 300µl of MMEC-plus with freshly added retinoic acid every 48 hours until confluence was reached. At this point, media in the upper chamber was removed to expose the confluent cell layer to air and the lower chamber was fed with MMEC-serum free (SF) (MMEC-basic supplemented with 1 mg/ml BSA, 5 µg/ml insulin, 30 µg/ml bovine pituitary extract, 5 µg/ml transferrin, 5ng/ml mouse epidermal growth factor, 0.025 µg/ml cholera toxin and 0.01 µM of freshly added retinoic acid). For immunocytochemistry of air-liquid interface cultures, media was aspirated and cells fixed with 4% freshly thawed PFA for 10 minutes then ice-cold methanol for 5 minutes. Staining steps were as described above. The transwell membrane was stained in whole mount with antibodies added into the transwell at 70µl of staining solution per transwell.

2.9 Genotyping

Mice ear snips were taken at 21 days after birth and placed into 1.5ml Eppendorf tubes with 50µl of ear snip buffer (1M Tris pH 8.0, 5M NaCl, 10% SDS and proteinase K at 20 mg/ml) and heated at 55°C for 3 hours with shaking at 300rpm. The samples were then heated 96°C to inactivate the proteinase K then centrifuged at 300 x g for 5 minutes and the supernatant

removed and diluted 1:10 in dH2O for subsequent genotyping using PCR according to the protocol as per Jackson laboratories shown in Figure 2-1.

A

PRIMER	5' LABEL	SEQUENCE 5' → 3'	3' LABEL	PRIMER TYPE	REACTION	NOTE
11341		GAA TTA ATT CCG GTA TAA CTT CG		Mutant Forward	A	directly after mCerulean
oIMR8545		AAA GTC GCT CTG AGT TGT TAT		Wild type Forward	A	
oIMR8916		CCA GAT GAC TAC CTA TCC TC		Common	A	

B

Reaction A	
COMPONENT	FINAL CONCENTRATION
ddH2O	
Kapa 2G HS buffer	1.30 X
MgCl2	2.60 mM
dNTP KAPA	0.26 mM
11341	0.50 uM
oIMR8545	0.50 uM
oIMR8916	0.50 uM
Glycerol	6.50%
Dye	1.00 X
Kapa 2G HS taq polym	0.03 U/ul
DNA	

Cycling			
STEP	TEMP °C	TIME	NOTE
1	94	--	
2	94	--	
3	65	--	-0.5 C per cycle decrease
4	68	--	
5		--	repeat steps 2-4 for 10 cycles (Touchdown)
6	94	--	
7	60	--	
8	72	--	
9		--	repeat steps 6-8 for 28 cycles
10	72	--	
11	10	--	hold

Figure 2-1 Polymerase chain reaction used to genotype mice using DNA extracted from pinna snips.

Genotyping protocol with PCR. Ear snips were obtained from 21-day old mice and DNA extracted. Genotyping was performed according to a validated protocol from JAX using a PCR-based method. A. Primers used for PCR. B. Reaction cocktail and PCR cycle protocol.

2.10 Flow cytometry

All staining steps were performed at 4°C and with cells protected from light. Cells were resuspended in FACS buffer (1% bovine serum albumin (BSA) in PBS) and subsequently incubated with mouse serum (1:10 dilution) (Sigma) for 20 minutes to block Fc receptors. Specific antibodies conjugated to an appropriate fluorophore were then added to the cells and the cells were incubated for 20 minutes. Cells were washed 3 times in FACS buffer before resuspending in FACS buffer and either run on an LSR Fortessa II (BD Biosciences), and analysed using FlowJo software (Tree Star, USA).

For intracellular antigen staining, cells were fixed for 15 minutes at room temperature in BD CellFIX (BD 340181) then after washing thrice in FACS buffer, antibody staining was performed with dilution in BD FACS Permeabilizing Solution (BD 340973). For non-conjugated antibodies, the blocking was performed as above before incubating with the primary antibody for 20 minutes, washing thrice in FACS buffer, then adding the appropriate secondary antibody for 20 minutes before washing again then proceeding to conjugated staining as above.

Isotype controls and FMO (fluorescence minus one) were used to set gates for analysis. Microbeads (BD) were used for single stained controls apart from for keratin-5 and isolectin-B4 for which cells were used.

Antibodies used are shown in Table 2.

Antigen:Conjugate	Details
CD31:APC	102410, Biolegend
CD45:PerCPCy5.5	103132, Biolegend
EpCAM (CD326):APC-Cy7	118218, Biolegend
Isolectin GS-IB4:Biotin-XX	I21414, Invitrogen
Streptavidin:Qdot605	Q10101MP, Invitrogen
CK5:AlexaFluor488	ab193894, Abcam
NGFR:PE	12-9400-42, Invitrogen
ITGA6:PE	12-0495-82, Invitrogen

Table 2. Flow cytometry antibodies.

All antibodies and secondaries were used at 1:100 dilution apart from for keratin-5 which was at 1:300.

2.11 Induction of Cre-recombinase

A stock solution of tamoxifen (Sigma-Aldrich T5648) was made by dissolving 1g of tamoxifen in 1ml of warm ethanol (55ºC) whilst being stirred. After the majority of the tamoxifen had dissolved, 49ml of corn oil (Sigma-Aldrich C8267) was added to generate a 20mg/ml stock solution and this was incubated in a water-bath at 37ºC for 15 minutes. 750µl aliquots were stored at -20ºC until needed. For induction of lineage tracing mice were given tamoxifen by oral gavage at a dose of 200µg/g, once a day for three consecutive days and provided with wet mash and weighed during this process.

2.12 Whole mounts

Mice were anaesthetised with a terminal dose of pentobarbital and perfused with ice cold 4% PFA. Then heads were skinned then post-fixed in 4% PFA for 16 hours at 4ºC. The mastoid bullae were dissected as described earlier and then decalcified for 14 days. The bulla was embedded into 1% agarose in a 10cm dish with the middle ear opening facing upwards and immersed in PBS. Fluorescence was visualised using an upright Leica SP8 or Zeiss LSM 710/880 confocal microscopes.

2.13 Clearing[40]

Mice heads were processed as for whole mounts up until the embedding stage. After decalcification bulla were immersed in RapiClear 1.52 (Sunjin labs RC152) in a 1.5ml Eppendorf. After this time, bullae were either embedded in agarose as above for whole mounts with RapiClear covering the bulla, or divided into dorsal and ventral sections and mounted onto Superfrost-plus slides with a RapiClear as mounting media.

Bone CLARITY was performed as specified by Greenbaum and colleagues[117]. After the decalcification step, hydrogel stabilisation was performed by embedding in 4% acrylamide for 16 hours at 4ºC followed by polymerization at 37ºC for 3 hours. Delipidation was then performed for 5 days in 8% SDS at 37ºC before washing in PBS then removing haem to quench autofluorescence by using amino alcohol at 37ºC. Finally, samples were placed in refractive index matching solution and embedded in 1% agarose for whole mount visualisation using confocal microscopy as above.

2.14 Spheroid assay

Enzymatically isolated mouse middle ear epithelial cells were fibroblast depleted and then 10,000 cells were mixed in a 1:1 ratio with growth factor reduced Matrigel (Corning 354230) and seeded into a 24-well 0.4µm pore transwell. MMEC-plus proliferation medium was added to the upper and lower chamber for 7-10 days after which MMEC-SF differentiation medium was

added instead. After 14-21 days ice cold 4% PFA was used to fix the spheroids, the Matrigel aspirated using a wide bore aspiration pipette and pelleted in ice-cold PBS by centrifuging at 300 x g for 5 min. The supernatant was aspirated and the samples were embedded in HistoGel (Richard Allan Scientific) and stored in 70% ethanol until ready for paraffin embedding and processing as described above.

2.15 Hypoxia induction

Cobalt (II) Chloride hexahydrate ($CoCl2 \cdot 6H2O$, MW=237.9) (Merck C8661) was used to chemically induce hypoxia inducible factor[118] at 50μM, 100μM and 200μM concentrations dissolved into MMEC-plus. Middle ear epithelial cells were initially isolated and cultured in MMEC-plus for 7 days before hypoxia induction for 7 days with alternate day media changes.

2.16 Statistics

All data points are represented as unadjusted mean ± standard error of mean unless specified otherwise. Data were analysed to establish normal distribution. Where data was normally distributed Student's t-test was performed. Non-parametric tests were used for non-normal data (Mann-Whitney Test) to establish significance. The significance threshold was set at $p < 0.05$. GraphPad Prism v8) (GraphPad Software, CA,USA) was used for all analyses.

Chapter 3 Establishing assays of middle ear epithelial homeostasis in vitro

The ability to analyse the proliferative and differentiation behaviour of epithelial cells in vitro requires a method of isolation of viable tissue from the region of interest. Here, middle ear epithelium was isolated using enzymatic techniques before a variety of assays used traditionally in respiratory epithelial biology were adapted and optimised to study the characteristics of the mouse middle ear epithelium.

3.1 Enzymatic dissociation using dispase and TrypLE can be used to isolate middle ear mucosal cells

Middle ear cells can be obtained by instrumental biopsy and removal of epithelial tissue, enzymatic dissociation strategies, or a combination of the two methods. Instrumental biopsy involves physically removing the lining from a dissected bulla. This has the advantage of directly visualising targeting regions and removing any influence exposure to dissociation enzymes may have on the cells. However, it may not yield enough tissue as the mucosal lining is thin during health and thus can be challenging to dissect out. In addition, single cell suspension would still need to be generated from this biopsy subsequently and this could be done via trituration or using enzymatic reagents.

Instrumental biopsy alone and enzymatic dissociation alone were tested in turn to identify the optimal method to yield adequate numbers of viable epithelial cells for further experimentation. All experiments below are in B6J mice of 8-12 weeks of age and a mix of sexes, unless otherwise specified.

The middle ear bullae were dissected out and the tympanic membrane with the surrounding bony annulus and ossicles removed to prevent contamination by tympanic membrane epithelial cells (Figure 3-1B). As the normal middle ear mucosal lining is a very thin layer, instrumental removal was challenging with only small fragmented biopsies being obtained. Instrumental removal of tissue from both bullae of an individual mouse did not yield enough tissue for further processing (n=3 attempts).

Enzymatic dissociation strategies consisted of placing both dissected bullae in entirety into a series of dissociation reagents (Figure 3-1A). It has been shown in the murine airway that pronase-based dissociation techniques results in cleavage of some extracellular epitopes such as CD31, CD45 and ITGA6[119]. As these markers would be used in gating strategies for flow cytometry, such cleavage can preclude from further flow cytometric analysis and sorting. However, the use of dispase followed by 0.1%trypsin conserves these epitopes better than pronase[119]. Thus, a dispase/trypsin based strategy may be a preferred methodology for isolation. The initial step was a comparison between this and with pronase-based isolation to assess cell yield and viability.

The pronase isolation was performed as per Mulay and colleagues[101]. For dispase based isolation, a technique from Hegab[120] was modified. Mice were euthanised and the bulla were dissected out with removal of the ossicles and tympanic membrane with bony annulus. Both bullae were placed in a 1ml Eppendorf with 16U of dispase in 1ml of mouse middle ear epithelial cell basic (MMEC-basic) media at room temperature. After 30 minutes, 0.5mg/ml of DNase I was added. After 20 minutes, the bullae were removed and placed in 1ml of 0.1% trypsin/EDTA. The previous reaction was quenched by diluting in 10% FBS in MMEC and the suspension stored on ice until later use. The bullae in trypsin were placed in a shaker at 37°C for 30 minutes. After this time, this reaction was also quenched with 10% FBS. The 3 solutions were pooled, filtered through a 70μm cell strainer and centrifuged at 500rcf for 10minutes at 10°C to maintain cell viability. The pellet was resuspended in 10% FBS and cell number and viability were assessed.

There was no difference between the two techniques in number of cells isolated or in number of non-viable cells as assessed by trypan blue staining (Figure 3-1C). The final isolation strategy was thus 16U Dispase in 1ml MMEC for 30 minutes, followed by 20 minute incubation with 0.5mg/ml DNaseI (to prevent cell clumping) and then a 30 minute incubation at 37°C in 1ml of TrypLE rather than trypsin/EDTA. This change to TrypLE was to further preserve epitopes[121] and to remove EDTA from the protocol which can affect basal cell viability[102].

This procedure is henceforth referred to as enzymatic isolation.

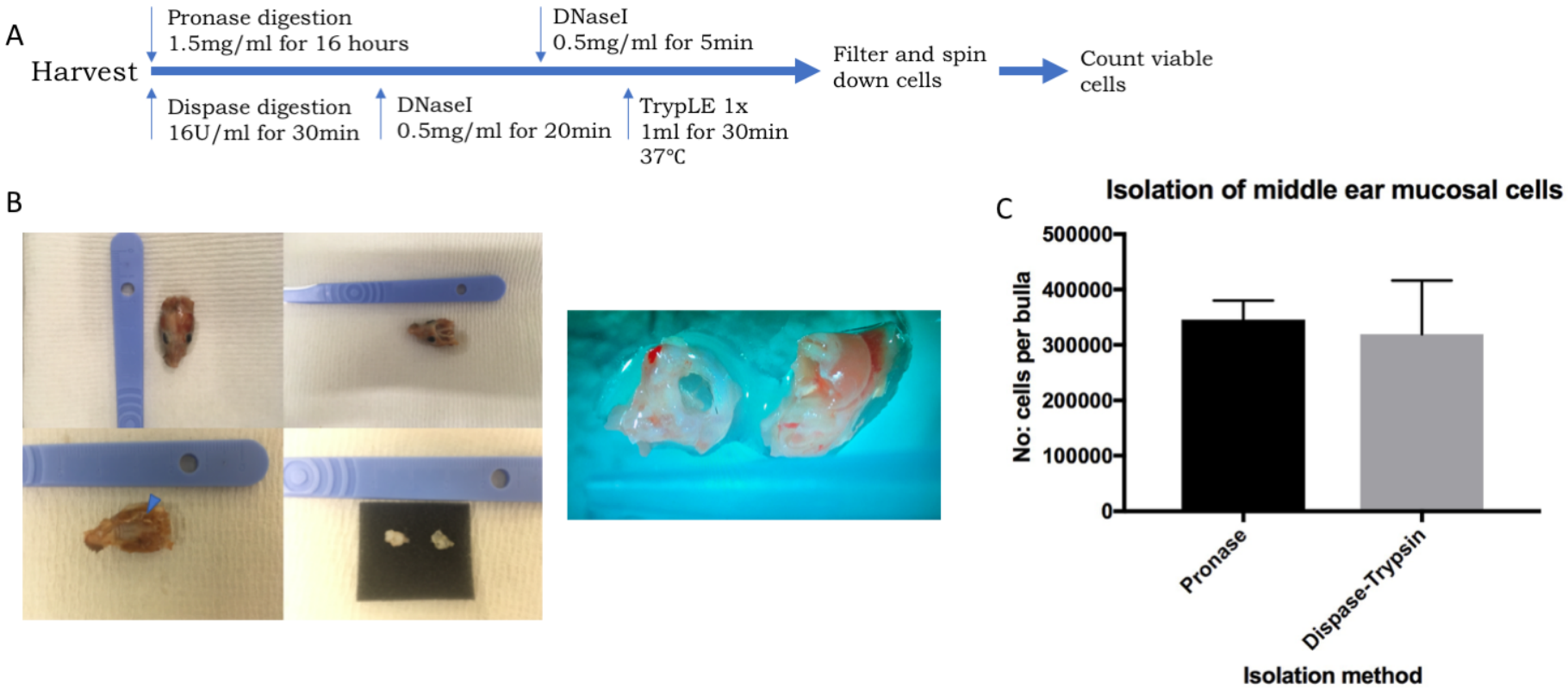

Figure 3-1 Enzymatic dissociation using dispase and TrypLE can be used to isolate middle ear mucosal cells.

Isolation of cells from the mastoid bullae. (A) Enzymatic dissociation was performed either using pronase alone or dispase followed by Trypsin/EDTA before generating a single cell suspension and counting viable cells using trypan blue. (B) Mice under terminal

anaesthesia were decapitated, skinned, and the middle ear bulla (blue arrowhead) dissected out. The tympanic membrane and ossicles were separated and discarded, leaving just the bulla cavity (right panel). (C) Bar graph shows mean yield of viable cells from each isolation method. No significant difference was seen between either method (Student's t-test, two tailed). Error bars show SEM. (n = 3 mice)

3.2 KRT5+ cells constitute 7% of middle ear epithelial cells

Keratin 5 (KRT5) is an intracellular cytokeratin that is expressed by the basal cell population of epithelial tissues[93]. The presence of basal cells in the middle ear has been known since Tos[73] identified such cells in histology of human temporal bones. Basal cells are known to express KRT5+[93] and the confirmation that KRT5+ expressing basal cells exist in the murine middle ear has recently been supported by immunohistochemistry, in vivo lineage tracing and cell culture[98,99,110]. However, it is still uncertain how many KRT5+ cells are present and what proportion of the epithelium they constitute. Here, flow cytometry was used to identify the proportion of cells in the middle ear epithelium that are KRT5+.

Using fresh enzymatically isolated middle ear cells from 3 mice, a gating strategy was used to remove immune and endothelial cells (excluded by gating on CD31- and CD45-negative cells) (Figure 3-2A), then to select for epithelial cells using the marker EpCAM [94] ([122,123] Ryan et al., 2020, unpublished data).

Cells isolated from the middle ear that were EpCAM positive were considered of epithelial origin (Figure 3-2B). Of these EpCAM+ cells, 7.02% (±1.35%) were KRT5+. KRT5+ cells were not found in the EpCAM- population, non-epithelial population (Figure 3-2C).

A

Epitope	Fluorophore	Dilution	Purpose
CD31	APC	1:100	Negative selection endothelial cells
CD45	PerCP-Cy5.5	1:100	Negative selection immune cells
EpCAM	APC-Cy7	1:100	Positive selection epithelial cells
KRT5	AF488	1:500	Basal cell marker
GSIB4	Qdot605	1:100	Test as surrogate marker for KRT5+ cells

B

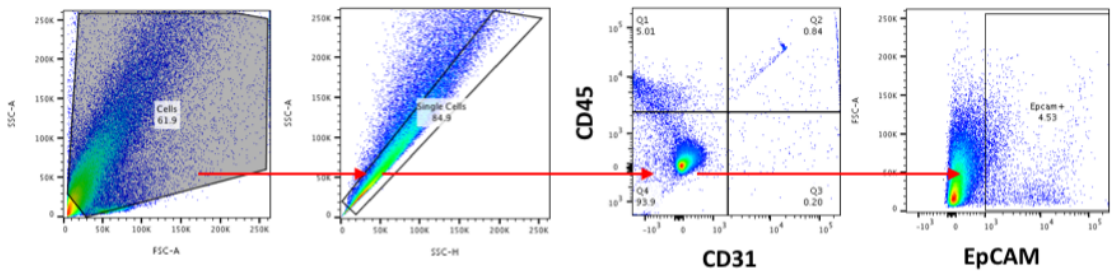

C

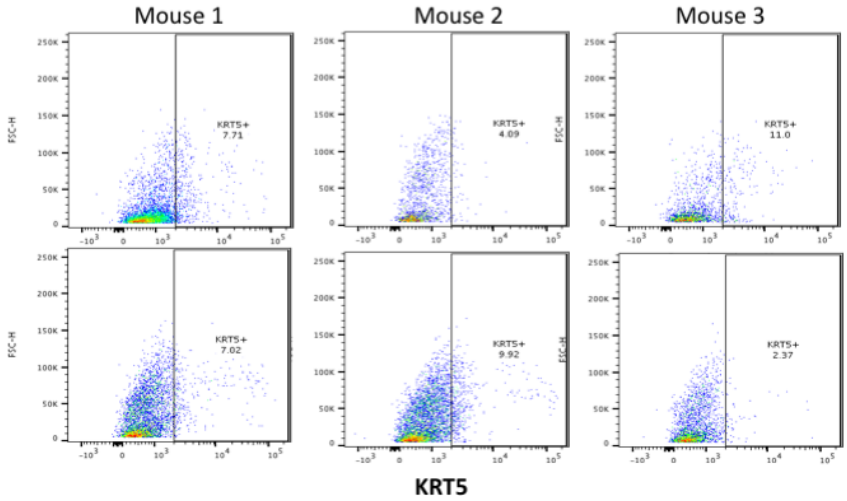

Figure 3-2 KRT5+ cells constitute 7.02% of middle ear mucosa.

Flow cytometric analysis of mouse middle ear epithelial cells. After enzymatic isolation, up to 100,000 cells per sample were seeded into each well of a 96-well plate and stained. B. A gating strategy was used to remove endothelial and haematopoietic cells (CD31-CD45-) followed by selection for epithelial cells using EpCAM positivity. C. Of the EpCAM+ population, 7.02% (±1.35%) were KRT5+. Each panel shows one bulla, columns are from individual mice. (n = 3 mice)

3.3 Cells with progenitor capacity are present in the middle ear epithelium

Colony forming assays can be used to assess for the presence of progenitor cells in mouse middle ear. This is one of the techniques used to study how epithelial linings are maintained by progenitor cells[102]. Colony forming assays work on the principle that when a single cell suspension is seeded in 2D adherent culture, any colonies that form must derive from a cell with progenitor potential – these are termed clones[124]. Colony forming efficiency is thus a ratio of the number of colonies formed relative to the number of cells plated. Culturing cells in such a manner can be used as an indicator of progenitor cell number, to analyse proliferative potential and characterisation of colony-forming efficiency, colony sizes and morphology to differentiate between cells with varying progenitor abilities[113].

In assays using skin epithelial cells, the density of seeding for colony forming analysis is classically 2500 cells per well of a 6-well plate assuming a pure basal cell population and the use of co-culture conditions with an inactivated mouse embryonic fibroblast feeder layer[102]. However, it is known that there can be strain specific differences in colony forming efficiency (up to 50x) between different congenic strains of mice[125]. In addition, the middle ear epithelium may have a different proliferation and turnover potential compared with airway[13]. It was therefore unclear what seeding density would be best to use for a colony-forming assay using cells isolated from the mouse middle ear.

To arrive at a *minimum* and range of seeding densities, the assumptions were:

- 6% of epithelial cells are KRT5+ cells (lower bound of the range of values from flow cytometry)
- the population of cells isolated after fibroblast depletion using differential adherence is 100% epithelial
- at least 2500 cells per well of a 6-well plate is needed
- the assay is terminated after 6 cell divisions have taken place[126]
- colonies should not have merged prior to the assay being terminated

Thus, we need approximately 2500/0.06 = 41,666 per well of a 6-well plate. This is likely the lower bound of the seeding density required. Initial attempts of culture at 50,000/well, 125,000/well and 250,000/well all grew some colonies but 250,000/well had >10 colonies seen in all wells. Therefore, the highest seeding density in this range was used that would permit technical triplicates from each bulla. This is specified in each experiment.

As some primary cell culture of tissues require collagen coating to ensure cell adherence and growth, colony-forming ability on collagen was then tested. Enzymatically isolated fibroblast-depleted *Figure 3-3A) mouse middle ear cells were prepared as a single cell suspension and seeded at 250,000 cells per well of a 6-well plate and grown for 2 weeks. Half the wells were coated with 150µl of 50µg/ml rat-tail collagen-I. Colonies with epithelial cell like morphology started to appear after 3-5 days in all wells. Colonies increased in size for the duration of the assay. Brightfield microscopy showed heterogeneous colonies; some displayed the typical cobblestone morphology of epithelial cells, others had enlarged cytoplasmic regions and less tightly packed cells which may suggest unhealthy cells, senescence or partial attempts at differentiation. This heterogeneity is in keeping with other murine colony forming work[102]. Contaminating fibroblasts were rarely seen and if identified they were excluded from the colony counts. After 2 weeks plates were fixed and stained using crystal violet. The overall colony forming efficiency was 0.005% for collagen coated and 0.007% for non-collagen coated wells (Figure 3-3C). There was no difference in morphology between the two conditions. The area of colonies seen in the plate ranged from 0.000068cm^2 to 0.083cm^2. Plotting this graphically shows a positive skew with the majority of colonies being small in size but a few larger outlying colonies evident (Figure 3-3D). There was thus no significant difference between culturing in collagen coated or non-coated condition and further cell culture was performed without collagen coating unless specified.

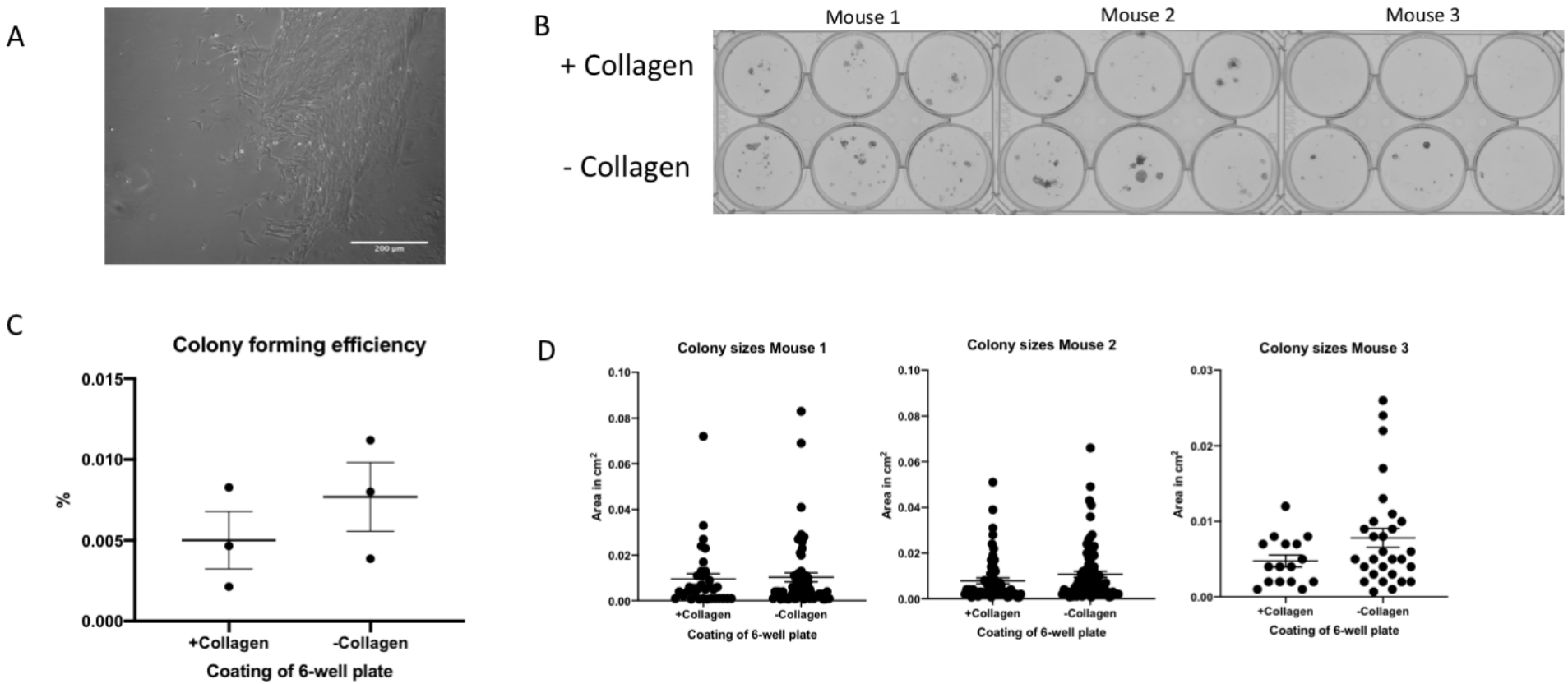

Figure 3-3 Single cell suspension of isolated middle ear epithelium has cells with colony forming ability.

A. Differential adherence on Primaria plates allows separation of epithelial and fibroblast populations. Fibroblast cells adhere more rapidly compared with epithelial cells and thus the supernatant is enriched for epithelial cells. Cells in Primaria plates were grown in

10% FBS with medium changed 3 times a week. Brightfield image of representative fibroblast colony in Primaria plate 5 days post differential adherence process. B. Middle ear mucosa has cells with colony forming potential. A single cell suspension of enzymatically isolated middle ear epithelial cells was seeded at a density of 250,000 cells per well of a 6-well plate with collagen coating (+C) or without collagen coating (-C). Each well in a culture condition is a replicate. Cells were grown in MMEC+ medium with media changes 3 times per week. After 2 weeks, cells were fixed in 4% paraformaldehyde and stained with 1% Crystal violet before imaging. Colonies derived from single cells can be seen in all wells. C. Colony forming efficiency of middle ear mucosa. Middle ear mucosa has a colony forming efficiency of 0.005% (collagen coated) 0.007% (non collagen coated). There was no significant difference between coated and uncoated efficiency ($p = 0.39$, unpaired t-test, two tailed). Error bars show SEM. D. Colony sizes of colonies formed. Middle ear epithelia derived colonies are $0.007cm^2$ in area (with collagen) and $0.01cm^2$ in area (without collagen). All mice had a positive skew with some comparatively large colonies. There was no significant difference between coated and uncoated sizes. ($p = 0.40$, Mann-Whitney-U, two tailed). Error bars show SEM. ($n = 3$ mice)

3.4 Colonies grown from progenitor cells express the basal cell marker KRT5

Having shown that cells with progenitor capacity exist in the middle ear using the colony forming assay, the next step was to check whether any of the colonies derived from these cells expressed the basal cell marker keratin-5 (KRT5). If positive, this would suggest that KRT5+ cells are found in the middle ear epithelium and also have progenitor potential, akin to other epithelial surfaces. Furthermore, it would show the current method as a way to isolated and culture progenitor cells which can then be used in assays of differentiation potential.

Enzymatically isolated mouse middle ear epithelial cells (MMEC) were seeded onto microscopy coverslips in a 6-well plate and grown for two weeks before fixing and staining for keratin-5 to visualise immunofluorescence. Colonies showed KRT5 positivity (Figure 3-4A) even when they did not display the classical tightly packed appearance (Figure 3-4C). A fibroblast contaminating population was nucleated and were KRT5- thereby serving as an internal control (Figure 3-4B). As found by Watt in skin culture and Mulay and colleagues in MMEC culture, 2D culture of murine epithelial cells had limited efficacy in growing a uniform stem cell population and heterogeneity of colonies was seen with some undergoing senescence or potentially undergoing differentiation or demonstrating altered morphology when grown on tissue culture plastic[102,110].

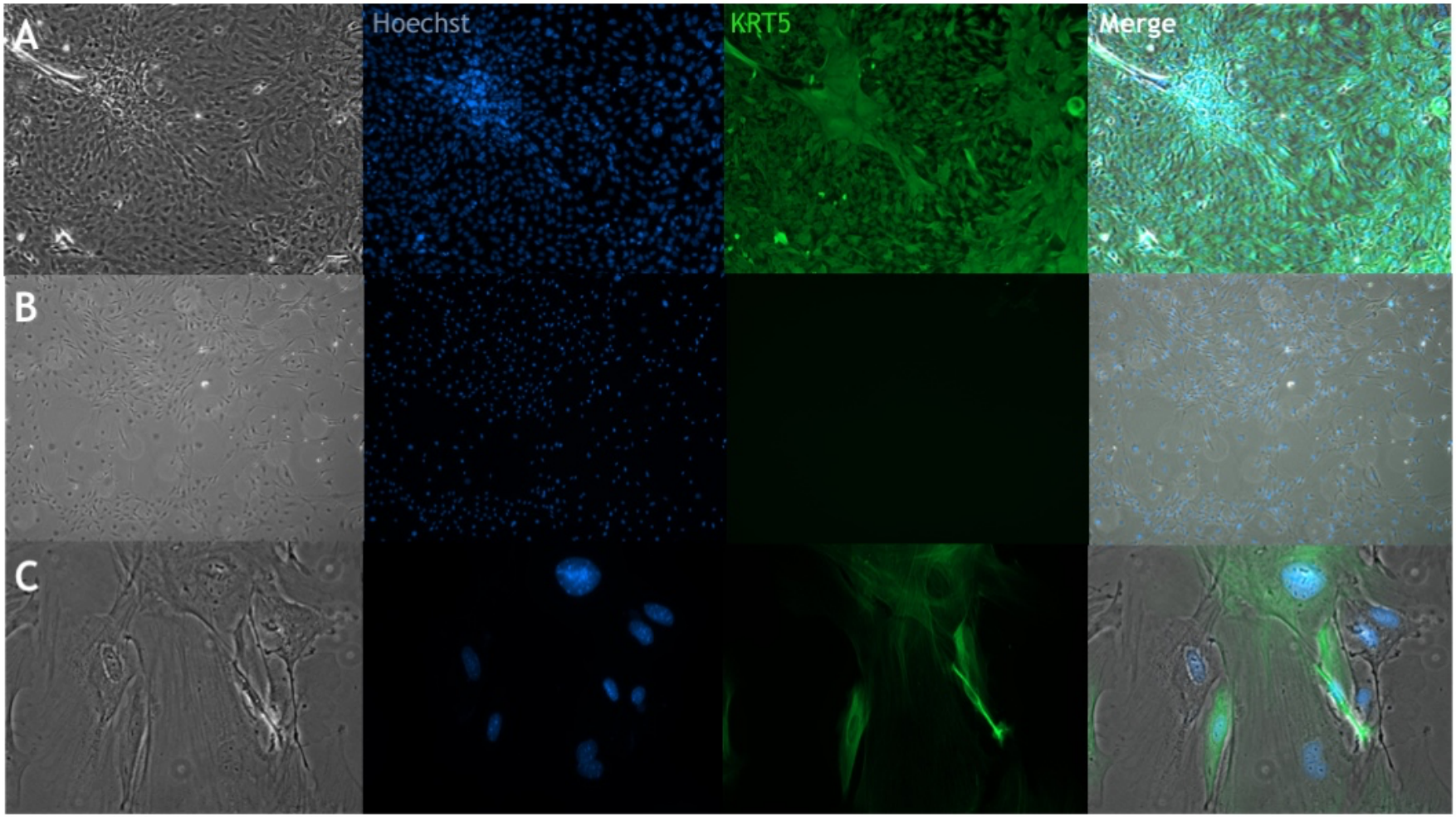

Figure 3-4 Colonies derived from middle ear epithelium are KRT5+ and show epithelial like morphology.

After enzymatic dissociation, 50,000 cells were seeded onto non-collagen coated coverslips in a 6-well plate and grown for 2 weeks with 3 media changes per week. Cells were then fixed with 4% PFA, permeabilised with ice-cold methanol and stained for keratin-5 (AlexaFluor-488 – shown here as green) and Hoechst-33342 (shown here as blue). Top row A. shows epithelial cell like colony and middle row B. shows fibroblast-like KRT5- control. C. Colonies with heterogeneous morphology also have some KRT5+ cells. Panel shows colonies with cells with less tightly packed cells and larger cytoplasmic regions. These also have KRT5+ cells as well as some KRT- cells. Scale bar shows 100μm. (n = 3 mice)

3.5 Differentiation potential of KRT5+ progenitors can be assayed using 3D air-liquid interface culture

The air-liquid interface (ALI) culture assay is well-established in respiratory biology as an in vitro model of differentiated airway epithelium. The process involves the generation of a confluent monolayer of submerged, undifferentiated basal cells in a transwell prior to air exposure to stimulate differentiation. Therefore, it is possible to study the differentiation potency of basal cells by observing the cell types that arise from differentiation of a confluent progenitor cell layer (Figure 3-5A).

Mulay and colleagues used a seeding density of 10,000 cells per well, but other groups have used higher densities. To confirm optimal seeding density, enzymatically isolated fibroblast depleted middle ear epithelial cells were seeded at 10,000/well, 50,000/well and 100,000/well densities in 0.4μm transwells in a 24-well format with and without 150μl of 50μg/ml collagen coating. Colonies did not grow without collagen coating (data not shown). In the collagen-coated transwells, small colonies were seen after 3-5 days. A higher seeding density resulted in better growth with 1/6 colonies grew at 10000/well whilst all transwells grew at the highest 100000/well density (Figure 3-4B). This is in keeping with the estimates that a 24-well transwell insert has a surface area of 0.33cm^2 and thus at confluence should have approximately 40,000 cells. Assuming 7% of epithelial cells are KRT5+, 0.07*100,000 is 7000 basal cells. Three population doublings (i.e. 7000 to 14000 to 28000 to 56000 cells over 3 doublings) would be needed to reach confluence and this is approximately 120 hours or 5 days as a minimum. This does not take into account cell death or the initial lag phase of 3-5 days in proliferation that occurs when MMEC are seeded[110].

Transwells were examined daily using brightfield microscopy. Growth rate between wells was variable but all wells that grew were confluent after 7-14 days. The confluent monolayer had the cobblestone like morphology of epithelial cells and less heterogeneity was seen than when grown in 2D plastic

culture (Figure 3-5C). At confluence, transwells were fixed and stained in whole mount and were positive for KRT5 and p63 (Figure 3-5D). This confirmed that the cells expressed markers of basal/progenitor cells when submerged, prior to air exposure and addition of differentiation medium to simulate differentiation.

A

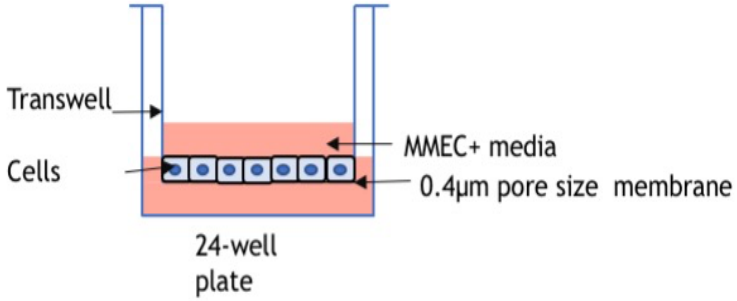

B

Seeding density/cm^2	Equivalent number of cells/24 well insert	Number of transwells grown to confluence
30303.0303	10000	1 out of 6
151515.1515	50000	4 out of 6
303030.303	100000	6 out of 6

C

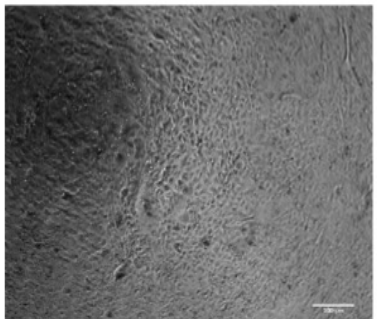

D

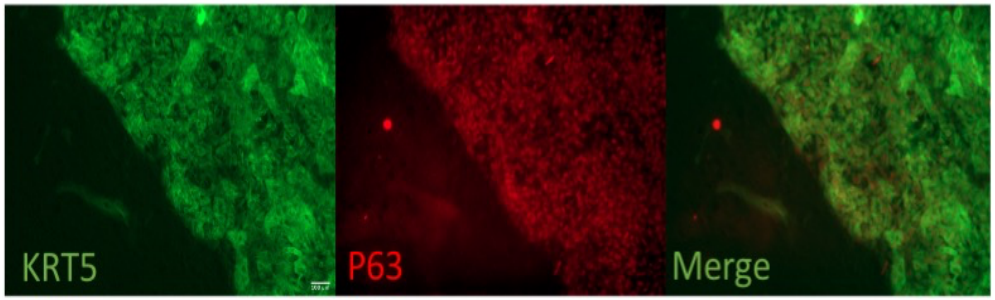

Figure 3-5 Air-liquid interface can be used as an assay for differentiation potential of basal cells

A. Freshly enzymatically isolated mouse middle ear cells were seeded at 10000/well, 50000/well or 100000/well of collagen coated and non-coated 0.4μm semi permeable transwells. The lower and upper chambers were fed with MMEC+ medium every other day. Transwell set up is as shown. B. Colonies were seen after 3-5 days and higher seeding densities seem to promote better growth. C. If growth was seen, colonies were confluent by 7-14 days and had epithelial cell like morphology. D. Immunofluorescence showed

positivity for KRT5 (AlexaFluor488 here shown as green) and P63 (AlexaFluor647 here shown as red). Scale bars show 100μm. (n = 3 mice)

3.6 KRT5+ cells can differentiate into cells with ciliated and goblet cell morphology

The middle ear epithelium has differentiated cells which are mainly ciliated and goblet cells. If KRT5+ cells represent progenitor cells of the middle ear, they should show an ability to differentiate into multiple cell types, and at least the ciliated and goblet cells seen in the middle ear. To test this, enzymatically isolated fibroblast depleted MMECs were seeded at a density of least 50,000 cells per transwell to generate a confluent monolayer (Figure 3-6A) before stimulating differentiation by removing the upper layer of medium and replacing the lower chamber medium with MMEC-SF (serum free). A change in morphology was seen after 5-7 days in most wells.

Brightfield microscopy revealed three predominant morphologies of cells, some with raised ciliated appearance; some with expanded vesicles with goblet cell like appearance, and some remaining cobblestoned and flat resembling undifferentiated basal cells (Figure 3-6B).

Transverse sectional histology was attempted by cutting out the transwell and paraffin embedding followed by haematoxylin and eosin staining. However, this resulted in a significant loss of sections from slides with staining with only 1 of 24 remaining adherent. However, the one remaining section did show areas of ciliation in transverse section too corroborating the brightfield visualisation (Figure 3-6C).

Although there is only one adherent section and thus repeats and other sectioning techniques are required, it does suggest that differentiation of KRT5+ cells have bipotent differentiation capacity as it has occurred once.

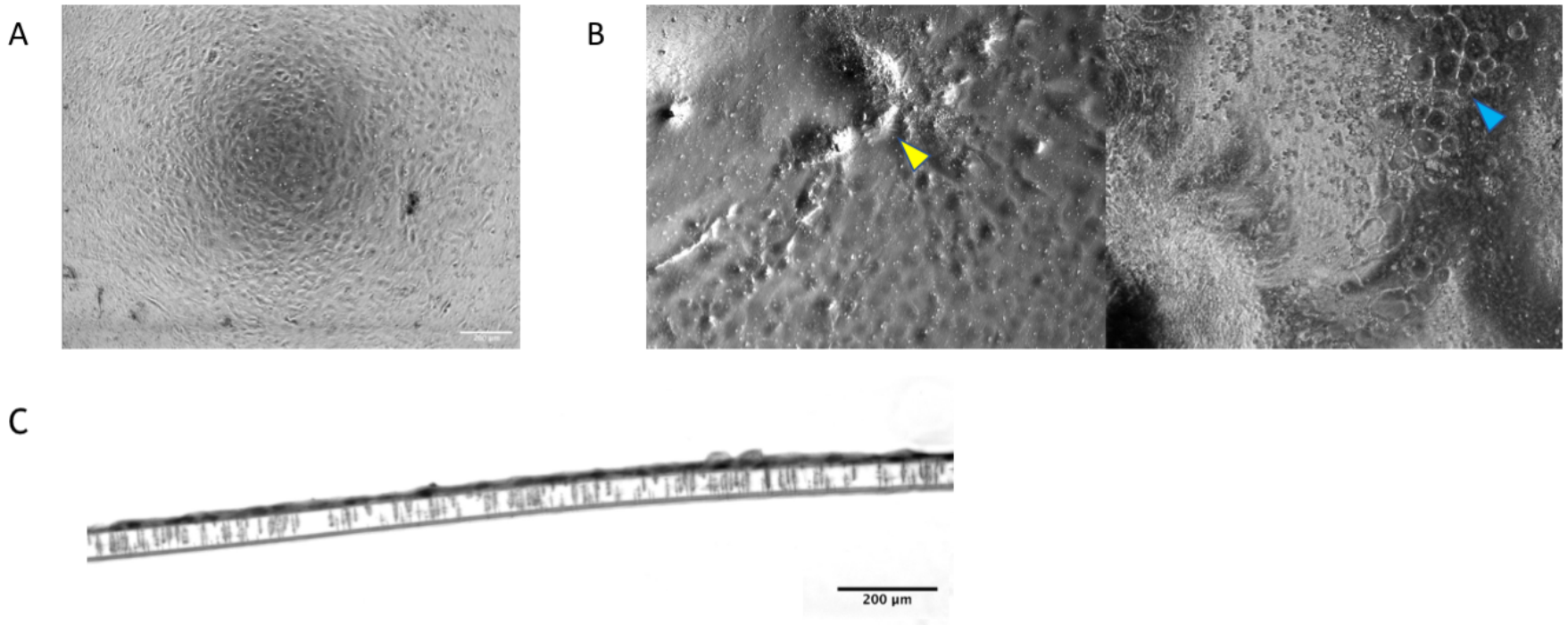

Figure 3-6 Differentiation of submerged cells gives rise to cells with ciliated, goblet-cell and basal cell like morphology.

After confluence, medium was removed from the upper chamber and the lower chamber replaced with MMEC-SF medium. A. Confluent monolayer visible before stimulating differentiation. B. Cells differentiated into three morphologies with regions of ciliation showing raised 3D cells (yellow arrowhead), goblet cell like regions showing vacuoles (blue arrowhead), and undifferentiated/epithelial cells with morphology as before. (Scale bar in A shows 200µm and applies to data in B) C. Transverse section histology using paraffin

embedding showed raised regions of pseudostratified/ciliated epithelium. Section was manually located using brightfield microscopy as the size was too small for automated locating in Nanozoomer. Scale bar shows 200μm. (n = 3 mice)

3.7 Microdissection of mastoid bullae into dorsal and ventral regions allows region-specific analysis of middle ear epithelial cells

It has been shown that the murine middle ear has a dual embryological origin with the dorsal aspect derived from neural crest cells and the ventral aspect from endoderm[72]. To explore whether this developmental region-specific difference has any functional significance, a surgical technique to reliably dissect and separate dorsal bulla from ventral bulla was optimised.

Mice under terminal anaesthesia were decapitated and skinned. The skull cap, lower jaw and brain tissue were removed. Subsequent dissection was performed under microscopic vision with the bulla always kept moist in MMEC basic medium. The dissection was also performed with ice underneath the dissection surface to keep the bulla cool and to maximise cell viability. The mastoid bulla were exposed on both side and separated from the rest of the skull. A small cut was made in the bone just medial the tympanic bony annulus and extended dorsally and ventrally to remove the tympanic membrane completely. The eustachian tube was also removed. The dorsal and ventral aspect of the bulla were then separated by horizontal cuts in the axial plane just above the eustachian tube orifice entrance (Figure 3-7).

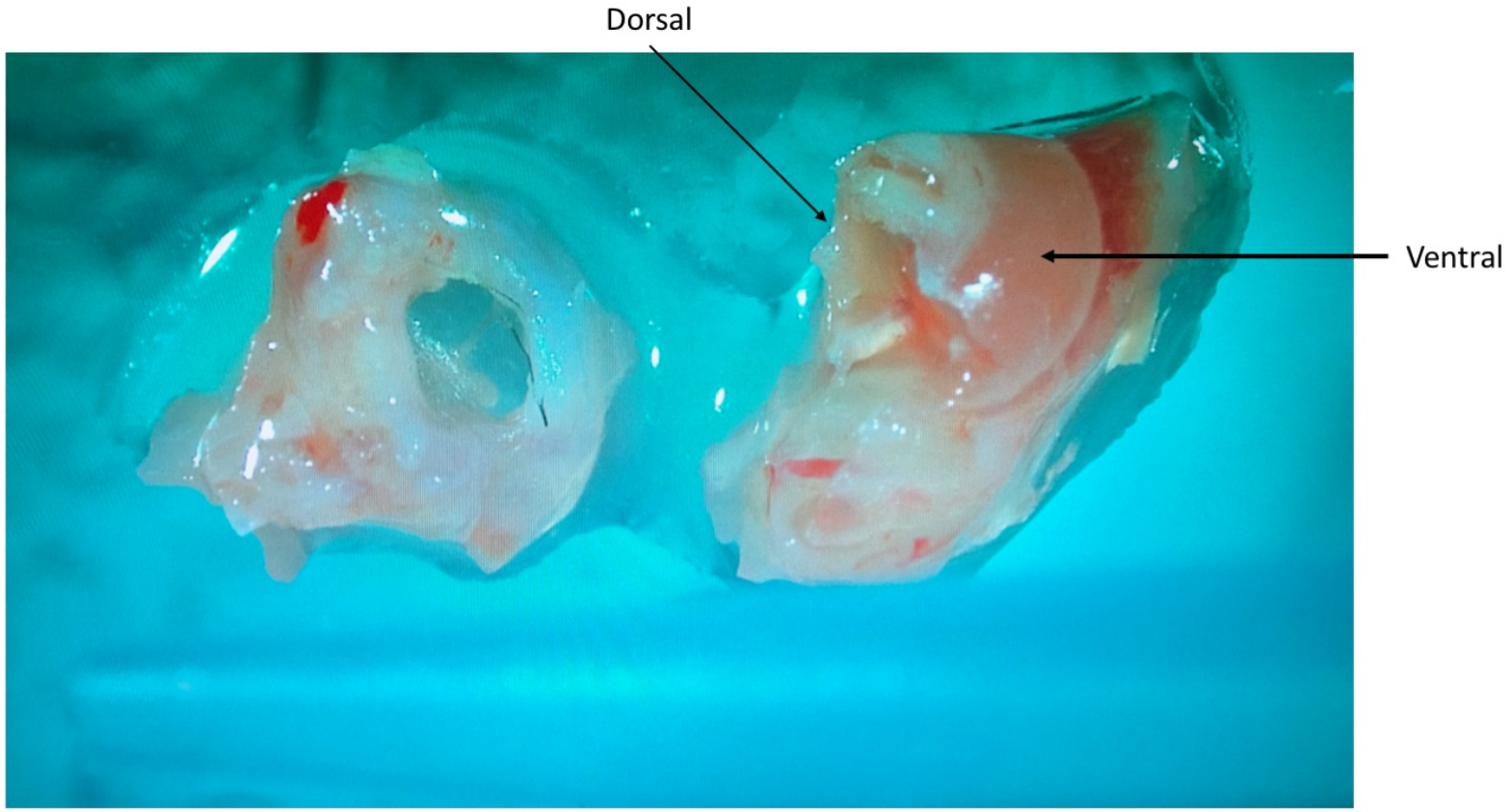

Figure 3-7 Microdissection of middle ear bulla can be used to separate dorsal and ventral regions.

Bullae were isolated as before with the tympanic membrane, bony annulus and ossicles removed. The bulla was then divided into two in the long axis to separate dorsal from ventral regions for further processing.

3.8 Ventral bulla derived epithelium has a higher colony forming efficiency and formed larger colonies than dorsal epithelium

To assess whether the different embryological origins of dorsal and ventral middle ear epithelium has an effect on progenitor cell function, mice were euthanised and dorsal and ventral regions of bullae dissected out separately. Enzymatic isolation was performed and cells were seeded onto 6-well plates as described earlier for colony forming assays. Two weeks later plates were fixed and stained with crystal violet to visualise colonies.

Colonies started to appear after 3-5 days in both dorsal and ventral region wells. Colonies had the cobblestone-like appearance of epithelial cells and showed similar heterogeneity with some looser packed colonies with larger cells (Figure 3-8A). No difference in morphology was seen between the regions of origin. Fewer colonies grew in the dorsal region wells compared with the ventral region wells but this was not significant (CFE of 0.035% for dorsal, 0.1292% for ventral, P=0.114, Mann-Whitney U, two-tailed) (Figure 3-8B). Colonies that grew from dorsal derived epithelium were of similar mean area to ventral derived epithelium (dorsal = 0,016cm^2, ventral = 0.029cm^2, p = 0.1143, Mann-Whitney U two-tailed) but had a higher number of outlier colonies >0.1cm^2 (Figure 3-8C and D).

Although non-significant, the trend towards region specific differences in colony forming efficiency ability may be due to a difference in the proportion of KRT5+ progenitors in dorsal and ventral epithelium. To analyse whether this was the case, flow cytometry was performed. Enzymatically isolated MMEC from dorsal and ventral regions was stained using the same gating protocol as described previously. KRT5+ cells constitute a smaller proportion of MMEC from dorsal bulla compared with ventral bulla. KRT5+ cells made up 1.26% of EpCAM+ cells in dorsal epithelium and 28.9% of EpCAM+ cells in ventral epithelium (Figure 3-8E).

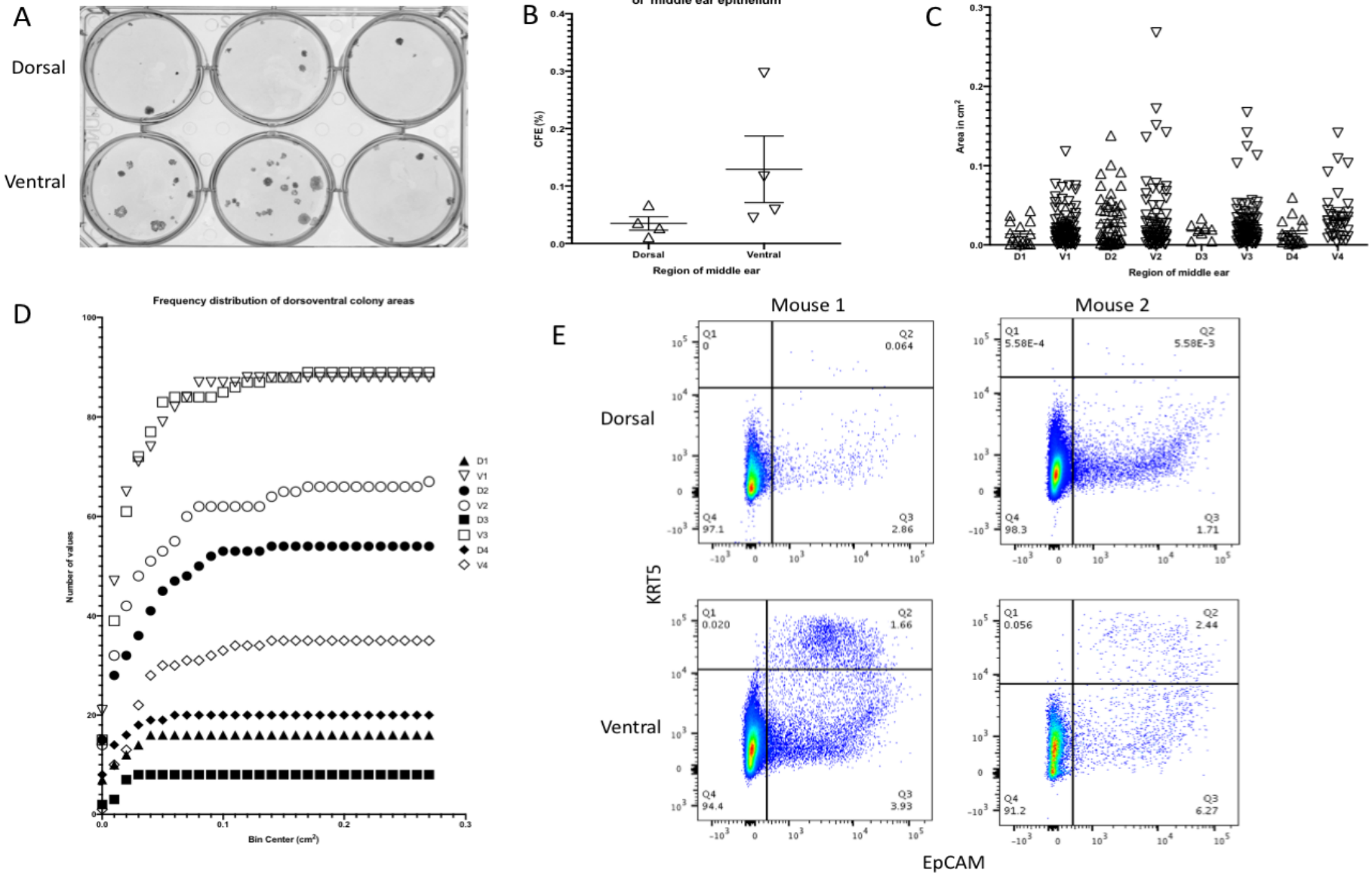
A
Dorsal
Ventral
B
Colony forming efficiency by region of middle ear epithelium
CFE (%)
Dorsal
Ventral
Region of middle ear
C
Areas of colonies formed by region of middle ear
Area in cm²
D1
V1
D2
V2
D3
V3
D4
V4
Region of middle ear
D
Frequency distribution of dorsoventral colony areas
Number of values
Bin Center (cm²)
E
Mouse 1
Mouse 2
Dorsal
Ventral
KRT5
EpCAM
Q1 0
Q2 0.064
Q4 97.1
Q3 2.86
Q1 5.58E-4
Q2 5.58E-3
Q4 98.3
Q3 1.71
Q1 0.020
Q2 1.66
Q4 94.4
Q3 3.93
Q1 0.056
Q2 2.44
Q4 91.2
Q3 6.27

Figure 3-8 Ventral epithelium has progenitor cells that form larger colonies than dorsal epithelium.

A. Enzymatically dissociated cells from dorsal and ventral bulla were seeded into 6-well plates for colony forming assays. Representative image of a 6-well plate after fixing and staining. Top row is dorsal epithelium and bottom row is ventral. Each well in a row is a replicate. B. Graph shows colony forming efficiency of dorsal and ventral epithelium from 4 mice. There was no significant difference in CFE between dorsal (0.035%) and ventral (0.1292%) (P=0.114, Mann-Whitney U, two-tailed). Error bars show SEM. C. Areas of colonies formed showed the ventral region had a positive skew with some large colonies, not seen in dorsal regions from the same mouse. The mean area was not significantly different (dorsal = 0,016cm2, ventral = 0.029cm2, p = 0.1143, Mann-Whitney U two-tailed). D1 = dorsal region mouse 1, V1 = ventral region mouse 1. D. Plotting the distribution to analyse skewness of the distribution shows that ventral derived cells have a positive skew with more colonies of larger size. D1 = dorsal region mouse 1, V1 = ventral region mouse 1. (n=4 mice) E. Flow cytometry showed that the proportion of KRT5+ cells is higher in ventral epithelium (1.66% and 2.44% of EpCAM+ cells) compared with dorsal (0.064% and 0.0005%) (n = 2 mice)

3.9 Enriching for KRT5+ cells is possible using ITGA6

Keratin-5 is an intracellular protein and staining for this marker requires fixation and permeabilisation of cells. Thus, this marker cannot be used to sort viable cells for further culture. Therefore, other markers used in airway epithelium as proxy markers for basal cells include integrin-α-6 (ITGA6), nerve growth factor receptor (NGFR) and GSI-B4 (isolectin B4 from *Griffonia simplicifolia*). The latter is an extracellular lectin that binds to glycoprotein on basal cells and allows for sorting airway basal cells in mouse[94].

Flow cytometry was performed as described previously.

For GSI-B4 the EpCAM+KRT5+ population, GSI-B4 was bound by 75.08% (±11.6 SEM) of the cells. Of the 37.17% (±3.73 SEM) of EpCAM+ cells that bound GSI-B4, only 22.08% (±4.64% SEM) were KRT5+ (Figure 3-9A). A mouse trachea control was used as a comparator with previously published data to check the protocol was working appropriately (Figure 3-9D).

For ITGA6 as an additional marker, from the EpCAM+KRT5+ population, ITGA6 was also expressed by 97.97% (±0.56 SEM) of cells. However, of the 72.69% of EpCAM+ cells that were ITGA6+, only 55.94% (±8.99 SEM) were KRT5+ (Figure 3-9B)

Thus, EpCAM+ITGA6+ will capture nearly all cells that are KRT5+ cells. However, this population will also have about half as KRT5- cells i.e. EpCAM+ITGA6+ as an enrichment strategy will result in a population of cells of which half are KRT5+.

NGFR+ cells only constituted 0.096% (±0.039 SEM) of EpCAM+ cells and thus further analysis was not performed as too small a population expressed this marker for it to be useful (Figure 3-9C).

Thus, an enrichment strategy that used EpCAM+GSIB4+ would result in a cell population of which a fifth were KRT5+.

Summary

This chapter establishes a platform of assays with which to assess the cell biology of the murine middle ear. This includes the ability to isolate and quantify putative progenitor cells and their colony forming ability. Differentiation assays have also been optimised to assess differentiation potential of progenitor cells. Limitations include the relatively small number of mice and restricted strains used.

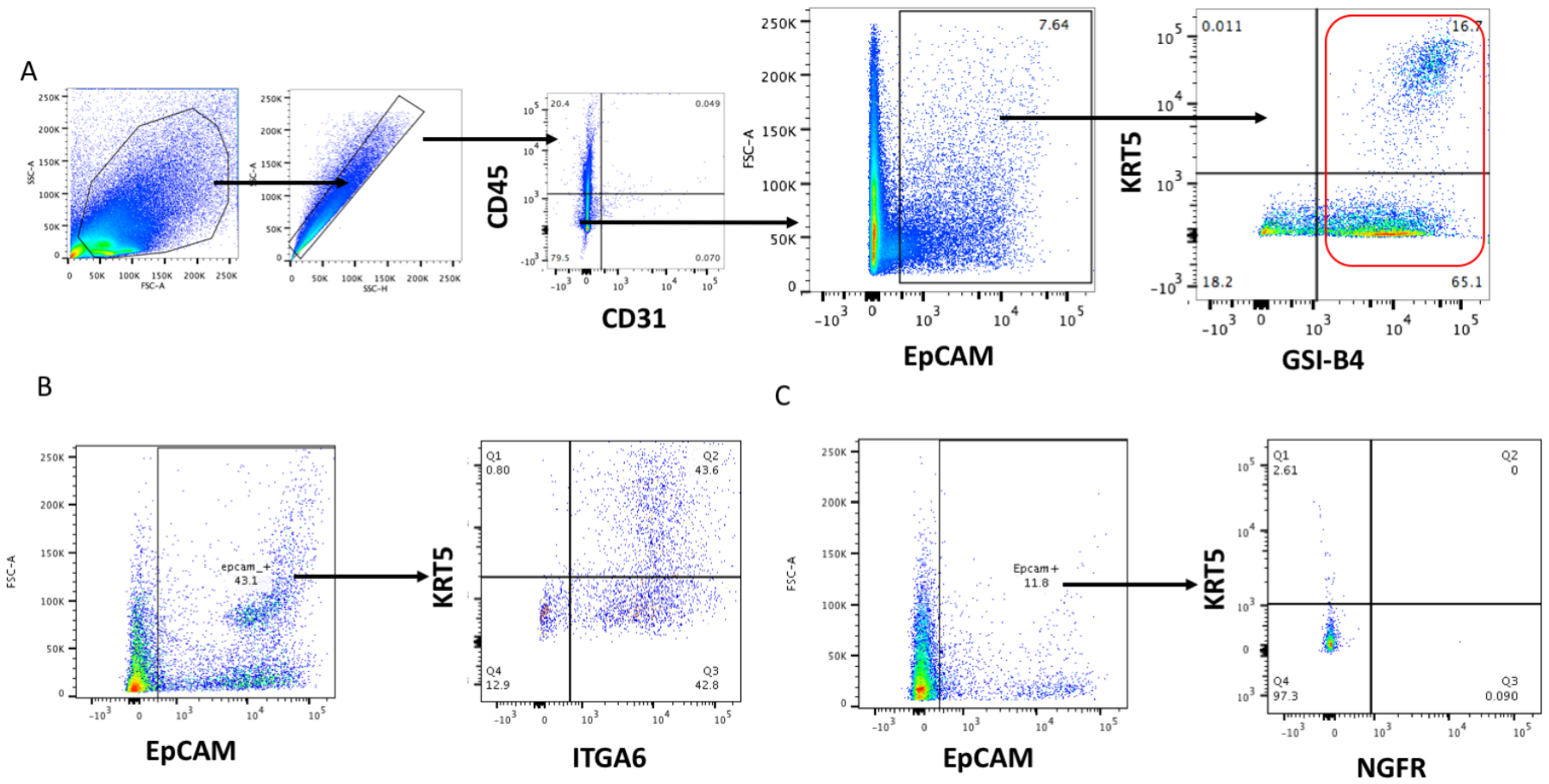
A
CD45
CD31
20.4
0.049
79.5
0.070
EpCAM
7.64
KRT5
GSI-B4
0.011
16.7
18.2
65.1
B
EpCAM
epcam_+
43.1
KRT5
ITGA6
Q1
0.80
Q2
43.6
Q4
12.9
Q3
42.8
C
EpCAM
Epcam+
11.8
KRT5
NGFR
Q1
2.61
Q2
0
Q4
97.3
Q3
0.090

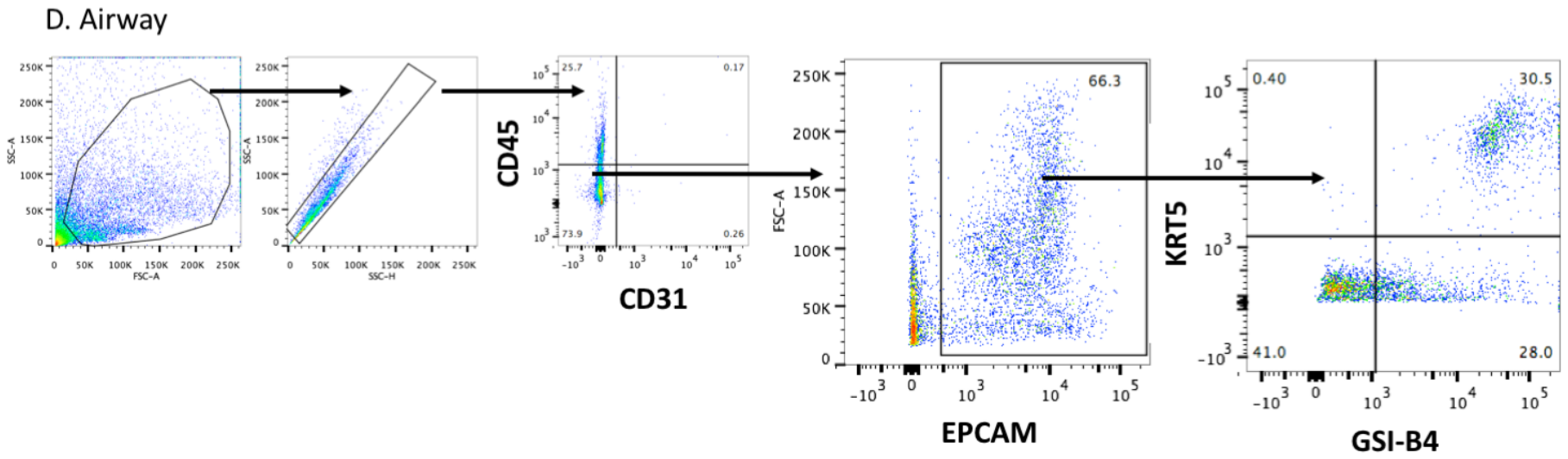

Figure 3-9 KRT5+ cells can be enriched for by ITGA6.

Fresh enzymatically isolated middle ear cells were made into a single cell suspension and then analysed for potential markers of KRT5+ cells. A. Cells that are KRT5+ are also GSI-B4+, but some GSI-B4+ are KRT5- with only 20% of EpCAM+GSIB4+ cells expressing KRT5 (Representative image from n = 3 mice). B. ITGA6 was a more useful extracellular marker for basal cells with approximately half the EpCAM+ITGA6+ population expressing KRT5. (Representative image from n = 4 mice) C. NGFR was expressed by very few EpCAM+ cells. D. Mouse trachea was used to check the protocol and the level of GSI-B4 based enrichment of KRT5+ cells was comparable to those of Rock et al., 2009.[94] (Representative image n = 3 mice). Antibodies used were CD31:APC; CD45:PerCPCy5.5; EPCAM:APC-Cy7; GSIB4:Qdot605; CK5:AF488., ITGA6:PE, NGFR:PE

Chapter 4 Changes in middle ear epithelial characteristics in an *fbxo11* mutant mouse model of otitis media

The Jeff mouse is a single gene mouse model of otitis media. Identified from an unbiased N-ethyl-N-nitrosourea mutagenesis screen, Jeff heterozygotes *(Fbxo11$^{Jf/+}$)* have a non-conservative glutamine to leucine change at amino acid 491 in exon 13 of the *fbxo11* gene [48]. These mice were found to have a reduced Preyer reflex (ear flick in response to sound) [127] and a conductive hearing loss[47]. This was caused by a bilateral otitis media that had developed in all mice by 3 weeks of age, even when the mice were grown in pathogen free conditions. As this weaning age of 21 days is the age at which the middle ear cavity is developed in mice, there is no developmental stage without an otitis media and a conductive hearing loss. The bilateral otitis media was shown by a middle ear histology that showed a fluid filled cavity with hyperplasia of the mucosal lining and a conductive hearing loss seen on auditory brain stem response testing. Much is now understood about the genetic basis of this model as well as the signalling pathways, in particular the TGF-ß and hypoxia pathways, that are affected by the Jeff *Fbxo11* mutation [53].

Multiple mouse models of otitis media exist [12,50] but mice with mutations in *Fbxo11* such as Jeff are particularly appealing as they are non-syndromic so do not develop otitis media solely due to anatomical features and also do not demonstrate other pathology. Furthermore, the role of the *Fbxo11* gene in otitis media has been confirmed in human genome wide association studies analysing recurrent otitis media, severe otitis media, and chronic otitis media with effusion [51,52]. However, as yet, the cell biology underlying the mucosal remodelling seen in Jeff mice with otitis media has not been fully explored.

Another mouse model of otitis media, the *Tbx1/+* mouse, shows a global mucosal remodelling in otitis media but certain middle ear regions demonstrate these epithelial hyperplastic changes more so than other regions – this is seen particularly in the hypotympanum and promontory akin to changes seen in COME in humans[99]. In addition, immunohistochemistry of the dorsal neural crest-derived regions in *Tbx1/+* mice with otitis media shows an increase in

the number of KRT5+ cells found here compared with the same region in unaffected mice. Epithelial remodelling therefore seems to be seen in focal areas of the middle ear and it is unclear why this is the case.

Thus, whilst it seems likely that otitis media involves cellular remodelling, the nature and cellular dynamics of this remodelling, as well as the role this remodelling has in in chronic or recurrent otitis media is unknown. Of note, as the expression of FBXO11 is identified in the middle ear epithelium between E18.5 and P21 before declining by P28[48], it suggests that at least in the *Fbxo11*$^{Jf/+}$ mouse model of chronic otitis media, there may be some abnormal developmental process that predisposes the middle ear to chronic disease. One hypothesis is that the progenitor cells in the middle ear epithelium lack an ability to proliferate or differentiate appropriately, or it may be that they cannot respond appropriately to stimuli such as hypoxia (for example as a result of Eustachian tube dysfunction) and respond with an aberrant remodelling response.

This chapter aims to explore whether there are changes in number, location and function of KRT5+ cells in the validated Jeff mouse model of chronic otitis media to help elucidate the impact of *Fbxo11* Jeff mutation in the pathogenesis of chronic otitis media

4.1 Jeff *Fbxo11*$^{Jf/+}$ mice with otitis media show middle ear mucosal hyperplasia

Whilst it has been shown that middle ear mucosal hyperplasia and cellular remodelling occurs in the Jeff mouse[48], it has not been specifically studied to see whether this remodelling is throughout the middle ear epithelium or whether there is a more region specific remodelling restricted to the dorsal or ventral epithelium (reflecting the different embryological origins of these tissues in mice and akin to the regional changes seen in the *Tbx1/*+ mouse). To answer this, histological sections from adult *Fbxo11*$^{Jf/+}$ mice were compared with *Fbxo11*$^{+/+}$ controls.

The middle ear of *Fbxo11*$^{Jf/+}$ mice with otitis media had fluid present in the cavity and demonstrated mucosal hyperplasia. This hyperplasia was global with a relative increase visible in both dorsal (albeit less obviously seen) and ventral regions of the middle ear in *Fbxo11*$^{Jf/+}$ mice compared with *Fbxo11*$^{+/+}$*.* This suggests remodelling occurs throughout the middle ear epithelium. This was seen across multiple sections and in multiple mice (Figure 4-1).

Therefore *Fbxo11*$^{Jf/+}$ mice demonstrate middle ear epithelial hyperplasia throughout the middle ear cavity. Tucker and colleagues have shown that there is an increase in the staining for KRT5+ cells in *Tbx1/*+ mouse model of otitis media [99]. The next step is to identify whether there are such changes in the number and distribution of KRT5+ progenitor cells that could underlie the remodelling seen in *Fbxo11Jf/+ mice*.

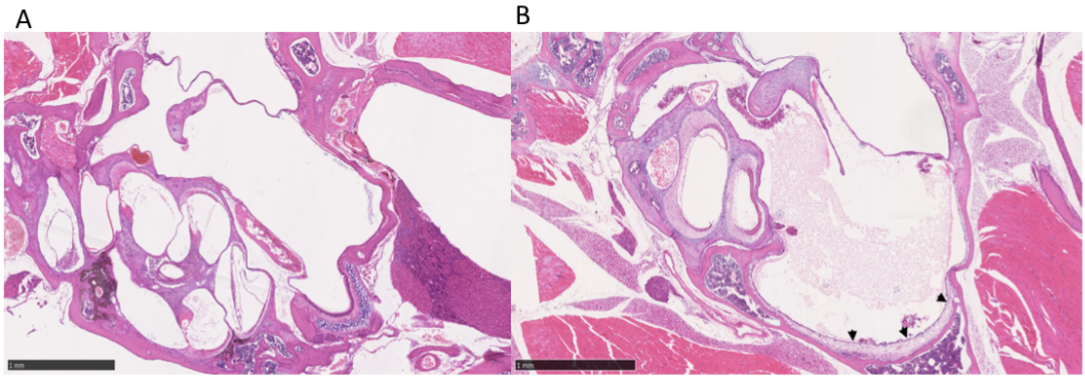

Figure 4-1 Middle ear mucosal remodeling is seen in *Fbxo11*$^{Jf/+}$ mutant mice with chronic otitis media

Middle ear mucosal remodeling is seen in chronic otitis media. Mice of 12 weeks of age were used for histological sections. A. Wild type control Fbxo11+/+ mice had a clear middle ear with minimal epithelial thickening. B. The middle ear was filled with fluid and there was a visible increase in the thickness of the mucosa both ventrally (black arrowheads) and dorsally in *Fbxo11*$^{Jf/+}$ mutant mice with chronic otitis media (n = 3 mice of each genotype)

4.2 *Fbxo11*$^{Jf/+}$ mice show a relative increase in KRT5+ cells particularly in the dorsal middle ear epithelium

Cellular remodelling occurs in epithelial linings secondary to proliferation and differentiation of local tissue resident cells with progenitor potential. KRT5+ cells are thought to be one of the progenitor cells of the middle ear and the proliferative and differentiation capacity identified in the previous chapter supports this hypothesis. These cells are found in both dorsal and ventral endoderm-derived epithelium but there seems to be trend towards a higher proportion being present ventrally as shown earlier in Chapter 3. This asymmetric distribution has also been found to some extent by others[99] and is thought to be a result of the differing embryological origin of the dorsal and ventral middle ear[72]. In otitis media, however, as studied using the *Tbx1/*+ mouse model[128,129], KRT5+ cells are found in regions such as the lining overlying the cochlea, whereas they are not normally present in this location in middle ear tissue from healthy controls[99]. To explore whether similar changes in the proportion and distribution of KRT5+ cells are also seen in the Jeff model of otitis media, middle ear epithelial cells from *Fbxo11*$^{Jf/+}$ and *Fbxo11*$^{+/+}$ mice were analysed using flow cytometry.

Mice under terminal anaesthesia were decapitated, skinned and the bulla dissected as described previously. Enzymatically isolated mouse middle ear epithelial cells (MMEC) were used to generate a single cell suspension which was stained for EpCAM and KRT5. As before, CD31+CD45+ cells were excluded from analysis (to remove endothelial and immune cells) using a negative gating strategy. There was a trend towards an increase in the proportion of KRT5+ cells seen in *Fbxo11*$^{Jf/+}$ mutant mice compared with controls (Figure 4-2).

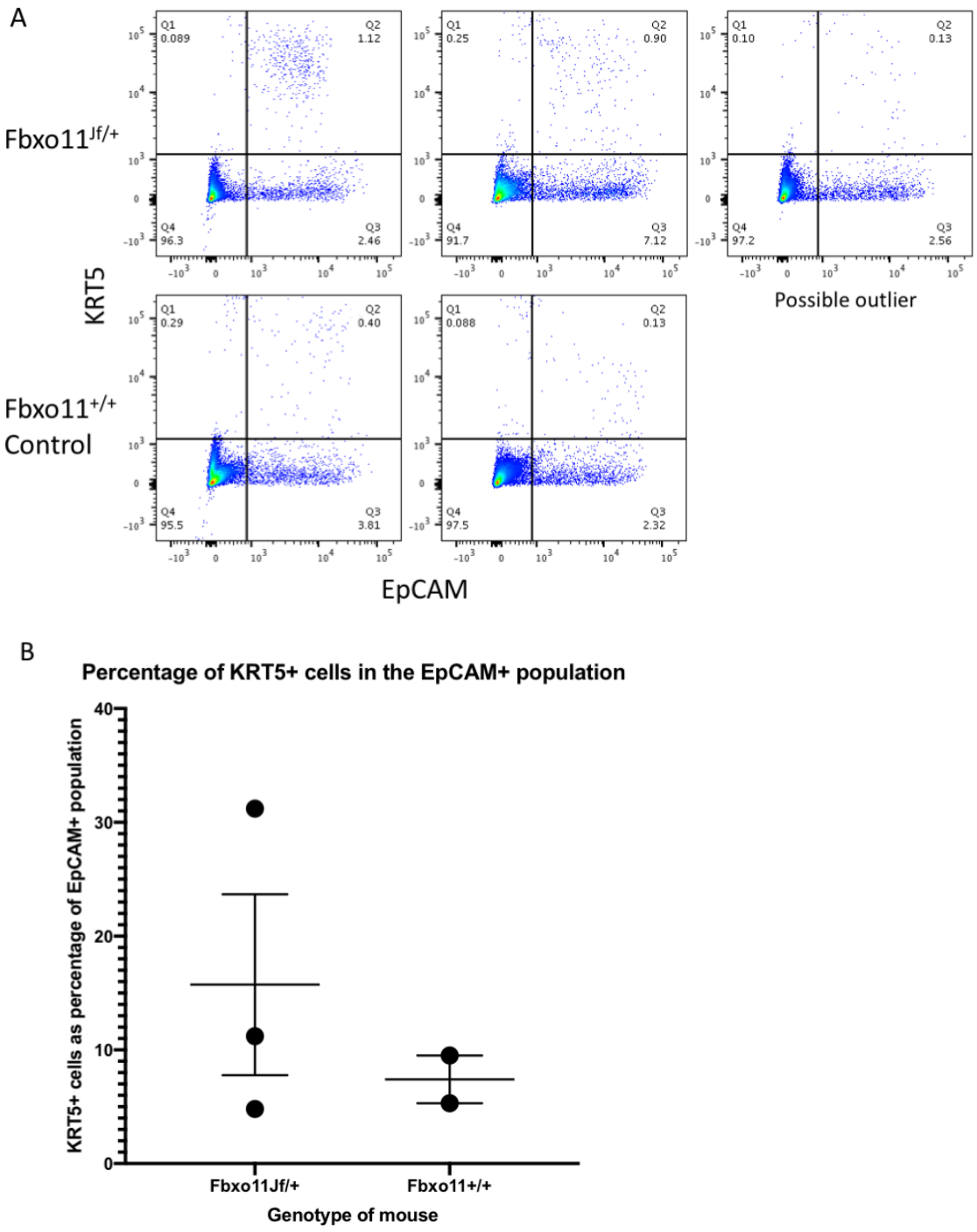

Figure 4-2 *Fbxo11*$^{Jf/+}$ mice show global increase in KRT5+ cells.

Flow cytometry was performed on *Fbxo11*$^{Jf/+}$ (n=3, top panels) and controls (n=2, lower panels) to analyse the number of KRT5+ cells in the entire bulla. Each panel represents one mouse. EpCAM is on the x-axis as an epithelial marker. KRT5 is on the y-axis. *Fbxo11*$^{Jf/+}$ have 31.2%, 11.2% and 4.8%

EpCAM+KRT5+ cells (upper right quadrant). Control mice have 9.5% and 5.3% KRT5+EpCAM+ cells. B. On average, *Fbxo11*$^{Jf/+}$ mice have more EpCAM+KRT5+ cells (15.73%) than control mice (7.40%) but this was not statistically significant (p=0.48, unpaired t-test, two-tailed). The *Fbxo11*$^{Jf/+}$ mouse in the top right may reflect a genotyping error or biological variation.

To explore whether any small increase in KRT5+ cells was hidden due to a dorsal or ventral region specific change in KRT5+ proportions, flow cytometry was performed on separate dorsal and ventral regions of the bulla from a *Fbxo11*$^{Jf/+}$ mutant mouse and a control *Fbxo11*$^{+/+}$ mouse (Figure 4-3). In the *Fbxo11*$^{+/+}$ mouse without otitis media the dorsal region contains few cells and there was no discernible positive population of KRT5+ cells. The ventral region had KRT5+ cells making up 7.78% of the EpCAM+ population. In *Fbxo11*$^{Jf/+}$ mutant mouse, there is a more discernible KRT5+ population seen in the dorsal middle ear derived cells constituting 18.3% of the EpCAM+ population. KRT5+ cells constituted 8.86% of the ventral epithelium derived cells in mice with *Fbxo11*$^{Jf/+}$ otitis media, comparable with the proportion in the *Fbxo11*$^{+/+}$ control mouse.

Whilst these findings align with the embryological dorsoventral asymmetry of the middle ear bulla, further biological and technical replicates are necessary to confirm these findings and the impact on proliferation and differentiation.

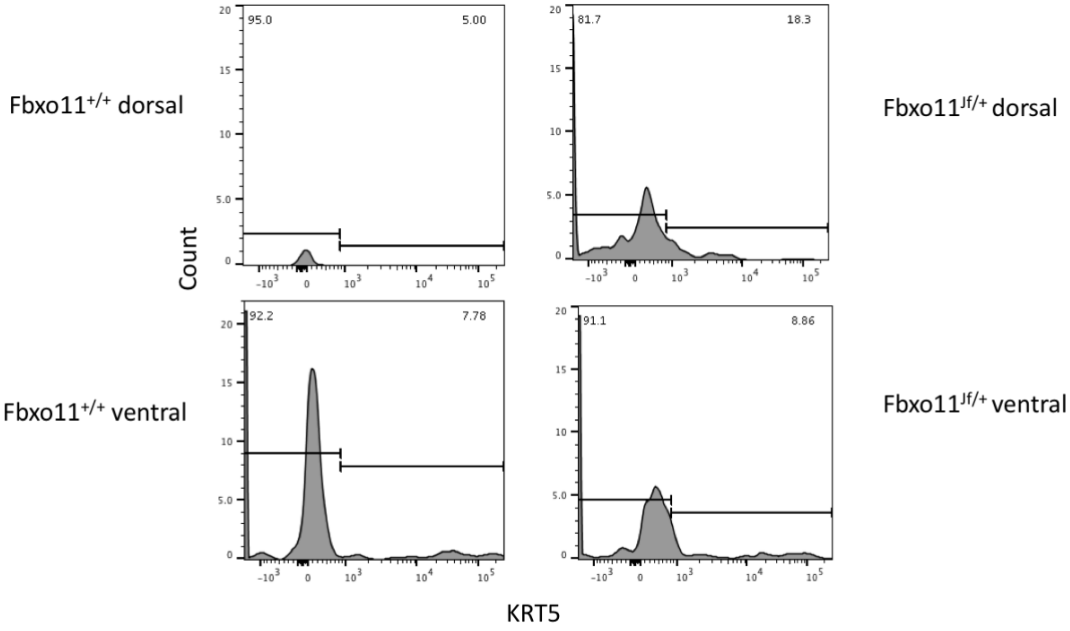

Figure 4-3 *Fbxo11*$^{Jf/+}$ mice show increased proportion of KRT5+ cells dorsally.

Flow cytometry was performed on one mouse of each genotype to assess whether there may be a difference in the number of KRT5+ cells. Whilst in Fbxo11+/+ KRT5+ cells were predominantly found ventrally making up 7.78% of the epithelium, dorsally it was difficult to find a population and there were fewer cells overall. In Fbxo11Jf/+ KRT5+ cells comprised 18.3% of the epithelium and more cells were found dorsally (n = 1 mouse of each genotype).

This increase in dorsal regions could be due to KRT5+ cell migration, clonal expansion of KRT5+ progenitors, or clonal proliferation followed by partial commitment of a higher order stem cell into KRT5+ cells. To see whether KRT5+ cells are more proliferative in otitis media, cell cycle analysis was performed using Hoechst-33342. If there was more proliferation evident in KRT5+ cells in *Fbxo11*$^{Jf/+}$ mutant mice with chronic otitis media compared with controls, this would suggest this is the proliferative population and add weight to this hypothesis, rather than to the alternative hypothesis of KRT5+

progenitor migration or expansion of a higher order stem cell into less pluripotent KRT5+ progenitors.

Enzymatically isolated middle ear epithelial cells from *Fbxo11*$^{Jf/+}$ mutant mice and controls were analysed on a dorsal and ventral region specific basis using the DNA marker Hoechst-33342 for cell cycle analysis. Results of this assay were inconclusive as the Hoechst-33342 staining did not provide suitable results for cell cycle analysis with difficulty in ascertaining peaks and each phase of the cycle on the histogram (Figure 4-4).

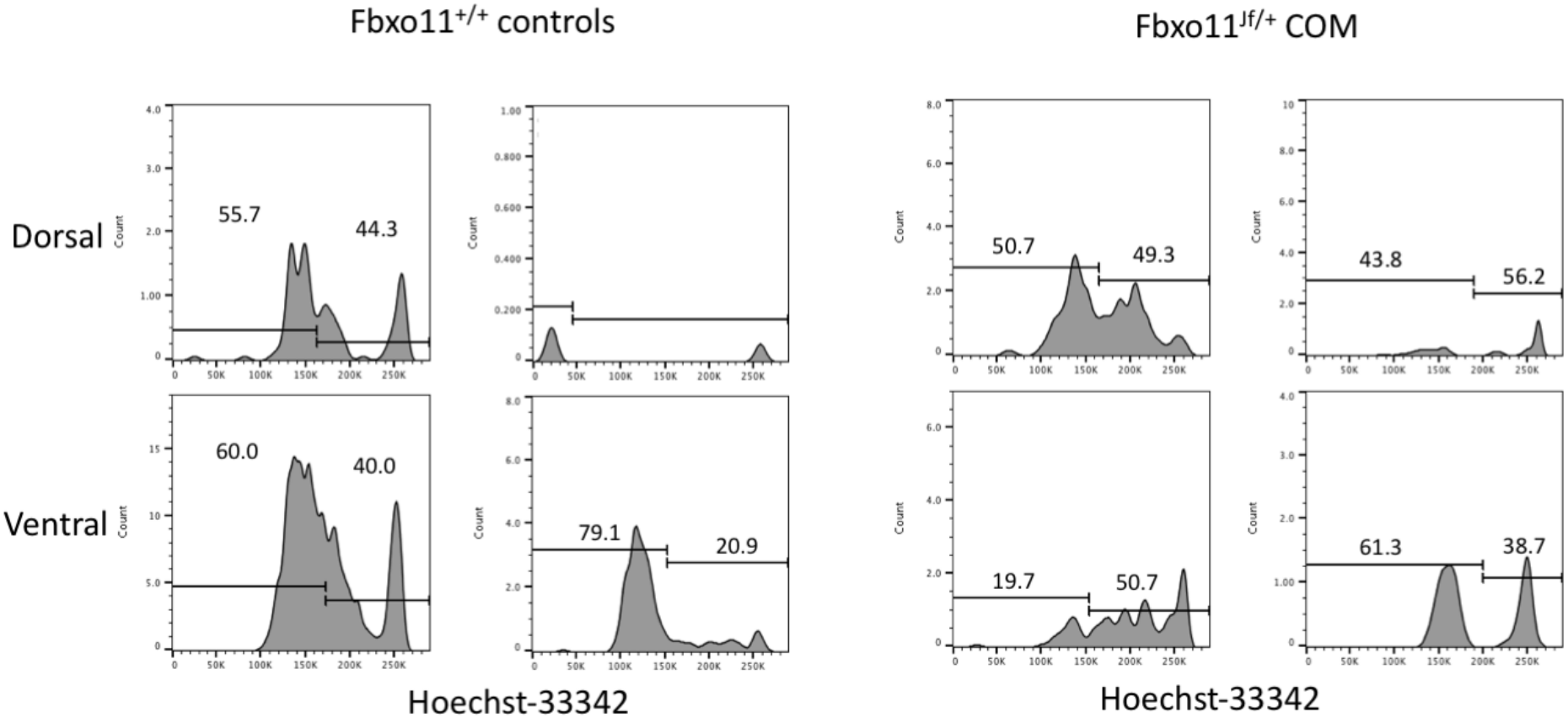

Figure 4-4 Cell cycle analysis of region-specific middle ear epithelium.

Primary isolated middle ear cells were analysed using flow cytometry. CD31-CD45- populations were removed and EpCAM+KRT5+ populations were analysed for G1/S/G2M phase of cell cycling using Hoechst-33342. Each column of panels represents one mouse with upper panels being dorsal and lower panel being ventral region epithelium. 2 mice of each genotype were analysed. Peaks were difficult to ascertain consistently on analysis and as such it was not possible to assign reliable proportions to G1, S and G2m phases of the cell cycle (n.= 2 mice of each genotype).

Taken together, although not significant, these results suggest there may be an increase in the relative proportion of KRT5+ progenitors, particularly in the dorsal middle ear epithelium, the *Fbxo11*$^{Jf/+}$ model of COME. Since *Fbxo11*$^{Jf/+}$ mice develop chronic otitis media with effusion even in specific pathogen free conditions, one hypothesis is that there may an intrinsic problem with the progenitor cell function which results in an inflammatory epithelial environment hence ongoing otitis media. Alternatively, it may be that progenitor cells respond abnormally to stimuli that would normally only cause transient inflammation, for example, hypoxia secondary to eustachian tube occlusion. The first step in studying which of these mechanisms is responsible is to explore whether there are any changes to progenitor cell function in the diseased mouse middle ear.

4.3 *Fbxo11*$^{Jf/+}$ show a reversal of the normal dorsoventral asymmetry in colony forming ability

To study the function of progenitor cells from healthy middle ears and from mice with otitis media, colony forming assays were performed using middle ear epithelial cells from *Fbxo11*$^{Jf/+}$ and *Fbxo11*$^{+/+}$ mice (n=3 heterozygotes n=2 wild type). Mice were euthanised and otitis media was visually confirmed by microscopic inspection. Middle ear epithelial cells were isolated as described previously. Cells were seeded in technical triplicates in 6-well plates for 2 weeks prior to fixing and staining to assess colonies.

There was no significant difference in mean colony forming efficiency (0.037% for *Fbxo11*$^{Jf/+}$ and 0.028% for *Fbxo11*$^{+/+}$, p=0.52) or in mean colony size (0.023cm^2 for *Fbxo11*$^{Jf/+}$ and 0.016cm^2 for *Fbxo11*$^{+/+}$, p=0.058) (Figure 4-5A). However, *Fbxo11*$^{Jf/+}$ mice with chronic otitis media had a sub-population of cells that resulted in very large colonies present that were not seen in *Fbxo11*$^{+/+}$, mice. This is visible as a positive skew in the distribution of colony areas (Figure 4-5B). Whilst such outlying colonies were also seen earlier in wild type B6 mice, these outliers are seen moreso in *Fbxo11*$^{Jf/+}$ mice with chronic otitis media than in littermate controls.

Others have shown that in otitis media, KRT5+ cells are found in regions of the middle ear where they are normally not present[99]. The flow cytometry data also suggest this to be the case in *Fbxo11*$^{Jf/+}$ mice. To verify whether there is a functional effect of this change in progenitor distribution, dorsal and ventral bulla were dissected separately from *Fbxo11*$^{Jf/+}$ mice and assessed for colony forming ability on a region-specific basis (n = 4 of each genotype). There was no difference in mean colony forming efficiency in *Fbxo11*$^{Jf/+}$ mice (dorsal 0.067%, ventral 0.060%, p = 0.88) (Figure 4-6A) but 3 out 4 mice had the sub-population of cells that form relatively large colonies present dorsally rather than ventrally with the positive area skew being more marked dorsally rather than ventrally (Figure 4-6C and D). Two *Fbxo11*$^{Jf/+}$ mice also showed outlying colonies larger (>0.30cm^2) than any other colonies seen. In contrast in *Fbxo11*$^{+/+}$ mice, a relatively large colony sub-population is seen in ventral region derived cells alone with a positive skew in area distributions seen.

The presence of a sub-population of dorsal progenitors with large-area colony forming ability could be due to a KRT5+ progenitor with high proliferative ability, however the proliferation data from the cell cycle analysis is inconclusive. As the cells have been found only in some of the mice, this may also reflect chance sampling of these cells in these mice alone from a range of cells with varying progenitor potential that all the middle ear epithelia possess.

In summary, it seems there is a trend towards an increase in the number of large colony forming KRT5+ cells in *Fbxo11*$^{Jf/+}$ mice dorsally compared with ventrally and this is the reverse trend of the situation seen in control *Fbxo11*$^{+/+}$ mice, although neither reached statistical significance. The next question is whether there are changes in differentiation potential.

A

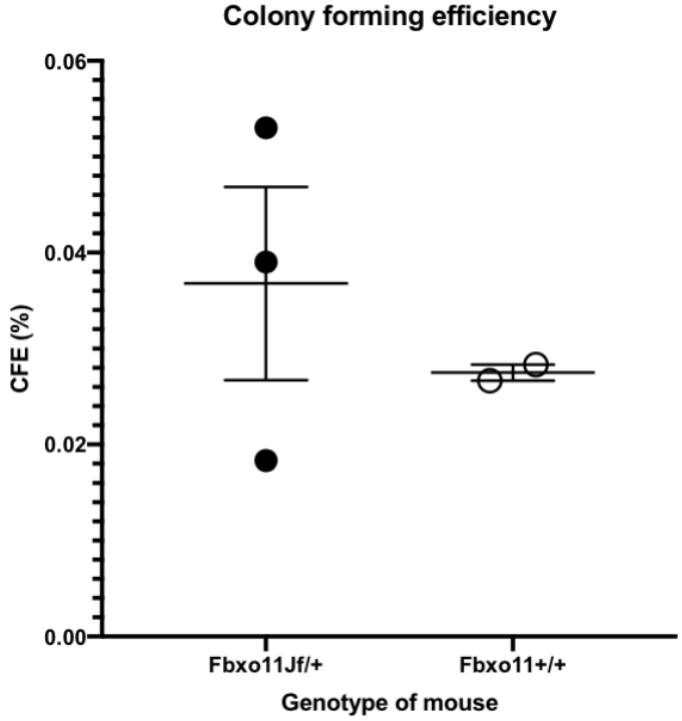
Colony forming efficiency
0.06
0.04
0.02
0.00
CFE (%)
Fbxo11Jf/+
Fbxo11+/+
Genotype of mouse

B

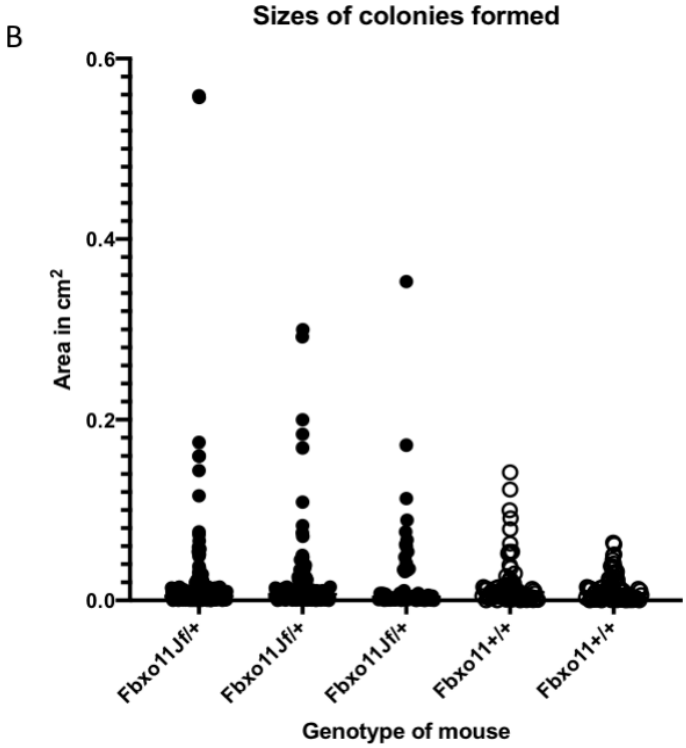
Sizes of colonies formed
0.6
0.4
0.2
0.0
Area in cm2
Fbxo11Jf/+
Fbxo11Jf/+
Fbxo11Jf/+
Fbxo11+/+
Fbxo11+/+
Genotype of mouse

Figure 4-5 Middle ear epithelial cells from *Fbxo11*$^{Jf/+}$ mutant mice show colony forming ability with a CFE of 0.037%

Middle ear epithelial cells from *Fbxo11*$^{Jf/+}$ mice have similar colony forming efficiency but positive skew in area of colonies. A. Middle ear epithelial cells from *Fbxo11*$^{Jf/+}$ mice have a colony forming efficiency of 0.037% whereas middle ear epithelial cells from *Fbxo11*$^{+/+}$ show a colony forming efficiency of 0.028%. There is no significant difference ($p = 0.8$, Mann-Whitney-U, two-tailed, n = 3 *Fbxo11*$^{Jf/+}$ *n*= 2 *Fbxo11*$^{+/+}$). B. In the area of colonies formed, *Fbxo11*$^{Jf/+}$ mice (filled circles) have some middle ear epithelial cells that give rise to colonies with large areas and these are not seen in middle ear epithelial cells from *Fbxo11*$^{+/+}$ mice (open circles). There is no significant difference in the mean area of the colonies formed (*Fbxo11*$^{Jf/+}$ 0.022cm^2, *Fbxo11*$^{+/+}$ 0.016cm^2, $p = 0.2$, Mann-Whitney-U test, two-tailed, error bars show SEM).

A

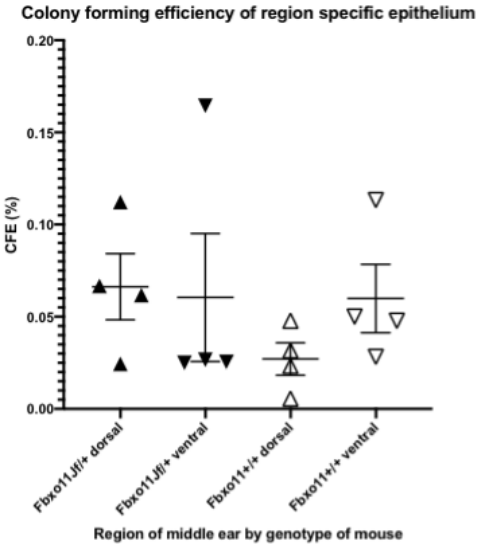
Colony forming efficiency of region specific epithelium
CFE (%)
0.20
0.15
0.10
0.05
0.00
Fbxo11Jf/+ dorsal
Fbxo11Jf/+ ventral
Fbxo11+/+ dorsal
Fbxo11+/+ ventral
Region of middle ear by genotype of mouse

B

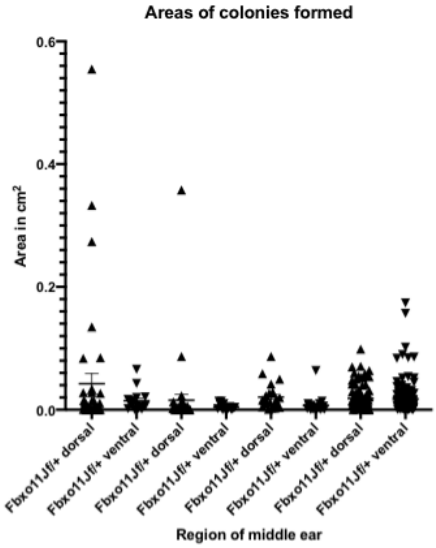
Areas of colonies formed
Area in cm²
0.6
0.4
0.2
0.0
Fbxo11Jf/+ dorsal
Fbxo11Jf/+ ventral
Fbxo11Jf/+ dorsal
Fbxo11Jf/+ ventral
Fbxo11Jf/+ dorsal
Fbxo11Jf/+ ventral
Fbxo11Jf/+ dorsal
Fbxo11Jf/+ ventral
Region of middle ear

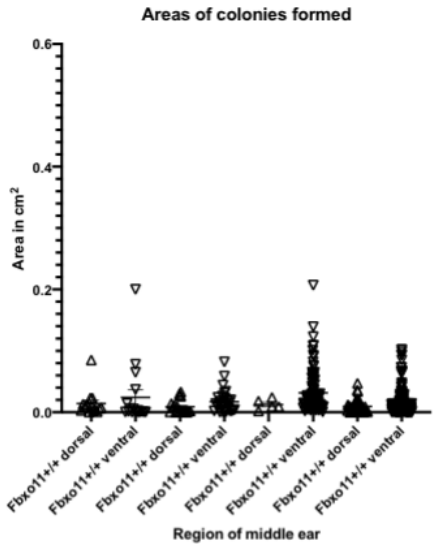
Areas of colonies formed
Area in cm²
0.6
0.4
0.2
0.0
Fbxo11+/+ dorsal
Fbxo11+/+ ventral
Fbxo11+/+ dorsal
Fbxo11+/+ ventral
Fbxo11+/+ dorsal
Fbxo11+/+ ventral
Fbxo11+/+ dorsal
Fbxo11+/+ ventral
Region of middle ear

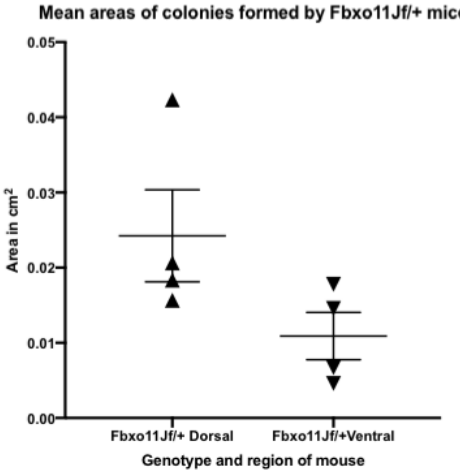
Mean areas of colonies formed by Fbxo11Jf/+ mice
Area in cm²
0.05
0.04
0.03
0.02
0.01
0.00
Fbxo11Jf/+ Dorsal
Fbxo11Jf/+Ventral
Genotype and region of mouse

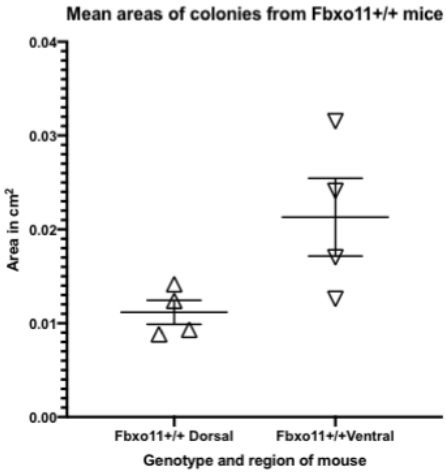
Mean areas of colonies from Fbxo11+/+ mice
Area in cm²
0.04
0.03
0.02
0.01
0.00
Fbxo11+/+ Dorsal
Fbxo11+/+Ventral
Genotype and region of mouse

C

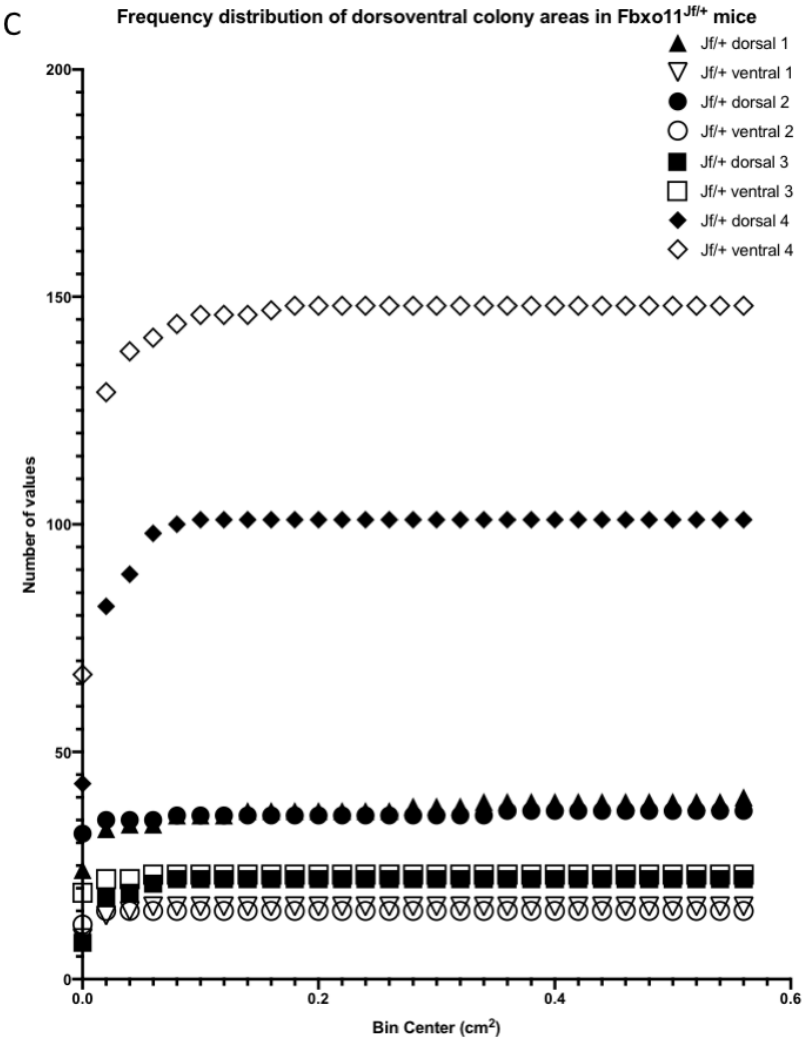
Frequency distribution of dorsoventral colony areas in Fbxo11Jf/+ mice
Jf/+ dorsal 1
Jf/+ ventral 1
Jf/+ dorsal 2
Jf/+ ventral 2
Jf/+ dorsal 3
Jf/+ ventral 3
Jf/+ dorsal 4
Jf/+ ventral 4
Number of values
Bin Center (cm2)

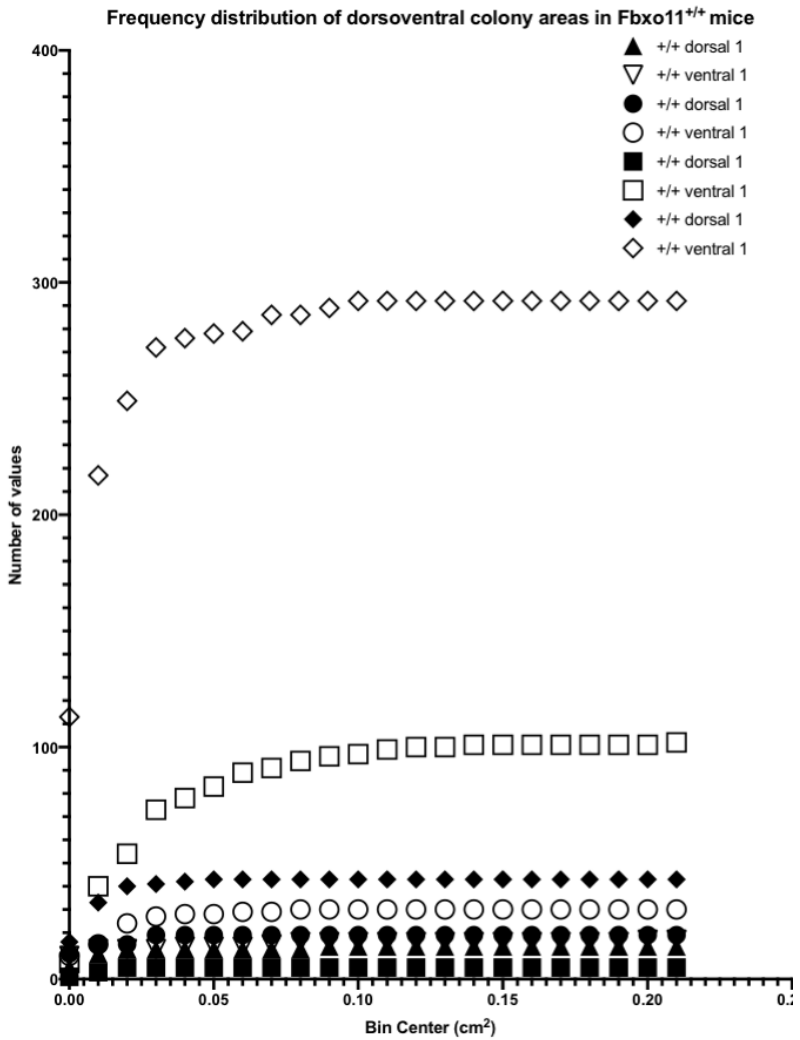
Frequency distribution of dorsoventral colony areas in Fbxo11+/+ mice
+/+ dorsal 1
+/+ ventral 1
+/+ dorsal 1
+/+ ventral 1
+/+ dorsal 1
+/+ ventral 1
+/+ dorsal 1
+/+ ventral 1
Number of values
Bin Center (cm2)

Figure 4-6 *Fbxo11*$^{Jf/+}$ and *Fbxo11*$^{+/+}$ mice have opposite dorsoventral asymmetry in the size of colonies formed by middle ear epithelial cells.

Larger colonies are found more often dorsally in Fbxo11$^{Jf/+}$ mice and ventrally in Fbxo11$^{+/+}$ mice. A. Cells from dorsal and ventral region epithelium of the middle ear were seeded for colony forming assays. No difference was seen in mean CFE between regions in either genotype of mice (*Fbxo11*$^{Jf/+}$ 0.067% dorsal; 0.060% ventral, p = 0.89, Mann-Whitney-U, two-tailed) (*Fbxo11*$^{+/+}$ 0.027 % dorsal; 0.060% ventral, p = 0.14, Mann-Whitney-U, two-tailed) (n = 4 mice of each genotype). Error bars show SEM. B. Top graph show areas of colonies formed from middle ear epithelial cells by region for *Fbxo11*$^{Jf/+}$ mutant mice (left) and *Fbxo11*$^{+/+}$ controls (right). Graphs below show mean middle ear epithelial colony sizes for each genotype. There was no significant difference in mean colony area for *Fbxo11*$^{Jf/+}$ (dorsal = 0.024cm^2, ventral = 0.011cm^2, p = 0.057, Mann-Whitney-U, two-tailed) or Fbxo11+/+ (dorsal = 0.011cm^2, ventral = 0.021cm^2, p = 0.057, Mann-Whitney-U, two-tailed). (n=4 mice of each genotype) Error bars show SEM. C. Cumulative frequency distribution of areas seen shows a reversal of the positive skew in areas is seen with *Fbxo11*$^{Jf/+}$ mice (left graph) having larger colonies predominantly in epithelial cells from dorsal middle ear whereas *Fbxo11*$^{+/+}$ controls have larger colonies in epithelial cells from ventral middle ear.

4.4 *Fbxo11*$^{Jf/+}$ middle ear progenitor cells show abnormal differentiation at air liquid interface

To investigate whether basal cells from *Fbxo11*$^{Jf/+}$ mice middle ears have a normal bipotent differentiation capacity, cells from *Fbxo11*$^{Jf/+}$ and *Fbxo11*$^{+/+}$ mice were isolated and cultured at air-liquid interface. Following the protocol of Mulay[101], cells from 3 mice of each genotype were pooled together and seeded at a higher density of at least 100000 cells per transwell to rapidly establish a confluent monolayer of basal cells prior to stimulating differentiation. 8 transwells were seeded from each genotype. Following this, the medium in the upper chamber media was removed to expose cultures to air and the media in the lower chamber replaced with MMEC-SF (mouse middle ear epithelial cell culture media-serum free) to stimulate differentiation.

Confluent monolayers of cells with epithelial basal cell-like appearance were seen within 14 days regardless of genotype. However, once the differentiation step was performed, cells from *Fbxo11*$^{+/+}$ mice differentiated into cells with ciliated and goblet cell-like morphology previously seen over a timescale of 7-21 days. Cells from *Fbxo11*$^{Jf/+}$ mice did not show a similar differentiation pattern. Cells became more elongated and fibroblast-like in appearance and only one region of ciliation was seen in one transwell, with the remainder either not differentiating or developing a mesenchyme-like morphology (Figure 4-7).

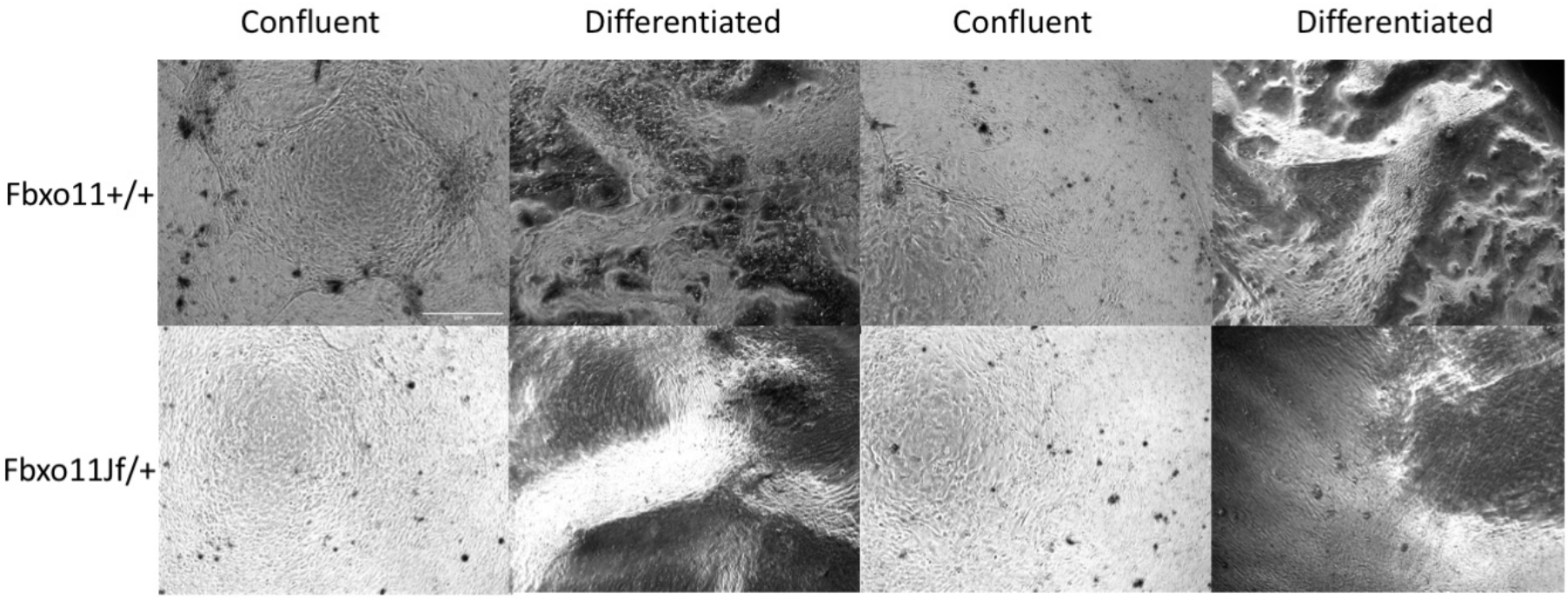
Confluent
Differentiated
Confluent
Differentiated
Fbxo11+/+
Fbxo11Jf/+

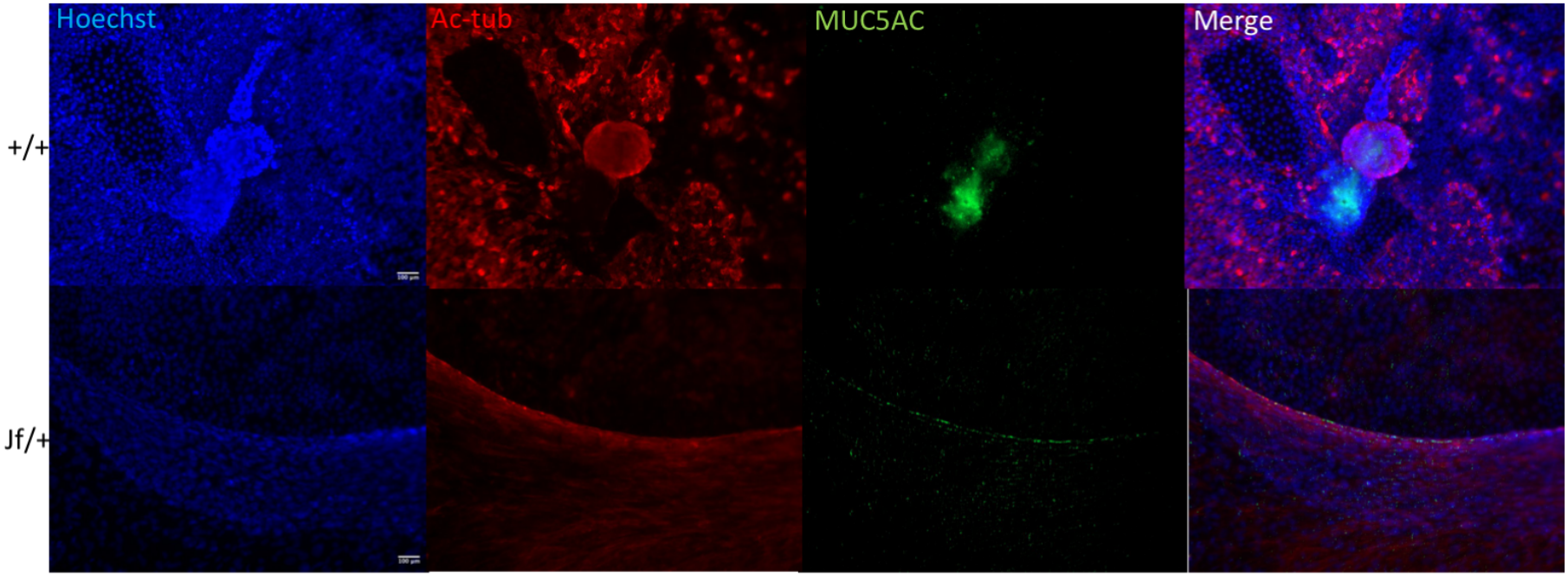

Figure 4-7 Fbxo11$^{Jf/+}$ show abnormal morphology on differentiation at air-liquid interface with few regions of goblet or ciliated cells.

Fbxo11$^{Jf/+}$ differentiate into more mesenchymal like cells at air liquid interface. Cells from Fbxo11$^{+/+}$ (top) and $^{+/-}$ (bottom) were grown at air liquid interface. At confluence all transwells that grew had epithelial like morphology with cobblestone like cellular appearance

upper figure. After differentiation was stimulated by air exposure and media change, *Fbxo11*$^{+/+}$ grew areas with pseudostratified morphology and ciliation/goblet cells, as confirmed by immunofluorescence in the lower figure (Hoechst-33342 here shown as blue, Ac-Tub-AlexaFluor 647 here shown as red, MUC5AC-AlexaFluor 488 here shown as green). Fbxo11Jf/+ however had large regions of mesenchymal appearing tissue with a fibroblast like morphology (lower panels). (n=3 mice pooled for 8 transwells per genotype)

To confirm whether this was the case and there was an intrinsic abnormality of differentiation, the air-liquid interface assay was repeated but this time without pooling using cells from individual mice (n=3 of each genotype) with technical replicates. Transwells that grew were confluent between 7-14 days. All three transwell replicates grew for 2 out of 3 *Fbxo11*$^{+/+}$ control mice and for 2 out of 3 *Fbxo11*$^{Jf/+}$ mice with chronic otitis media. Transwells from the control mice all differentiated into ciliated and non-ciliated morphology (Figure 4-8A). For *Fbxo11*$^{Jf/+}$ mice with chronic otitis media, one set of transwells showed differentiation into ciliated cells in two wells (Figure 4-8B) but mesenchymal appearance in the other well (Figure 4-8B'). The other mouse had the mesenchymal appearance as described before (Figure 4-8C). To clarify this result in differentiation potential, an assay of individual cell differentiation rather than a global pooled population of cells derived from middle ear epithelium a different assay was optimised.

A

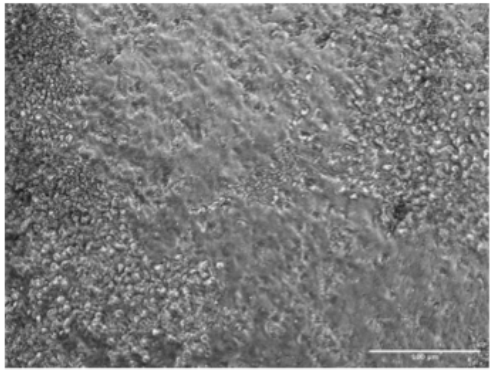

B

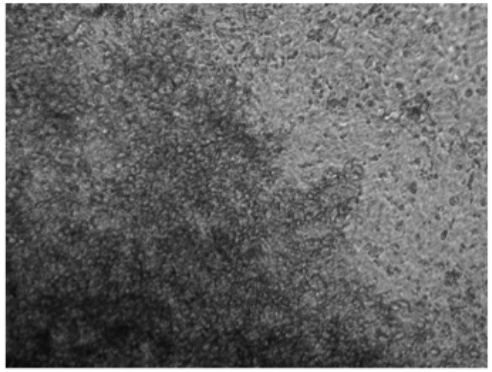

C

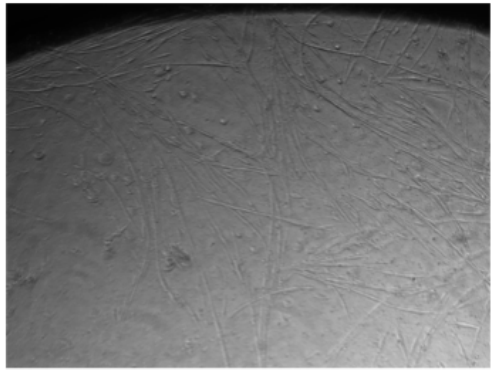

B’

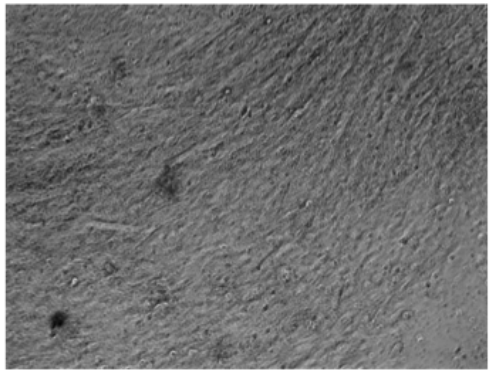

Figure 4-8 Air-liquid interface assay of non-pooled mice suggests *Fbxo11*$^{Jf/+}$ mutants have aberrant differentiation potential.

Air-liquid interface assay was repeated with cells from 3 individual mice of *Fbxo11*$^{Jf/+}$ and *Fbxo11*$^{+/+}$ control genotypes, without pooling of cells. 3 transwells were seeded with middle ear cells from each mouse. Transwells from 4 out of the 6 mice grew to confluence (2 of each genotype). Upon differentiation, progenitors from both the *Fbxo11*$^{+/+}$ control mice showed ciliated pseudostratified morphology. A. Example of normal differentiated epithelium from *Fbxo11*$^{+/+}$ middle ear cells . B. Cells from *Fbxo11*$^{Jf/+}$ mutant mice showed two morphologies. The first was normal differentiation as shown here. However, one of the transwells from the same mouse became mesenchymal in appearance as seen in B'. C. Shows a transwell of cells from the second *Fbxo11*$^{Jf/+}$ mutant with only abnormal cells seen. Scale bar shows 100μm (n =3 mice of each genotype).

4.5 3D spheroid assays offer an alternative higher throughput method of assessing progenitor cell function and modelling the middle ear

The small number of progenitor cells with large colony forming ability suggests there may be a heterogeneity of progenitor cells in the mouse middle ear and this heterogeneity changes in otitis media. This is in keeping with other epithelial surfaces where progenitor cells are grouped into three types - termed holoclones (most stem like), meroclones and paraclones (most committed to a differentiated phenotype) – depending on their subsequent clone forming ability when single cells are isolated from colonies and their proliferation potential assessed.

The air-liquid interface assay can only assess the middle ear progenitor cell function at a cell population level as it requires a confluent monolayer of progenitor cells prior to differentiation. It may be that a subpopulation of middle ear epithelial cells that form large colonies overgrow in the submerged phase of air-liquid interface and these cells may not be able to differentiate properly. To assess whether there is heterogeneity within progenitor cells in terms of differentiation ability, a different assay is required that can assess differentiation from single cells. One such assay used in airway biology that can be adapted to address this question is the 'tracheosphere assay.' Here a single cell suspension is mixed with an extra-cellular matrix -hydrogel known as Matrigel[94,130]. Each single cell has the potential to give rise to a 3D sphere of differentiated epithelium composed of all the cell types of the airway. This protocol was adapted in an attempt to generate 'spheroids' – 3D spheres derived from middle ear epithelium.

Enzymatically dissociated middle ear epithelial cells were mixed in a 1:1 ratio in growth factor reduced Matrigel at a density of 10000 cells per well and seeded into 24-well transwells. MMEC+ proliferation medium was added in the lower and upper chamber for 7-10 days to stimulate proliferation. After this period the media was replaced with MMEC-SF differentiation medium for 7 days. Two morphologies of 3D spheres were seen after differentiation was

stimulated (Figure 4-9). The first was a multicellular clump with no lumen – this was seen predominantly in transwells from *Fbxo11*$^{Jf/+}$ mice with chronic otitis media. The second was a more obvious 3D spheroid with a lumen resembling the tracheospheres seen in airway culture of spheroids – these were found in the in transwells from *Fbxo11*$^{+/+}$ control mice. Attempts at staining of these was unsuccessful but would be helpful in confirming the morphological appearances and assess for presence of ciliation and mucus secreting cells.

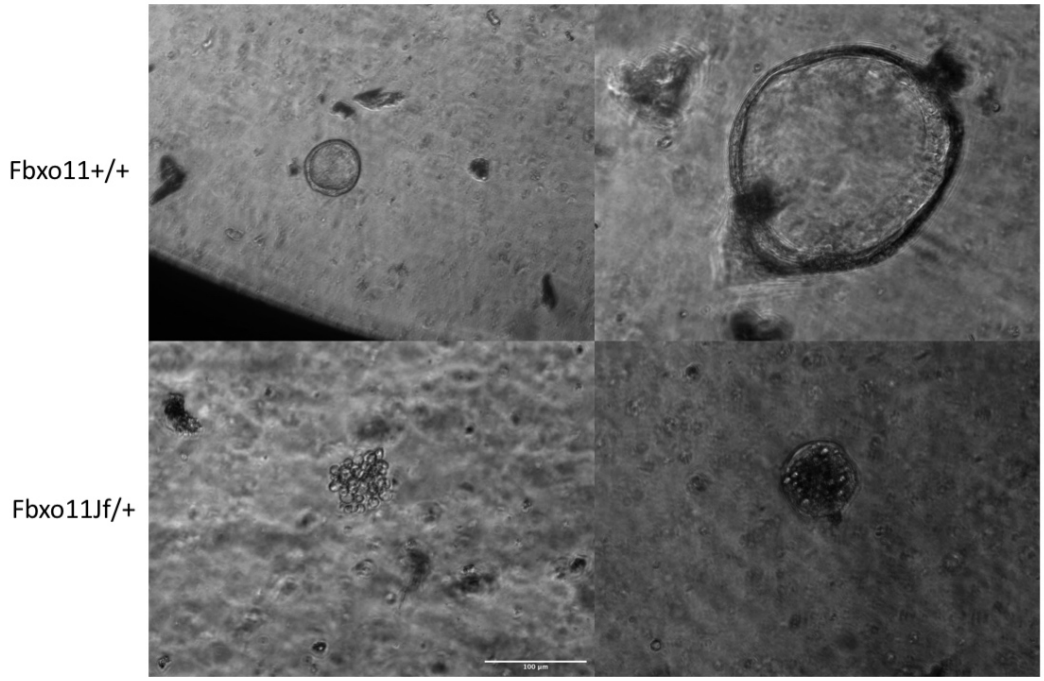

Figure 4-9 Mouse middle ear epithelial cells can give rise to 'spheroids.'

Spheroids from middle ear epithelial cells of *Fbxo11*$^{Jf/+}$ mice show abnormal morphology. A single cell suspension of primary isolated cells was cultured in Matrigel in a 24-well transwell format with proliferation media (MMEC+) for 7 days before differentiation was stimulated with MMEC-SF. Cells from *Fbxo11*$^{+/+}$ grow spheroids with conventional appearance with an outer layer of cells and a lumen (top panel), cells from *Fbxo11*$^{Jf/+}$ grew spheroids with clusters of cells with no obvious sphere like appearance or lumen. Scale bar shows 100μm. (n=3 mice pooled for technical duplicates).

4.6 Addition of Cobalt II chloride hexahydrate to mimic hypoxia by inducing HIF-1/3α reduces colony forming ability in *Fbxo11*$^{Jf/+}$ mice

Thus far it has been shown that middle ear epithelial cells from *Fbxo11*$^{Jf/+}$ mutant mice may have an intrinsic change in colony forming ability (in terms of size) and differentiation ability. It has previously been shown using pimonidazole staining in immunohistochemistry that the middle ear of *Fbxo11*$^{Jf/+}$ mice is hypoxic[57,58]. The hypoxia in *Fbxo11*$^{Jf/+}$ mice is restricted to inflammatory and immune cells in the middle ear fluid and in infiltrative cells in the mucosa but hypoxia is not seen in the mucosal lining itself. The known function of FBXO11 is ubiquitination with a subsequent breakdown of HIF-1α. As such, loss-of-function mutations in *Fbxo11* such as in the Jeff mouse would be expected to cause continued expression of HIF-1α. However, pimonidazole staining only detects hypoxia when oxygen tension is less than 1.3%. Thus, the lack of staining may be that there is a milder level of hypoxia i.e. with oxygen levels above 1.3% present in the epithelial cells, hence there is no pimonidazole staining seen. Hypoxia may also be a trigger for chronic disease, perhaps secondary to eustachian tube dysfunction for example.

To explore whether hypoxia affects *Fbxo11*$^{Jf/+}$ mice with chronic otitis media differently from *Fbxo11*$^{+/+}$ mice, a colony forming assay was performed (n= 3 mice of each genotype). After 7 days, cobalt II hexahydrate - an inducer of HIF-1/3α[131] was added to the cell culture media at a concentration of either 50 μM, 100 μM or 200 μM. After 14 days in total, cultures were fixed and stained to assess the impact of hypoxia on colony forming efficiency and colonies.

Colonies from *Fbxo11*$^{Jf/+}$ and *Fbxo11*$^{+/+}$ mice middle ear epithelial cells had a difference in dose-response sensitivity to cobalt II chloride hexahydrate exposure with a 50% reduction in colony forming efficiency at 0.00276μM of cobalt II hexahydrate for *Fbxo11*$^{Jf/+}$ and 0.0225μM for *Fbxo11*$^{+/+}$ showing middle ear epithelial cells from *Fbxo11*$^{Jf/+}$ mice are affected by cobalt II hexahydrate at a lower concentration (Figure 4-10). Of note, the sub-population of large colonies that were seen previously were not evident in either genotype.

One explanation may be that a lower level of cobalt II chloride hexahydrate is required for hypoxic induction in *Fbxo11*$^{Jf/+}$. As CFE is an assay of stem/progenitor cell readout, the results here suggest progenitor cells from *Fbxo11*$^{Jf/+}$ are more sensitive to hypoxia in terms of survival. However, this does not explain whether hypoxia affects proliferation per se. Performing CFE and proliferation assays under hypoxic conditions using a hypoxia chamber together with Western Blotting for HIF to check the level of hypoxia in the cells[118].

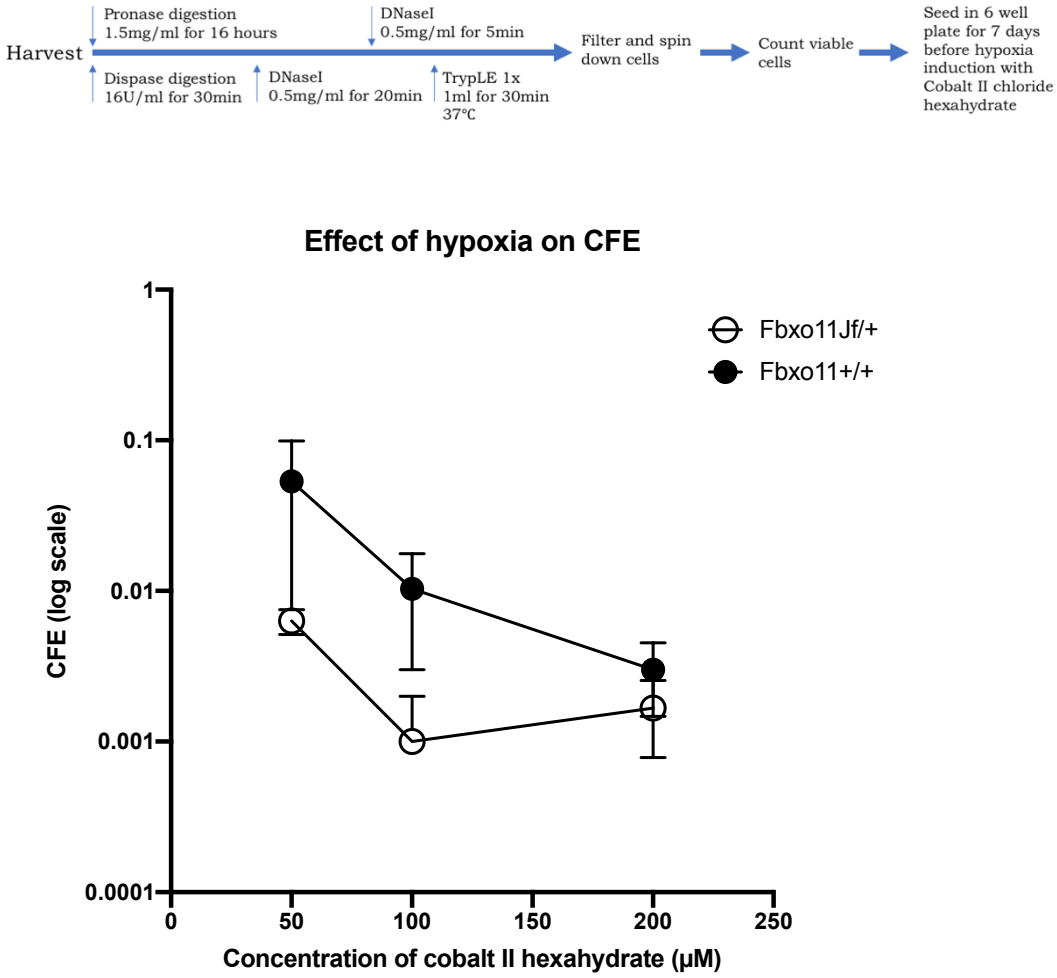

Figure 4-10 *Fbxo11*$^{Jf/+}$ show increased dose response sensitivity to HIF-1α stabilization.

Middle ear epithelial cells from *Fbxo11*$^{Jf/+}$ mutant mice and controls were cultured in media containing 50μM, 100μM or 200μM of cobalt II chloride hexahydrate to simulate hypoxic pathway activation. Both genotypes showed a reduction in colony forming efficiency with increasing concentration of cobalt II hexahydrate. Calculating regression of the curves showed that *Fbxo11*$^{Jf/+}$ middle ear epithelial cells showed a 50% reduction in CFE at a concentration

of 0.00276μM of cobalt II hexahydrate compared with 0.0225μM for *Fbxo11*$^{+/+}$ epithelial cell. (n = 3 mice of each genotype).

Summary

This chapter used the Jeff mouse model of otitis media to assess the role of KRT5+ cells may in the pathogenesis of otitis media. A number of effects have been identified but a limitation of this work is the relatively low numbers of mice used which warrants further investigation to robustly test disease specific effects.

Chapter 5 Multicolour lineage tracing of the mouse middle ear

The middle ear mucosa is a dynamic structure that contributes towards maintaining a well ventilated and clear middle ear cavity. Histological analysis of middle ear sections in humans and mice has shown that both acute and chronic otitis media result in a cellular remodelling with hyperplasia of both epithelial and stromal components. Underlying this remodelling must be the proliferation and differentiation of middle ear progenitors in response to some stimulus. As has been shown earlier, the epithelial lining of the middle ear contains keratin 5 (KRT5)+ cells that demonstrate features of progenitor cells, possess a bipotent differentiation capacity and display a dorso-ventral asymmetry of distribution in the middle ear, which is reversed in chronic otitis media.

The characterisation of progenitors can be performed using in vitro growth assays, in vivo transplantation assays to assess regenerative capacity, and in vivo lineage tracing [102,113,132]. In the middle ear, there has been particular interest in the last of these techniques with short-term and longer-term lineage tracing experiments demonstrating the presence of label-retaining cells and KRT5 positivity predominantly in the ventral regions of the ear; these studies showed KRT5+ cells have the ability to form ciliated cells[98,99]. However, whether the dorsal epithelium has a sparse population of KRT5+ during normal homeostasis as shown by Tucker and colleagues or whether it too has a comparable number of progenitors as suggested by Luo and colleagues is still debated[99,133]. The previous work in the chapters suggests that KRT5+ cells are bipotent and there may be a more sparse distribution dorsally during health that changes in COME.

It also remains unanswered how the remodelling that is seen during inflammation in chronic otitis media occurs at a cellular level. The earlier work in this thesis suggests that the dorsal epithelium does have a sparse population in normal homeostasis but during chronic otitis media in the *Fbxo11*$^{Jf/+}$ mouse model of otitis media, the dorsal population increases and progenitor cells with the ability to form large colonies are found. Whether such changes are seen in vivo remains to be answered.

Lineage tracing is now well established as a technique used to tag a target cell of interest in a way that all progeny derived from that cell also possess the same tag[132,134]. One common way to tag cells is to use a fluorescent protein such as green fluorescent protein (GFP). The number of cells tagged in such a way needs to be of a suitable 'clonal' density. This is to achieve a balance between an adequate number of cells being marked to effectively locate and visualise tagged patches of their progeny (termed clones as they are derived from a single cell) in a given region of tissue, but not marking so many cells that two neighbouring cells showing the same tag could be two individually marked cells rather than one marked cell that has divided. This density requirement is necessary both for analysis as well as the practicalities of imaging the tissue. The task of analysing how progenitor cells contribute to tissue homeostasis requires locating and visualising a density of tagged cells that is low enough for clones to form without merging but high enough to visualise multiple clones within a given field of analysis. One way to make this task easier is multicolour fluorescent lineage tracing, for example using the Confetti reporter line[107,108]. This uses four different colours, GFP, yellow fluorescent protein (YFP), red fluorescent protein (RFP) and cyan fluorescent protein (CFP), expressed at random after activation under an inducible promoter to tag the target cell of choice. This helps mitigate the difficulties of clonal density induction but also allows clonal dynamics (the mathematical analysis of number, size, shape and evolution of clones over time) to be studied for a given region. In addition, fluorescent cells allow for flow cytometric sorting of individual marked cells at a population level for transcriptomic analysis and further culturing as required.

To explore the contribution of KRT5+ cells to middle ear epithelial maintenance, KRT5-Cre^{ERT2} mice were crossed with R26R-Confetti reporter mice to generate double transgenic mice. The tamoxifen inducible expression of Cre recombinase in cells that expressed the KRT5 promoter meant KRT5+ cells will randomly express one of the four Confetti fluorophores (RFP, GFP, CFP, YFP) in a temporally restricted manner for the duration of tamoxifen exposure. After tamoxifen exposure has finished, no new progenitor cells will express fluorophores, only those KRT5+ progenitors already tagged and their

progeny (Figure 5-1). A ligand dependent Cre-mediated recombination was chosen with tamoxifen-based induction of Cre using the Cre^{ERT2} recombinase. The ER^{T2} used to minimise leakiness (inappropriate activation from endogenous oestrogen). This is owing to the triple mutant form of the human oestrogen receptor in the ER^{T2} form that prevents binding of the endogenous oestrogen ligand at physiological concentrations. Thus the receptor will only be activated by exogenous administration of tamoxifen (which is metabolised to the active 4-hydroxy-tamoxifen in vivo). Although doxycycline-based induction is also possible using mice with a different allele combination (rtTA/tetO-Cre/LoxP) based recombination, this was not chosen for two reasons. Firstly, as some cases of chronic otitis media studied are infective in nature (e.g. chronic suppurative otitis media in the Junbo model of otitis media caused by non-typeable haemophilus influenza), it was desirable to have a model that would not require antibiotic administration to allow maximum utility. Secondly, three alleles are required to generate these mice rather than the two in the KRT5-Cre^{ERT2};R26RConfetti crosses. Furthermore, to generate lineage traceable models of chronic otitis media would require mice with three alleles, as well as heterozygosity for the Jeff *Fbxo11* mutation (discussed in previous chapter). Breeding strategies to achieve this can become complex and so reducing the number of alleles required to the two allele KRT5-Cre^{ERT2} model was another benefit[134].

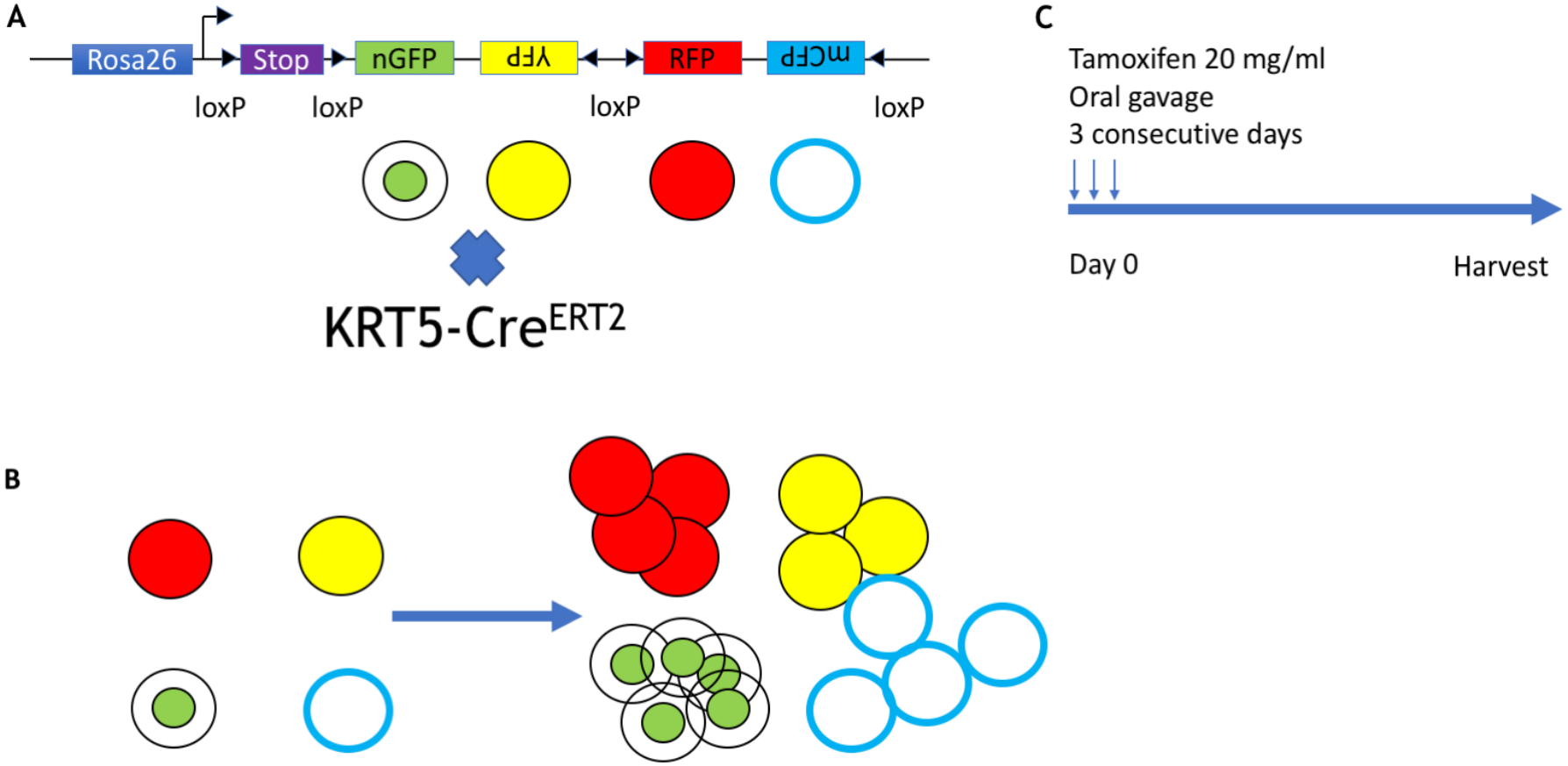
A
Rosa26
Stop
nGFP
YFP
RFP
mCFP
loxP
loxP
loxP
loxP
KRT5-CreERT2
B
C
Tamoxifen 20 mg/ml
Oral gavage
3 consecutive days
Day 0
Harvest

Figure 5-1 Lineage tracing can be used to track the progeny of a marked cell over time.

Lineage tracing methodology. This is a method to tag a progenitor cell using a fluorescent reporter protein so that all progeny of the cell will also carry the same fluorophore as the parent cell. A. Here a Brainbow 2.1 cassette under the ubiquitous Rosa26 promoter has a stop codon that is excised when combined with Cre-lox based recombination. Thus, when bred to mice that express Cre recombinase, such as the KRT5-CreERT2 mouse in which Cre is on the KRT5 promoter and inducible by tamoxifen. The resulting offspring are induced to potentially have a recombination event that will result in the random expression of GFP, YFP, RFP or CFP within the *Cre*-expressing tissues. By placing them downstream of the CAG promoter, all daughter cells, termed clones, will also express the same colour (as shown in B). C. Tamoxifen induction protocol used to activate Cre based recombination.

5.1 Rederivation of inducible lineage specific multicolour reporter lines

KRT5-Cre^{ERT2} transgenic mice on a mixed C57BL/6 x C3H background were a kind gift from Emma Rawlins (Cambridge). These mice (MGI ID 4358332 - Tg(KRT5-cre/ERT2)1Blh) have a 6 kb human promoter with a Cre^{ERT2} as transgene inserted at an unknown location. They were initially created by inserting the construct into fertilised zygotes and identifying and developing the subsequent line that showed best recombination in the airway [94] (http://www.informatics.jax.org/allele/key/569731). This mouse has a KRT5 transgene and express cre-recombinase under control of the KRT5 promoter/enhancer region. It is not possible to ascertain where this transgene has integrated into the genome as the allele integrates randomly into the genome at an unknown location. As such, the expression of the gene may not reflect normal physiological KRT5 expression. This model has been used to study airway cell biology [94] as for a while it was the only model available to the research community It is also acceptable the proof-of-principle experiments described initially here. However, quantitative lineage tracing experiments in which the aim is to accurately study the clonal dynamics of the middle would benefit from a mouse model that is more representative of physiological location and expression of KRT5, ideally using the endogenous murine KRT5 promoter. This knock-in mouse has a targeted insertion of the KRT5-Cre^{ERT2} at the endogenous locus using homologous recombination. As such it can be more representative of normal physiology. This knock-in mouse was obtained after the initial pilot experiments and rederived for further use – it is specified when it is used.

For these pilot experiments, a heterozygous breeding pair of Rosa26R-Confetti multicolour reporter mice were purchased from JAX (Stock 013731). Initial experiments to ascertain the feasibility of multicolour middle ear lineage tracing were performed using FVB/N mice as the background strain. This was as offspring were also being generated for epithelial tumorigenesis experiments (led by Dr. Gomez-Lopez). Both KRT5 and Brainbow strains were backcrossed at least four times (N4) onto an FVB/N background for subsequent colony generation. FVB/N;R26R-Confetti mice were bred to

generate mice homozygous for the Confetti allele, and FVB/N;KRT5-Cre^{ERT2} bred to generate mice homozygous for the KRT5-Cre^{ERT2} allele. These homozygous mice were then used to generate litters of KRT5-Cre^{ERT2};R26R-Confetti double transgenic mice on an FVB/N background for experiments.

5.2 Four colour confocal microscopy can be used to visualise multicolour clones

An unbiased approach to analysing clonal dynamics requires robust detection of all fluorophores without overlap over a large enough sampling area of the tissue of interest i.e. using whole mounts rather than processed histological sections which may not preserve native morphology and cell-cell relations [134]. The imaging of the middle ear native epithelium posed unique challenges specific to the tissue, in addition to the generic challenges of multicolour confocal microscopy of the Brainbow cassette.

The excitation and emission spectra of the four fluorophores are GFP - 488 nm; (~498 and 510 nm); EYFP 514 nm (~521 and 560 nm); RFP 561 nm, (~590 and 620 nm); CFP 458 nm, (~466 and 495 nm). As there is significant potential for cross-excitation and detection, it was necessary to work through options of linear unmixing, on-line fingerprinting, and a setup of a main beam splitter that minimises cross-excitation and emission detection. In addition, the imaging set up needed to be optimised balancing the minimum excitation time for detection that will prevent bleaching of fluorophores.

Specific challenges included the conical cavity shape of the middle ear bulla, the hard bone of the mastoid cavity enclosing the epithelium, the thin nature of the epithelial lining during health meaning the target area was small, autofluorescence of bone, and rapid accurate dissection of the bulla whilst preserving tissue architecture. The approaches devised below will be helpful in mitigating many of these challenges to effectively visualise endogenous fluorescence in whole mounts of the middle ear.

5.3 Tamoxifen induces multicolour expression in pinna skin that is preserved by EDTA decalcification

Tamoxifen was initially administered for 3 days to check clonal labelling density whilst minimising risk of toxicity from tamoxifen exposure. The first challenge was to ensure effective decalcification of the bony bulla whilst still preserving endogenous fluorescence. Mice were euthanised at 4 weeks after tamoxifen induction to allow adequate time for cell divisions to take place and increase chances that enough fluorescent cells would be present. The pinna skin was used as a positive control as KRT5+ cells are found in high levels in skin and this region was relatively hairless and thus required little further dissection or processing. Murine mastoid bulla have not been visualised in 3D whole mount previously. As such, optimisation was required to obtain a suitable sample for imaging. The bulla were dissected as described previously with the ear drum and ossicles removed. Both bullae were immediately placed in 4% PFA protected from light at 4°C for 16 hours on a roller. Subsequently, specimens were washed in PBS thrice and then placed in EDTA protected from light at 4°C on a roller, with alternate day EDTA exchanges. The bony cavity was grossly soft to compression by 72 hours and completely soft within 14 days. At this time, the pinna skin was assessed for fluorescence using an upright fluorescence microscope to confirm the presence of fluorescence before formal visualisation using confocal microscopy (Figure 5-2).

A

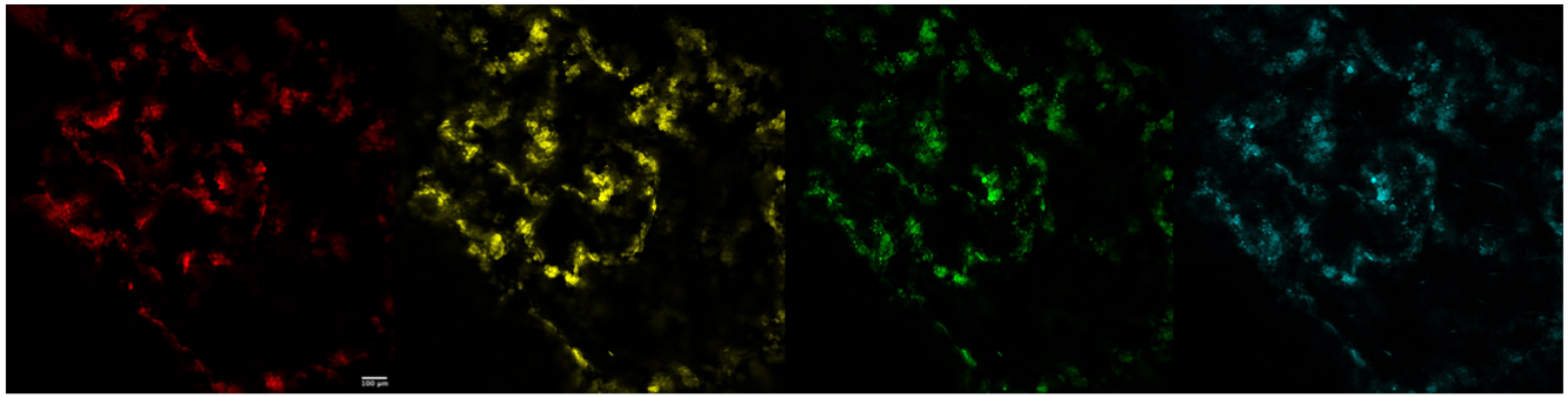

B

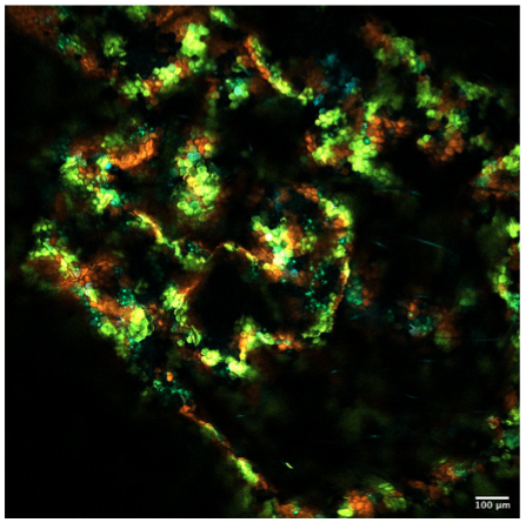

Figure 5-2 Tamoxifen induces multicolour expression in pinna skin that is unaffected by decalcification.

Pinna skin allows assessment of fluorescence. Pinna skin was dissected from mice at the time of bulla harvest and processed simultaneously in an identical manner to the bulla, including EDTA immersion/decalcification steps, as a positive control. Upright fluorescence microscope was used to check for fluorescence before confocal microscopy formally confirmed it was present in all four fluorophores. A. RFP, YFP, GFP and CFP of the confetti cassette were visible after decalcification. B. Merged image of above pinna skin showing all four fluorophores at once but there is some cross-excitation of YFP and GFP in particular. Scale bars show 100μm

5.4 Dissection and decalcification of middle ear bulla in toto can be used to prepare whole mount sections

Whole mount preparation options included thick sections embedded in agarose with sectioning using a vibratome, whole tissue compression between slides[135]or holding the bulla upright and visualising into the middle ear cavity[99].

As the cavity is hollow and the epithelial lining is only a thin layer during health, compression was not chosen as the tissue layers may end up in contact with each other. Furthermore, the bony layer when decalcified would be too thick and prevent adequate laser penetration. The vibratome would only partially overcome the previously discussed disadvantages of sectioning and limited sampling of tissue regions. As such, the upright embedding method was chosen for optimisation. A 1% agarose gel was cast in a 10 cm dish and cooled rapidly on ice. When the gel was almost cooled and set but still soft a bulla sample was placed in it with the cavity opening facing upwards (Figure 5-3). The sample was not inserted when the gel was too hot to protect the tissue and fluorophores from the heat. This was then covered in cold PBS to prevent drying out of the sample and for compatibility with a water dip lens.

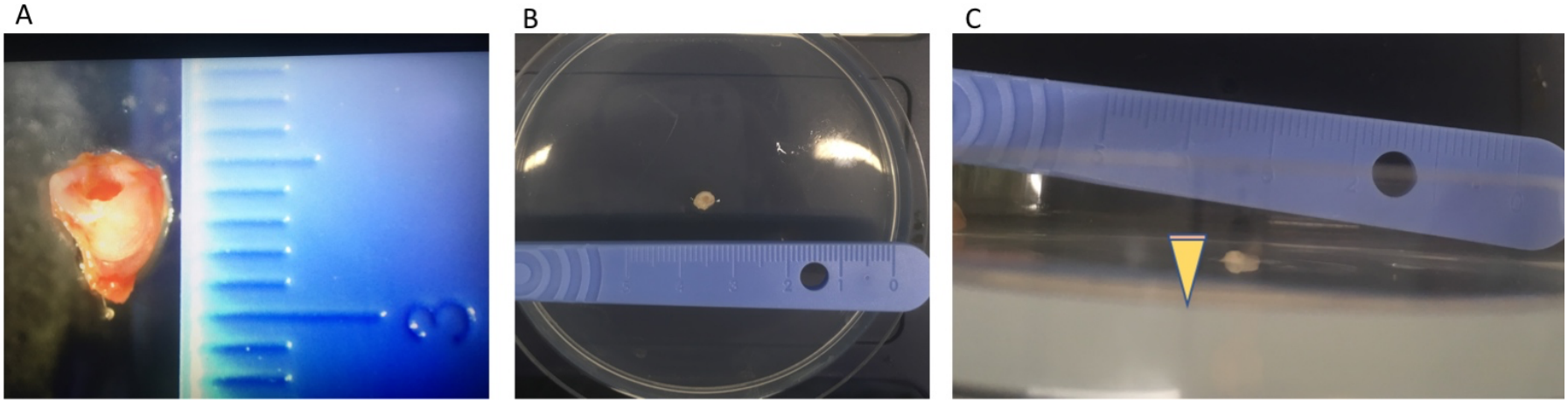

Figure 5-3 Dissection and decalcification of middle ear bulla in toto can be used to prepare whole mounts.

Whole mount dissection and mounting protocol. A. Mice were euthanised and the middle ear was dissected in its entirety and the tympanic membrane and bony annulus removed. B. A 1% agarose gel was cast in 10 cm tissue culture dish and allowed to cool rapidly on ice. When still flowing but cooled, the bulla was embedded with the tympanic opening facing outwards and upwards and covered with PBS to protect the specimen. C. Transverse view of the embedded specimen. Note a small amount is above the agarose to allow the objective to approach as close as possible. Accidental contact of the bulla by the objective will displace the positioning and risk damaging the objective.

As one bulla only allows one entire whole mount, attempts were also made at paraffin embedding the middle ear and obtaining multiple histological sections from one mouse. However, this processing quenched endogenous fluorescence and also caused unacceptably high levels of autofluorescence from bone especially (data not shown). Whilst these sections would have been beneficial to counterstain for multiple other markers from the same tissue, such as MUC5AC and ACT, the quenching and autofluorescence precluded from such further analysis.

5.5 Multicolour KRT5+ derived clones can be visualised in middle ear and show an increase in size with time

For whole mount preparations, initial attempts at visualisation were tested using a 5x, 10x and 20x, inverted lens set up on a Zeiss LSM880. The laser lines used were 458 nm, 488 nm, 514 nm and 561 nm and the set up used was based on that of Amitai-Lange and colleagues[136].

However, with the inverted lens set up, the focal length and working distance of the objectives was insufficient to penetrate through the dish, agarose and then the relatively thick bulla to visualise the epithelial lining within. As the bulla cavity is hollow and the region of interest was the inner surface of the bulla, another option was to use an upright lens with immersion capabilities to image the specimen from a closer distance. By having the objective closer to the epithelial layer within the bulla, the working distance could be reduced to minimise laser energy dissipation.

A set up using an upright objective (HC APO L U-V-I 10x/0.30) with water immersion function on a Leica SP8-vis microscope was subsequently tested. The laser lines and detection set up were as for the Zeiss LSM880.

Imaging was obtained over a 1024x1024 field with 8 bits per pixel and bidirectional scanning in Z-stack mode with a single laser at one time. The dwell time was 0.0000004s and the scan speed was 600Hz. This set up provided the optimal compromise between balancing fluorophore excitation, avoiding cross-excitation and detection, and minimising bleaching. This yielded better results with successful visualisation of fluorescence of all four colours in the middle ear bulla (Figure 5-4) similar to the positive control of the pinna skin. Clones were seen at the 4-week time point. The general size of visualised clones was larger in a 12-week sample. Again, cross-excitation of YFP and GFP was seen in parts and background autofluorescence was present in the GFP and CFP channels. Only background fluorescence was seen in the sample from a no tamoxifen negative control mouse and no discrete patches of fluorescence or fluorescent cells were seen.

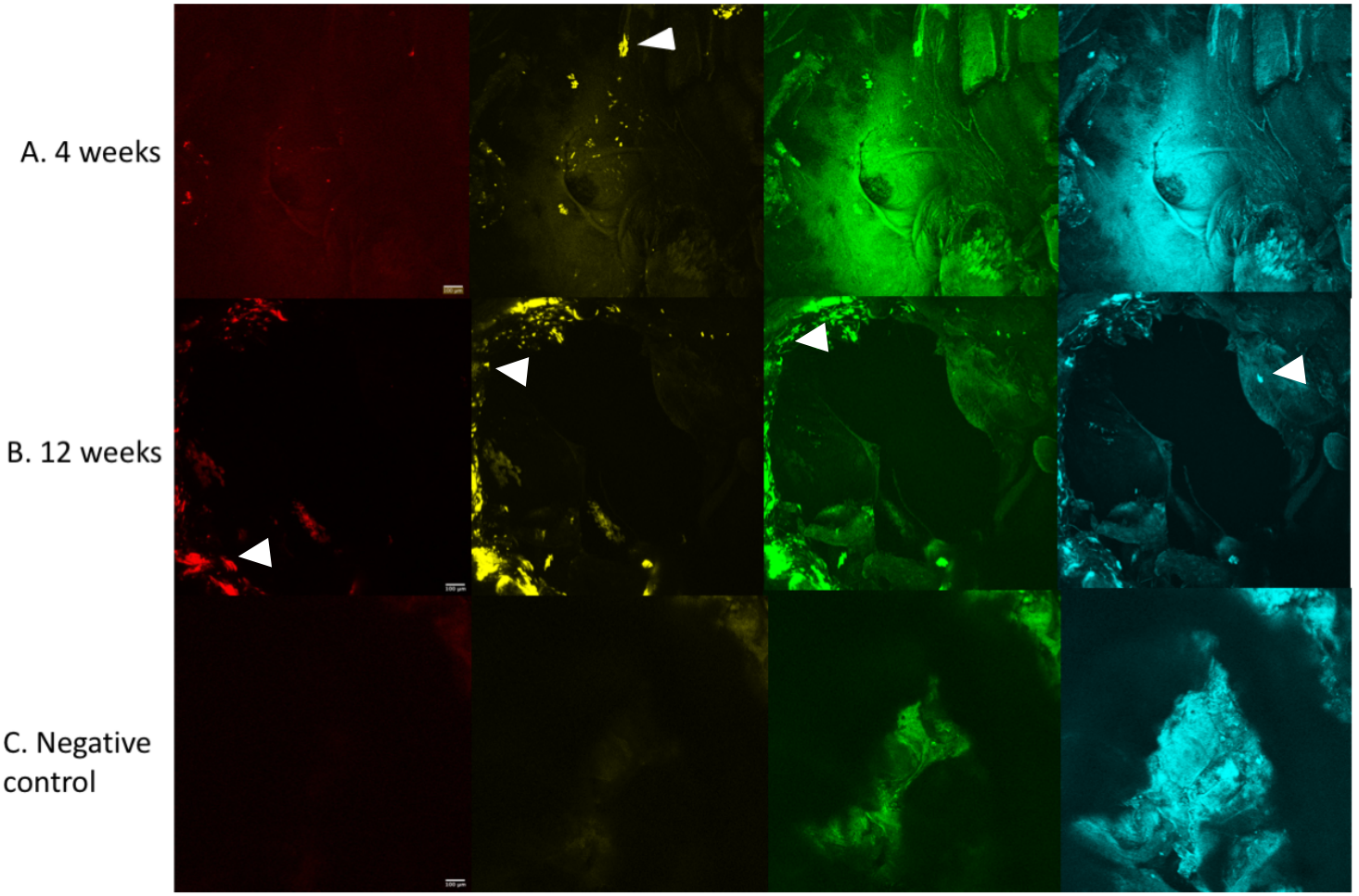

Figure 5-4 Multicolour KRT5+ derived clones can be visualised in middle ear and are larger in size with time.

KRT5+ clones in bulla were visualised using Leica SP8 confocal microscopy**.** Agarose embedded whole-mount specimens were imaged using an upright water immersion objective. **A.** KRT5+ clones were seen after 4 weeks (white arrowhead top panel) of RFP, YFP, GFP and CFP. **B.** Clones seen were generally larger in size at a 12-week time point (white arrowhead). Cross-excitation is seen with correlating patches of GFP cells that are also yellow. **C.** Negative control bulla from a tamoxifen unexposed mouse did not have any focal patches of fluorescence seen with only background autofluorescence. Scale bar shows 100 μm. (Representative images of n = 3 mice at time points)

Whilst the upright immersion set up provided adequate visualisation of endogenous fluorescence, there was cross-excitation of the fluorophores resulting in some cells that were visualised as both green and yellow. Modelling clonal dynamics robustly requires three components to be optimised as best possible – effective separation of fluorophores, maximal speed of acquisition to minimise sample exposure time, and adequate resolution to delineate individual cells and patches of cells. These can be potentially overcome by a multi-channel gallium arsenide phosphide (GaAsP) detector, on-line fingerprinting, a FAST module and an Airyscan set up. The GaAsP detector has higher sensitivity than a photo-multiplier tube (PMT) used in confocal microscopy and is thus useful for rapid image acquisition.

5.6 A novel 3D reconstruction method of whole mounts shows KRT5+ derived clones in multiple regions of middle ear

To use these tools to improve visualisation, a different microscope set up using the Zeiss platform with an LSM880 and GaAsP detector but without a FAST module was used. Another benefit of this microscope was a comparable Zeiss set up was available at both MRC Harwell and UCL. The objective used was a W Plan-Apochromat 10x/0.5 M27 75mm. The complete set up was as below:

Laser	Excitation(nm)	MBS	Dye detection
DPSS 561-10	561	MBS 458/561	ECFP
Diode 405-30	458	MBS 458/514	mRFP1.2
ArgonRemote	514	MBS 488	EYFP
HeNe594	488	MBS T80/R20	EGFP

Using this set up provided better visualisation by reducing cross-excitation of fluorophores, more rapid imaging with reduced bleaching and increased sensitivity. This meant more of the bulla could be imaged and allowed reconstruction of the data into a 3D image of the specimen (Figure 5-5). Of note, as this was for optimisation, the data were obtained over a shorter timescale than normally would be required for the level of imaging needed for clonal analysis. However, there was a requirement for further specimen optimisation. In particular, the issue of background autofluorescence particularly of GFP and CFP channels was high and likewise also present from endogenous vasculature. To overcome this, mice were perfused with ice cold PFA and post-fixed again using PFA after dissection for future specimens [117].

This method also provided the option of testing various clearing methods to examine whether better transparency and autofluorescence quenching aided data collection.

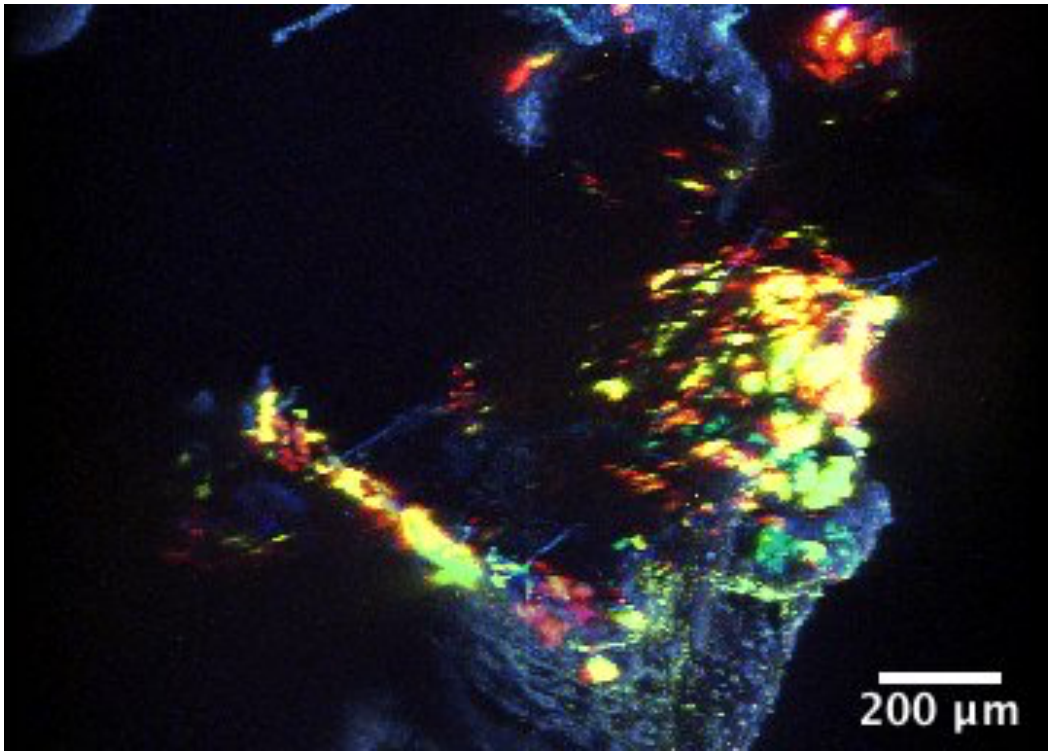

Figure 5-5 3D reconstruction of whole-mount shows KRT5+ derived clones in multiple regions of middle ear.

3D reconstruction allows visualisation of bulla looking where tympanic membrane would be. Dissected and decalcified bulla were embedded in an agarose gel and imaged using a water immersion objective on LSM880. 3D reconstruction of the merged Z-stack was possible to reconstruct the imaged bulla region, showing fluorescence in the ventral region of the middle ear (lower half of panel) and the dorsal part (upper half of panel). Scale bar shows 200µm. (Video also available)

5.7 Clones can be seen in KRT5-Cre^{ERT2} knock-in mice in multiple regions of the middle ear

Having established the visualisation of the middle ear fluorescence from a multicolour reporter line is a viable technique, the next step was to refine the model as some limitations existed. Firstly, the cassette used is a transgene using the human KRT5 promoter and thus the location and comparison with physiological expression is unknown. Secondly the mice are on an FVB/N background which is different from that of Jeff (C3H/B6). To overcome both these issues, knock-in mice on a B6 background would be most suited. Knock-in mice for KRT5 with tamoxifen inducible Cre-recombinase expression in KRT5+ cells by the endogenous promoter/enhance elements (B6N.129S6(Cg)-Krt5tm1.1(cre/ERT2)Blh JAX:029155) were obtained and rederived[109]. These were maintained on a B6N background but were not initially made homozygous as advised by the creating group. These were crossed to the Brainbow reporter line to generate double transgenic mice.

Tamoxifen was administered by oral gavage for 3 days and labelling checked after 2 weeks in the pinna skin (used as a positive control) and middle ear using whole mounts.

Fluorescence was visible in patches in the pinna skin as previously (Figure 5-6A).However, whilst the middle ear epithelium appeared to have many fluorescent cells, discrete patches were less obvious (Figure 5-6B). Whilst this showed that the model was viable as a middle ear lineage tracing set up, whether this difference in labelling with multiple adjacent colours seen rather than discrete clonal patches reflects a change in KRT5+ progenitor behaviour or reflects an increased sensitivity to tamoxifen based induction will require further analysis.

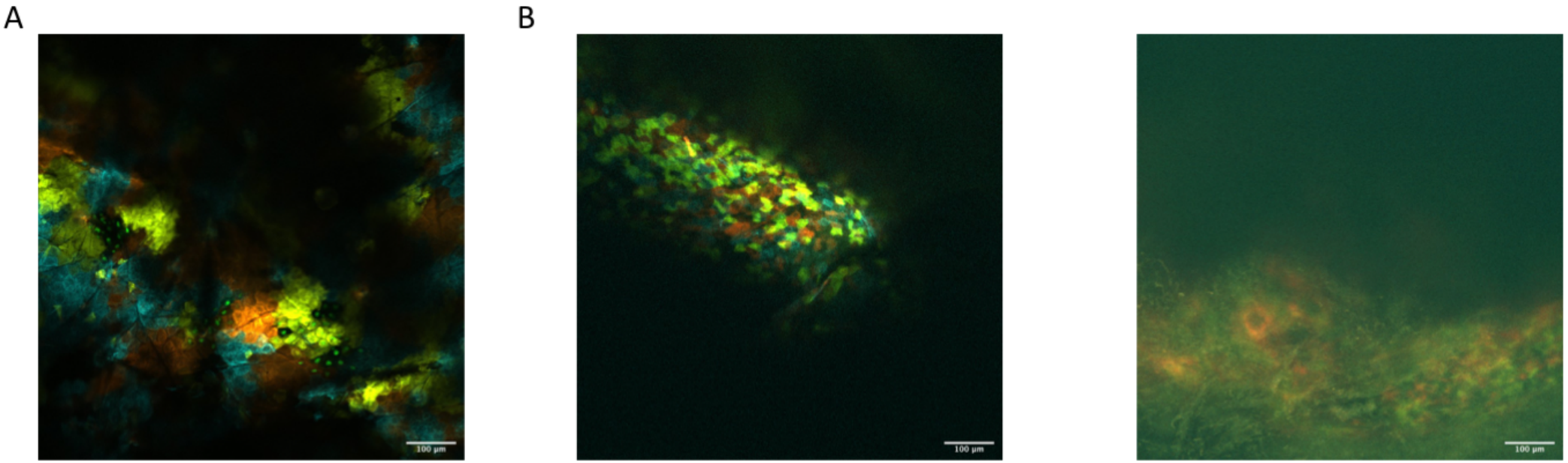

Figure 5-6 Endogenous fluorescence is visible in the KRT5 knock-in reporter line with the allele expressed at the physiological locus.

A. Mice were harvested and the pinna skin used as a positive control. Pinna skin showed all four endogenous fluorophores (RFP, YFP, CFP, GFP) in clonal patches after 2 weeks. B. Bulla whole-mounts were imaged and again showed fluorescence by cyan was poorly visualised. Distinct clonal patches were less evident and multiple colours were seen close together. Fluorescence was seen both close to (left) and distally from (right) the removed tympanic membrane. The distal image has more autofluorescence owing to the presence of more bone near here. Scale bar shows 100µm. (Representative images of n = 3 mice)

5.8 Tissue clearing of middle ear is possible with Bone CLARITY and RapiClear

Tissue clearing is now a common technique used to improve transparency of specimens to enable better visualisation of fluorescence. The most popular recent methods are modifications of CLARITY (*C*lear *L*ipid-exchanged *A*crylamide-hybridised *R*igid *I*maging/Immunostaining/In situ-hybridisation-compatible *T*issue-h*Y*drogel) based techniques [137]. Initially pioneered in the brain, CLARITY has now been successfully used to visualise bone marrow progenitor cells in long bones of mice [117]. However, this is a labour intensive and equipment reliant technique. Initial clearing methods tested were ScaleA/2 and CUBIC. Whilst both methods increased the specimen transparency, the bone was not completely clear (even with decalcification) and furthermore there was quenching of fluorescence (data not shown).

As such, two other tissue clearing methods were tested - Bone CLARITY or the use of the clearing agent RapiClear. For Bone CLARITY, the protocol included steps for specimen fixing, decalcification, stabilisation of hydrogel, autofluorescence quenching, and then CLARITY based clearing over a 1 month time period. For the RapiClear protocol, the steps included fixation and decalcification alone prior to addition of RapiClear.

Both protocols increased the transparency of the specimen with RapiClear providing better clearing. This may be secondary to the lack of available equipment for the Bone CLARITY set up. As such, oil-based degassing was performed rather than using a nitrogen chamber and a roller for agitation and flow-based clearing rather than a mixer. Since RapiClear provided comparable clearing in a shorter timescale RapiClear was chosen as the clearing method of choice for future samples (Figure 5-7).

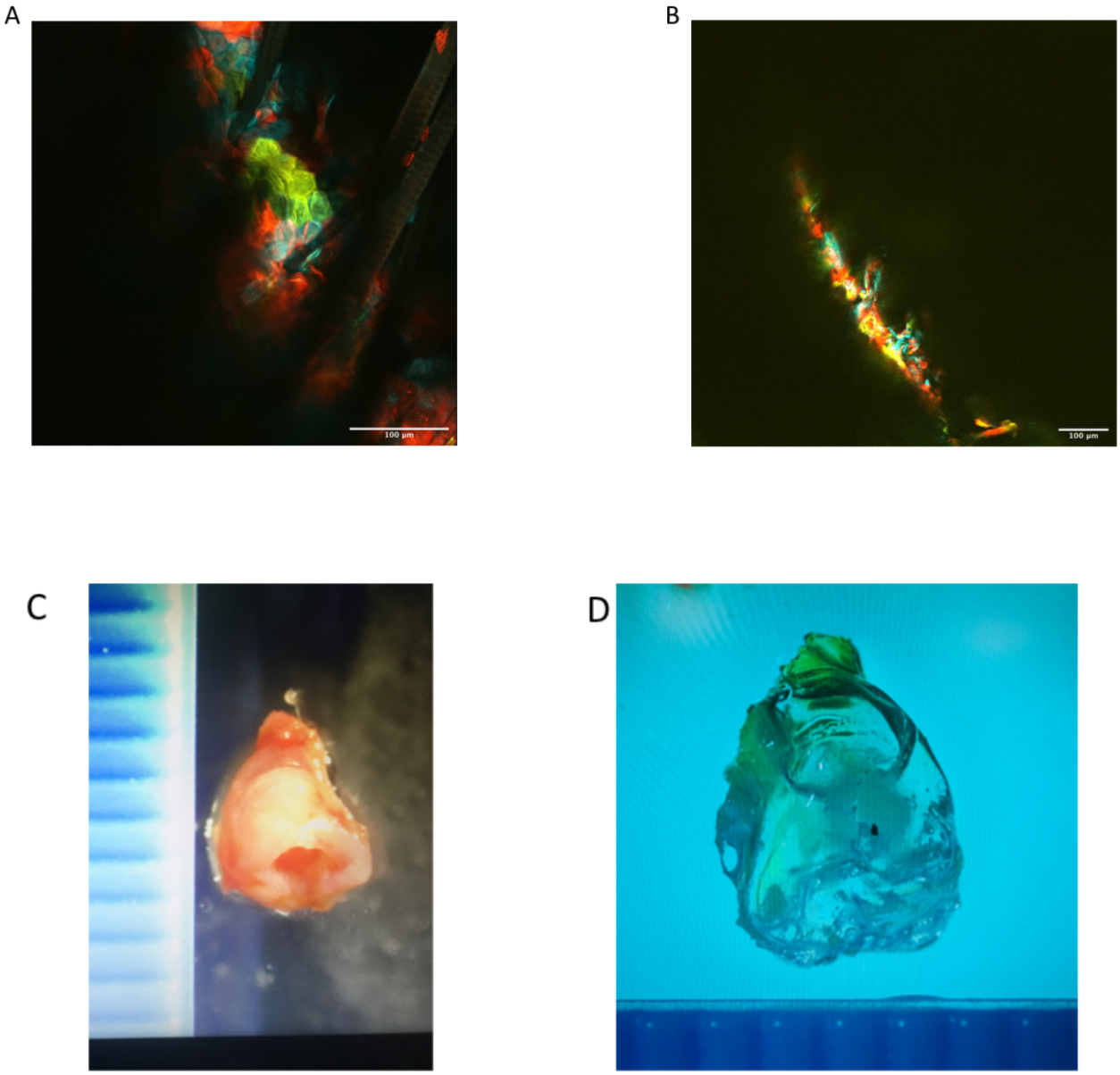

Figure 5-7 RapiClear allows clearing of tissue samples without quenching of endogenous fluorescence.

Tissues from Brainbow reporter mice were placed into RapiClear for 16 hours. A. Pinna skin as a positive control shows preservation of endogenous fluorescence and cellular architecture. B. A small region of middle ear bulla was also tested in thick section and this also showed preserved endogenous fluorescence with less autofluorescence than previously seen in uncleared samples as in Figure 5-4. C. Freshly dissected bulla before clearing. D. Example image of bulla after decalcification and clearing with RapiClear. Scale bar shows 100μm.

5.9 KRT5-Cre^{ERT2};Brainbow do not show histological signs of otitis media

To ensure the double transgenic mice and tamoxifen induction did not have otitis media and thus reflected normal tissue homeostasis rather than a pathological state, histological paraffin sections were obtained from mice without tamoxifen administration and 4 weeks after 3 days of tamoxifen administration. No signs of epithelial hyperplasia or middle ear fluid were seen in the mice (Figure 5-8).

Summary

This chapter demonstrates a viable approach to in vivo lineage tracing of middle ear progenitor cells using fluorescent reporter mouse lines. Future work will involve an adequately powered pulse chase experiment to model the clonal dynamic of the middle ear during homeostasis as well as during the chronic disease state.

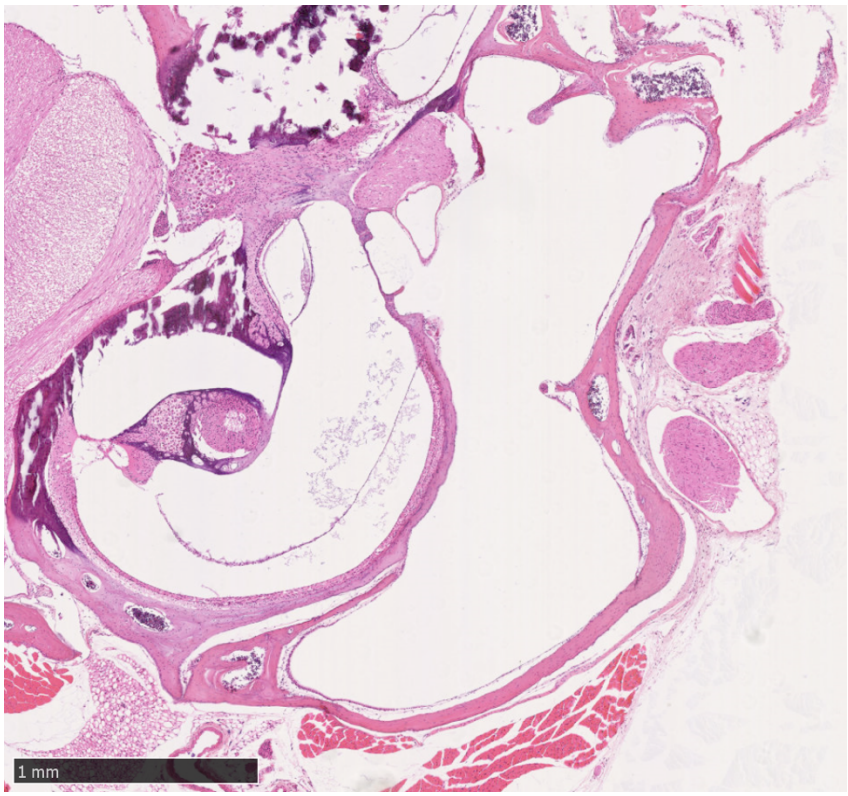

Figure 5-8 KRT5-Cre^{ERT2};Brainbow do not show histological signs of otitis media.

KRT5-Cre^{ERT2};R26RConfetti mice were used to obtain paraffin embedded sections at 12 weeks of age. The middle ear was clear with no fluid visible on inspection or on histological sections. The middle ear epithelium was also not thickened and comparable to wild-type B6 mice. Scale bar shows 1mm.

Chapter 6 Discussion

The work in this thesis has optimised a platform of assays for assessing the epithelial homeostasis of the murine middle ear. The work builds on existing research in middle ear biology, a field in which there is increasing focus on the function of the epithelial lining. The work has drawn on methodologies and concepts from the fields of airway biology and general epithelial biology to help address the question of how middle ear epithelial homeostasis is maintained and how this may be perturbed in chronic disease. Below, we consider the potential implications of the findings of this, limitations, and strategies for taking this research forward.

6.1 Summary of findings

The middle ear contains KRT5+ cells with progenitor cell capacity . These constitute approximately 7% of the middle ear epithelium during health. KRT5+ cells are asymmetrically distributed in the dorso-ventral axis – progenitors in the ventral middle ear are more common and also possess a sub-population of cells that can grow into large colonies in vitro. KRT5+ progenitors demonstrate bipotent differentiation capacity in vitro and can give rise to cells that are ciliated as well as cells that produce mucin. *Fbxo11*$^{Jfl/+}$ mice with chronic otitis media with effusion are known to show epithelial remodelling with hyperplasia. Middle ear epithelial cells from these mice seem to show a reversal in the dorso-ventral asymmetry of KRT5+ progenitors seen in health. There is an increase in the number of dorsal region progenitor cells and present in this dorsal KRT5+ population is a subpopulation of progenitors that can grow into large colonies in vitro, something usually only seen in ventral epithelium derived cells. Differentiation assays at air-liquid interface and

spheroid assays show middle ear progenitors from *Fbxo11*$^{Jf/+}$ have aberrant differentiation giving rise to cells with an abnormal mesenchyme like morphology. Progenitors from *Fbxo11*$^{+/+}$ controls give rise to ciliated and goblet cells. This aberrant differentiation is also seen at the single cell level in spheroid assays. Finally, multicolour lineage tracing using a KRT5-Cre^{ERT2};R26RConfetti reporter in vivo combined with tissue cleared 3D whole mount visualisation shows KRT5-derived clones are present in multiple regions of the murine middle ear. This model will allow detailed analysis of the cellular remodeling and in vivo progenitor cell clonal dynamics to be assayed in health and disease.

6.2 Limitations

The main limitation of the work is limited number of mice in experiments meaning whilst trends towards significance were seen, it is likely experiments were underpowered. As many of these assays are being performed for the first time in middle ear epithelium power calculations were not possible and numbers were based on existing literature of other epithelial biology fields. Further work building on this can design robust suitably powered experiments using data from this thesis.

6.3 Assaying middle ear epithelial homeostasis in vitro

The ability to study the proliferative behaviour of epithelial cells in vitro using colony forming analysis was pioneered by Howard Green and Jim Rheinwald[138,139] and is now standard practice for a variety of epithelial tissues most notably the skin[102,113]. Similar methodology has been adapted to the other epithelium including the airway epithelium especially of the

trachea[124,140,141]. As the airway and middle ear have similarities in cellular architecture with a basal cell layer consisting of KRT5+ progenitors and a pseudostratified layer of ciliated and goblet cells above this, the same techniques are now being used to probe the dynamics of the middle ear epithelium[98-101,110,142,143].

In this work, the middle ear epithelium has been analysed in bulk after a fibroblast depletion step - that is without selecting for epithelial cell subpopulations based on flow cytometric markers. This form of global analysis of the entire epithelium provides a useful initial insight into the middle ear epithelium as a whole but does not allow analysis of the cellular heterogeneity that exists within epithelial surfaces. This work focussed in particular on the role of KRT5+ cells that have been shown to have stem/progenitor capabilities in multiple other epithelial linings and recently in the middle ear[99]. The presence of KRT5+ cells in mouse middle ear has been shown by other groups using short-term lineage tracing, immunohistochemistry and in vitro cell cultures[98-100,110]. However, their number, distribution and differentiation potential is still an area of active research.

Here for the first time the epithelium has been analysed using colony forming ability and flow cytometry to quantify and localise KRT5+ cells in bulk and investigate their progenitor cell potential. These assays provides further evidence that KRT5+ cells are present in the middle ear and have progenitor cell capacity. KRT5 positivity is seen in colonies derived from single cells when grown in 2D culture in colony forming assays. Flow cytometry of primary mouse middle ear derived cells shows KRT5+ cells constitute about 7% of the middle ear epithelium. There is a trend towards a dorso-ventral asymmetry of distribution and function with a greater proportion KRT5+ cells present in the ventral epithelium.

Isolating cells from the mouse middle ear was standardised using an enzymatic dissociation protocol with dispase, DNase I and TrypLE. Dispase is a bacillus polymyxa-derived metalloprotease that works on fibronectin and type IV collagen, but not laminin, type V collagen, serum albumin or transferrin[144] and is quenched by dilution or spinning down of cells. It helps maintain cells in single cell suspension and the DNase I was used to remove released DNA to help prevent cell clumping. TrypLE was used rather than TrypEDTA as it is reportedly more gentle on cells to maximise viability and also to preserve extracellular epitopes, which would allow flow cytometric sorting of subpopulations if required[145]. The dissection of the bulla has been modified from existing work in two ways. Firstly, the bulla can be divided into dorsal and ventral regions along a horizontal axis from the diameter point of the annulus to a point just above the eustachian tube orifice. Existing dissection instructions advise removing the tympanic membrane and ossicles to minimise contamination but also remove the dorsal aspect, which may contain relevant cells [101]. As such, here the dissection for whole bulla analysis retained the dorsal bulla region and separated this for region specific analysis.

The dorso-ventral asymmetry aligns with the findings of Tucker and colleagues and Luo and colleagues who show that KRT5+ cells are predominantly found in the ventral middle ear and less frequently in the dorsal middle ear during routine homeostasis in health [98,99]. From literature searches, there have been no other attempts at quantification of the number of KRT5+ cells or colony forming ability of middle ear epithelium thus far although scRNAseq work in ongoing (Ryan et al., 2020, unpublished data). There is variation in the stem cell readout seen in colony forming assays and heterogeneity in the colonies seen. Visualisation of colonies showed some colonies with unhealthy appearing cells with enlarged cytoplasm/vacuoles perhaps reflecting senescence, poor growth, or partial differentiation attempts in 2D conditions

not conducive to full differentiation. Of note, there was generally more uniform cobblestone appearance seen in submerged ALI culture with better differentiation, which would be expected and has also been seen by others [110]. As such CFE is best used as a relative readout of progenitor cell capacity between two experimental conditions rather than an absolute readout of progenitor cell number.

Options to improve the colony forming potential may be co-culture using inactivated mouse embryonic fibroblasts as a feeder layer either from legacy 3T3-J2 or NIH-3T3 fibroblasts[102], TGF-ß inhibition[103]or dual-SMAD inhibition [146]. Co-culture of epithelial linings has been well characterised and even used for therapeutic potential in human skin regeneration and transplantation [104] and recently co-culture with 3T3-NIH murine fibroblasts has also been used to expand human middle ear epithelial cells for air liquid interface work [147]. This is thus a viable option but would require quantification of the relative effect on colony forming potential of mouse middle ear cells as it may be that whilst there is improvement, it still does not reflect a true readout of middle ear progenitors. As such, in this work CFE was used mainly in comparative assays between conditions (e.g. regions of the middle ear and hypoxic pathway activation).

The flow cytometric pipeline shows for the first time the proportion of KRT5+ cells that are present in the epithelial compartment of the middle ear and what region-specific differences exist. The ability to perform flow cytometry also opens up avenues to sort and enrich for subpopulations of cells. As KRT5 is an intracellular cytokeratin, extracellular markers of enrichment known to help sort for basal cells in the airway were tested. This showed that ITGA6+ and binding of GSI-B4 help enrich for KRT5+ cells but NGFR is not useful. Whilst the enrichment enabled by GSI-B4 and ITGA6 is comparable with the utility of

these markers in the murine airway, the inability of NGFR to help is different. This may be due to lack of NGFR expression in the middle ear or it may be that the cellular isolation technique used affected this epitope and prevented antibody binding.

Cell-cycle analysis using Hoechst-33342 to look at proliferation did not provide suitable data to assess proliferation of KRT5+ cells in the middle ear. This assay will require repeating or alternatively, using the modified thymidine analogue EdU (5-ethynyl-2'-deoxyuridine) that incorporates into DNA during synthesis and can subsequently be detected using flow cytometry or fluorescent microscopy.

Another experimental step would be to sort for KRT5+ enriched and non-enriched population and identify what proliferative/differentiation differences exist between these two populations to better understand the role of KRT5+ cells and identify what other progenitors may be present in the middle ear. Another alternative to sort for a pure KRT5+ population would be to use a constitutive KRT5-tdTomato mouse line where all KRT5+ cells would express the tdTomato protein and hence allow FACS using this fluorophore as a marker. Single-cell RNAseq is also a useful option to characterise the middle ear epithelium as a whole and also identify markers to purify the KRT5+ population. Such work is being performed by the Ryan group in USA (unpublished data); the results will doubtless help identify further markers as well as helping to further characterise the cell atlas of the mouse middle ear. The ability to sort human cells to enrich for a progenitor cell population is also appealing for potential therapeutic and diagnostic purposes.

Two in vitro differentiation assays were used to explore differentiation potential of middle ear epithelial progenitors. The majority of the work used the air-liquid

interface assays and built on protocols optimised by Mulay and colleagues [101]. The seeding density used was different in this work as optimisation assays showed higher densities provided better growth of transwell cultures. It is unclear why this difference exists, as the strain of mice used and culture conditions are similar. Of note, the isolation protocol is different in two ways – firstly, in this work dorsal bulla as well as ventral bulla was used to provide middle ear epithelium whereas Mulay and colleagues only used half bullae. As such, since the dorsal region contains a smaller proportion of progenitors, there may be more epithelial cells without progenitor potential in the initial single cell suspension. Secondly, different reagents were used (dispase/DNaseI/TrypLE compared with pronase) and it may be that the pronase used by Mulay and colleagues results in better progenitor cell viability. However, the use of dispase, DNaseI and TrypLE has been used by other stem cell biology protocols with a suitable cellular yield and functional outcome so this does not fully explain the discrepancy.

Differentiation of middle ear progenitors at air-liquid interface showed that a confluent layer of KRT5+ cells gives rise to both ciliated and non-ciliated cells that express MUC5AC, suggesting that KRT5+ cells are bipotent. This is in agreement with the findings of Luo et al.[98] who used short term lineage tracing of KRT5+ cells in mouse middle ear to show that KRT5+ cells give rise to ciliated and non-ciliated cells both dorsally and ventrally. Tucker and colleagues also find that some ciliated cells are present in the dorsal mouse middle ear. These may be of a neural crest origin or could be secondary to migration of cells from the ventral middle ear region where cells are predominantly endodermally derived during development. A small number KRT5+ cells are found in dorsal epithelium derived cells on flow cytometry, colonies from dorsal derived epithelium form in colony forming assays, and KRT5+ cells seem to have bipotent differentiation ability. It therefore seems

likely that KRT5+ progenitors underlie the generation and maintenance of at least some of the dorsal epithelium and a greater amount of the ventral epithelium. Attempts at region specific epithelium air-liquid interface assays in this work were inconclusive, but further attempts or use of the spheroid assays (as described below) may help clarify the role KRT5+ progenitors play in different regions of the middle ear. Likewise, multicolour lineage tracing will also aid in this.

Thus, the modified bulla dissection technique to include the entire bulla, colony forming assays, flow cytometry and the air-liquid interface assay provide a useful foundation with which to assay the middle ear epithelium in vitro. These techniques were subsequently applied to answer the question of how KRT5+ cell characteristics change in the *Fbxo11*-mutant mouse model of otitis media.

6.4 Middle ear epithelial cells *Fbxo11*$^{Jf/+}$ mutant mice show abnormal proliferation and differentiation

Mouse models of otitis media provide an essential resource to understand middle ear disease in a genetically tractable model. The Jeff *Fbxo11*$^{Jf/+}$ model has a mutation in the *Fbxo11* gene. This gene has been implicated in recurrent and chronic otitis media in multiple cohorts in human GWAS. As such, Jeff is a useful model to probe to understand mechanisms of how chronic middle ear disease can occur. Here, progenitor cell capacity and differentiation function were compared between *Fbxo11*$^{+/+}$ controls and *Fbxo11*$^{Jf/+}$ mutants. In the *Fbxo11*$^{Jf/+}$ mutant mice with otitis media, The major limitation of this section was underpowering with low n numbers meaning although trends were seen, significance was not reached. KRT5+ cells seem to increase in number in the dorsal epithelium; the progenitor cells here form larger colonies, and progenitor

cells lack the normal ability to form ciliated and non-ciliated cells instead achieving a more mesenchyme-type appearance. The combination of abnormal proliferation and aberrant differentiation could result in an inability of the middle ear epithelium to effectively ventilate and clear the middle ear cavity and result in a chronic inflammatory state as seen in COME.

The change from the normal ventral predominant distribution of KRT5+ progenitors to dorsal has been seen by immunohistochemistry from work by other groups studying otitis media in the *Tbx1/+* mouse[99]. Whether this is due to migration or proliferation of resident KRT5+ progenitors is still unanswered. Another hypothesis is that lineage negative progenitors (i.e. a higher order non KRT5+ progenitor) divide to give rise to KRT5+ progenitors[148]. Further work to clarify this could include lineage tracing and EdU-based proliferation assays as the Hoechst-based assay used in this work was sub-optimal. Likewise, isolation and analysis of an enriched progenitor population using ITGA6 as a FACS marker from dorsal and ventral regions could show the progenitor cell capacity, proliferative ability and differentiation potential of KRT5-enriched and KRT5-unenriched populations, thus finding whether other progenitor populations exist.

FBXO11 is a ubiquitin ligase that has downstream targets including BCL6 and neddylation of p53[63,66]. These are both involved in cell cycle regulation and proliferation. Thus, mutations in *Fbxo11* could result in abnormal cell cycle regulation and increased proliferation. However, this would not fully explain why there is a tendency towards a potentially region-specific remodelling and change in KRT5+ progenitors. One hypothesis that is difficult to test practically is the effect of gravity in that the dependent regions of the middle ear are exposed more to middle ear fluid and will be submerged compared with the dorsal regions.

The abnormal differentiation was a surprising result but again aligns with findings by Del-Pozo and colleagues[71] who showed that *Fbxo11*$^{Jf/+}$ mutant mice have a cavitation defect during development. This results in persisting mesenchyme that does not undergo the expected mesenchyme-to-epithelial transformation usually seen during development[72] and persisting as mesenchyme.

As such, the lack of normal differentiation may be due to an intrinsic inability of all KRT5+ progenitors from Jeff mice to differentiate owing to the *Fbxo11*$^{Jf/+}$ mutation. Alternatively, it may be that a subpopulation of progenitors alone is affected. Large colonies formed from dorsal region derived epithelium in 2D colony forming assays. It may be that these cells outcompete other progenitors in ALI during establishment of ALI confluence and this population may alone have aberrant differentiation. To assess progenitor function of single progenitor cells, a spheroid assay was optimised. When single cells were cultured in Matrigel, a spheroid with a lumen was only seen in cells derived from the control mice rather than from the *Fbxo11*$^{Jf/+}$ mutants. Staining and further analysis of this is required to fully characterise the cell types seen. As such, it seems that the *Fbxo11*$^{Jf/+}$ mutant mice have progenitor cells with abnormal colony forming ability (in terms of size) and differentiation. Once again whether this is triggered by a particular stimulus such as hypoxia or the middle ear epithelial cells are primed to function poorly due to abnormal FBXO11 function during development [55,71] needs to be explored.

A possible pathway that could explain why this occurs is the TGF-ß pathway. This has already been shown to affect stem cell proliferation[103] and is involved in other chronic inflammatory conditions such as lung fibrosis[149]. *Fbxo11*$^{Jf/+}$ mutant mice have abnormal TGF-ß signalling as shown by an increase in nuclear localisation of the downstream component pSMAD2[53]. The other

mutants identified from the unbiased ENU screen, namely Edison and Junbo, also have abnormal signalling in the TGF-ß pathway implicated. The fact that the *TGIF1*-/- mouse also develops otitis media, in a case when TGF-ß signalling is inhibited, suggests that both high and low TGF-ß affect cellular homeostasis. TGF-ß may also interact with the hypoxia pathway and hypoxia could potentially be a trigger[57,58]. The HIF-1α stabilising experiments show that *Fbxo11*$^{Jf/+}$ mutant mice seem to have a greater reduction in CFE at lower levels of cobalt II chloride hexahydrate exposure although Western blotting is required to quantify the extent of HIF activation in this assay. Further work to assay proliferation and differentiation in a hypoxic chamber would be useful. Another experiment would be to repeat the proliferation and differentiation assays in conditions of TGF-ß inhibition and stimulation under normoxic and hypoxic conditions.

The work on the *Fbxo11*$^{Jf/+}$ mutant mice does have a number of limitations. As well as the limitations of the assays and power described earlier, the findings have only been shown in one mouse model of otitis media. Thus, it will be necessary to corroborate these using other mouse models such as Junbo and Edison to see if mechanisms are common in suppurative forms of otitis media. Secondly, the mechanisms underlying these changes are still putative and it is unclear whether the progenitor cells intrinsically have abnormal proliferation and differentiation and thus cause COME, or is this seen in response to COME i.e. whether these changes are causal for chronic otitis media or caused by the environment is still unanswered. One way to answer this may be to engineer mutations in FBXO11 in vitro using viral vectors and to test proliferation and differentiation following this; likewise using other mouse models of COM would also demonstrate whether proliferation and differentiation changes are seen ubiquitously in COM. In addition, the assays used could be improved to provide a higher throughput method of screening

as ALI is mouse and labour intensive. The spheroid assay may thus be a viable alternative here as it can also be performed in 96-well plates [94,130]. Finally, the work has only been shown in mice models and human tissue verification is also required in future. However, some experiments are not possible using primary human tissue such as lineage tracing in vivo and this is where the platform of mouse model and 3D visualisation established will be invaluable in helping understand middle ear biology.

6.5 Multicolour lineage tracing can be used to model clonal dynamics in murine middle ear

Multicolour lineage tracing using an inducible Cre-recombinase in combination with the four colour Confetti reporter (RFP, YFP, CFP, GFP) has been used to study cellular homeostasis of numerous organs including lung, skin, mammary gland and gut [132]. The KRT5-Cre^{ERT2} mouse model exists in transgenic Tg(KRT5-cre/ERT2)1Blh[94] and knock in B6N.129S6(Cg)-Krt5tm1.1(cre/ERT2)Blh/J[109] variations and both have been well used in lineage tracing experiments. The use of a knock-in reporter line may provide a better comparison with normal physiology rather than the KRT5 transgene as the KRT5-Cre^{ERT2} is inserted in a targeted fashion at its normal locus in the mouse genome.

Visualisation of four colours with close excitation and emission spectra requires careful microscopy as well as suitable laser lines, filter sets and detectors that can excite the fluorophores specifically and rapidly and detect only the emission of interest. A further challenge specific to the middle ear is the bony cavity which houses the middle ear epithelium requiring decalcification and dissection without damaging the tissue of interest. Finally,

whole mount imaging is desirable to view a large enough field of interest to analyse cellular homeostasis.

The microscopy set up here using the upright water-immersion objectives in combination with a GaAsP detector and Airyscan allowed a balance between speed and resolution of imaging. Autofluorescence of the bony cavity was a problem even after decalcification. The CLARITY and RapiClear based clearing strategies tested helped with visualisation and reduction in autofluorescence. Regardless, the middle ear is a difficult anatomical site to effectively visualise and 3D whole mount four colour confocal is still a labour and time intensive process. One way to speed up the imaging data acquisition is by using a lightsheet microscope. In such a set up a sheet of illumination from a laser or a low numerical aperture source is used to illuminate a cleared tissue section with detection of fluorescence in a different orthogonal plane to reduced contamination from fluorescence that is not in the plane of interest. The main benefit of light sheet is adequate resolution but a many fold reduced time of acquisition. Another useful improvement would be to optimise counterstaining of the bulla whole mount for markers of cilia and goblet cells to verify what KRT5+ progenitors give rise to in vivo. Finally, the ability to sort the fluorescent KRT5+ derived cells can be useful for transcriptomic analysis of a KRT5+ cell derived population. Multicolour lineage tracing has been performed in the tympanic membrane, single/dual colour lineage tracing has been performed in the middle ear, and whole mounts have been used for 2D/stack reconstruction. However, this work is the first time these have been combined to effectively visualise multicolour fluorophores in 3D whole mount of the murine middle ear. This affords a potent opportunity to study the cellular dynamics of the middle ear. Furthermore, crossing this reporter line with models of COM will allow a hitherto unseen level of analysis of how the middle

ear epithelium changes in disease and how KRT5+ progenitor cells contribute to this remodelling.

6.6 Chronic otitis media is likely a result of interplay between multiple host and environmental factors

The research described here has focussed on studying the maintenance of the murine middle ear epithelial lining in health and how these processes change in, and may contribute to, chronic otitis media with effusion. There are multiple other factors that likely also play a role such as environmental stimuli, infection, eustachian tube dysfunction triggering hypoxia, the immune system, craniofacial anatomy, ciliary function, aberrant resolution medicine pathways and many more. The prevalence and heterogeneity of chronic otitis media with effusion (as well as other heterogeneous forms of chronic otitis media such as CSOM) means it is likely there is a varying degree of interplay between these factors. Analogous to a concept known as the Anna Karenina principle from the Tolstoy novel that states:

> "All happy families are alike; each unhappy family is unhappy in its own way."

all of these above factors need to be working correctly for effective middle ear homeostasis, whilst a problem in any one alone can result in a pathological disease state. The challenge faced by clinicians and researchers addressing the problem of chronic otitis media is identifying common treatable targets across this broad heterogeneous spectrum of disease.

6.7 Future work

The next steps building on the work in this thesis will comprise firstly using the enrichment protocols to purify KRT5+ cells and refining the spheroid assay to generate a higher throughput proliferation and differentiation screening platform. This will enable both cell intrinsic as well as exogenous pharmacological manipulation effects to be studied at scale. The aims of this will be to help identify putative mechanisms of aberrant remodelling as well as potential therapeutic compounds for further testing.

6.8 Conclusion

The work here shows that studying the stem/progenitor cell biology of the middle ear can help in understanding normal homeostasis and pathogenesis of disease. The long-term hope would be that this work can help in improving therapeutics in three ways. Firstly, it can help in understanding current treatments by creating lineage traceable COM mouse models to study how myringotomy (and other treatments) works in rescuing cellular remodelling. Secondly, there is an opportunity to identify new treatments. For example, if there is an intrinsic progenitor cell problem then therapy would need to involve surgical removal of the abnormal epithelium and regenerating sheets of healthy epithelium ex vivo for transplant [105]. Thirdly, if it is a signalling problem, for example, in the TGF-ß pathway, the spheroid assay can be used in a cheaper drug screening pipeline and eventually perhaps even optimised for primary human tissues. This would then allow the ability to personalise treatments by generating in vitro disease models using primary human tissues for patient-specific treatment.

Overall, chronic otitis media in all its forms poses a high burden disease with significant potential consequences and has been an issue since at least the

1600s. The hope is the work here will contribute towards improving our understanding of the condition, help other researchers use the assays in their work, and ultimately help deliver better patient care.

Bibliography

1. Livingston, G.*, et al.* Dementia prevention, intervention, and care. *Lancet* **390**, 2673-2734 (2017).
2. Anthwal, N., Joshi, L. & Tucker, A.S. Evolution of the mammalian middle ear and jaw: adaptations and novel structures. *J Anat* **222**, 147-160 (2013).
3. Smith, C.A. Inner ear. in *Form and Function in Birds* Vol. 3 (ed. King, A.S., McLelland, J.) 273-310 (Academic Press New York, NY, 1985).
4. Aoki, K.*, et al.* Relationship between middle ear pressure, mucosal lesion, and mastoid pneumatization. *The Laryngoscope* **108**, 1840-1845 (1998).
5. Felding, J.U., Rasmussen, J.B. & Lildholdt, T. Gas composition of the normal and the ventilated middle ear cavity. *Scand J Clin Lab Invest Suppl* **186**, 31-41 (1987).
6. Ikarashi, F. & Tsuchiya, A. Middle ear gas exchange via the mucosa: estimation by hyperventilation. *Acta oto-laryngologica* **128**, 9-12 (2008).
7. Shupak, A., Tabari, R., Swarts, J.D., Bluestone, C.D. & Doyle, W.J. Effects of middle ear oxygen and carbon dioxide tensions on eustachian tube ventilatory function. *The Laryngoscope* **106**, 221-224 (1996).
8. Schilder, A.G.*, et al.* Otitis media. *Nat Rev Dis Primers* **2**, 16063 (2016).
9. Monasta, L.*, et al.* Burden of disease caused by otitis media: systematic review and global estimates. *PLoS One* **7**, e36226 (2012).
10. Bakaletz, L.O. Immunopathogenesis of polymicrobial otitis media. *J Leukoc Biol* **87**, 213-222 (2010).
11. Kubba, H., Pearson, J.P. & Birchall, J.P. The aetiology of otitis media with effusion: a review. *Clin Otolaryngol Allied Sci* **25**, 181-194 (2000).
12. Bhutta, M.F., Thornton, R.B., Kirkham, L.S., Kerschner, J.E. & Cheeseman, M.T. Understanding the aetiology and resolution of chronic otitis media from animal and human studies. *Dis Model Mech* **10**, 1289-1300 (2017).
13. Tos, M. Pathogenesis and pathology of chronic secretory otitis media. *Ann Otol Rhinol Laryngol Suppl* **89**, 91-97 (1980).
14. Robb, P.J. Childhood otitis media with effusion. *Clin Otolaryngol* **31**, 535-537 (2006).
15. Leach, A.J.*, et al.* Panel 6: Otitis media and associated hearing loss among disadvantaged populations and low to middle-income countries. *Int J Pediatr Otorhinolaryngol*, 109857 (2020).
16. Bhutta, M.F. Epidemiology and pathogenesis of otitis media: construction of a phenotype landscape. *Audiol Neurootol* **19**, 210-223 (2014).
17. Organisation, W.H. Chronic suppurative otitis media: Burden of Illness and Management Options. in *Child and Adoloscent Health and Development - Prevention of blindness and deafness* (2004).

18. Schilder, A.G. Assessment of complications of the condition and of the treatment of otitis media with effusion. *Int J Pediatr Otorhinolaryngol* **49 Suppl 1**, S247-251 (1999).
19. Baumann, I., Gerendas, B., Plinkert, P.K. & Praetorius, M. General and disease-specific quality of life in patients with chronic suppurative otitis media--a prospective study. *Health Qual Life Outcomes* **9**, 48 (2011).
20. Brouwer, C.N.*, et al.* Health-related quality of life in children with otitis media. *Int J Pediatr Otorhinolaryngol* **69**, 1031-1041 (2005).
21. Roditi, R.E., Liu, C.C., Bellmunt, A.M., Rosenfeld, R.M. & Shin, J.J. Oral Antibiotic Use for Otitis Media with Effusion: Ongoing Opportunities for Quality Improvement. *Otolaryngol Head Neck Surg* **154**, 797-803 (2016).
22. Centre., N.I. Hospital Episode Statistics. (2010).
23. Rosenfeld, R.M.*, et al.* Clinical Practice Guideline: Otitis Media with Effusion Executive Summary (Update). *Otolaryngol Head Neck Surg* **154**, 201-214 (2016).
24. Khodaverdi, M.*, et al.* Hearing 25 years after surgical treatment of otitis media with effusion in early childhood. *Int J Pediatr Otorhinolaryngol* **77**, 241-247 (2013).
25. Cohen, S.G. Jean Riolan (1580-1657) French physician and pioneer anatomist. *Allergy Proc* **16**, 285-286 (1995).
26. Simon, F.*, et al.* International consensus (ICON) on management of otitis media with effusion in children. *Eur Ann Otorhinolaryngol Head Neck Dis* **135**, S33-S39 (2018).
27. Schilder, A.G.*, et al.* Panel 7: Otitis Media: Treatment and Complications. *Otolaryngology--head and neck surgery : official journal of American Academy of Otolaryngology-Head and Neck Surgery* **156**, S88-S105 (2017).
28. Casselbrant, M.L. & Mandel, E.M. Genetic susceptibility to otitis media. *Curr Opin Allergy Clin Immunol* **5**, 1-4 (2005).
29. Casselbrant, M.L.*, et al.* Otitis media: a genome-wide linkage scan with evidence of susceptibility loci within the 17q12 and 10q22.3 regions. *BMC Med Genet* **10**, 85 (2009).
30. Schlanser, A. *Practical Otology, Rhinology and Laryngology*, (Howard Kingston, London, 1938).
31. Daly, K.A.*, et al.* Epidemiology, natural history, and risk factors: panel report from the Ninth International Research Conference on Otitis Media. *Int J Pediatr Otorhinolaryngol* **74**, 231-240 (2010).
32. Allen, E.K.*, et al.* A genome-wide association study of chronic otitis media with effusion and recurrent otitis media identifies a novel susceptibility locus on chromosome 2. *J Assoc Res Otolaryngol* **14**, 791-800 (2013).
33. Mouse Genome Sequencing, C.*, et al.* Initial sequencing and comparative analysis of the mouse genome. *Nature* **420**, 520-562 (2002).

34. Venter, J.C., *et al.* The sequence of the human genome. *Science* **291**, 1304-1351 (2001).
35. Giebink, G.S. Otitis media: the chinchilla model. *Microb Drug Resist* **5**, 57-72 (1999).
36. Jinek, M., *et al.* A programmable dual-RNA-guided DNA endonuclease in adaptive bacterial immunity. *Science* **337**, 816-821 (2012).
37. Nolan, P.M., *et al.* A systematic, genome-wide, phenotype-driven mutagenesis programme for gene function studies in the mouse. *Nat Genet* **25**, 440-443 (2000).
38. Brown, S.D., Chambon, P., de Angelis, M.H. & Eumorphia, C. EMPReSS: standardized phenotype screens for functional annotation of the mouse genome. *Nat Genet* **37**, 1155 (2005).
39. Stottmann, R. & Beier, D. ENU mutagenesis in the mouse. *Curr Protoc Mouse Biol* **4**, 25-35 (2014).
40. Susaki, E.A., *et al.* Advanced CUBIC protocols for whole-brain and whole-body clearing and imaging. *Nat Protoc* **10**, 1709-1727 (2015).
41. Hardisty, R.E., Mburu, P. & Brown, S.D. ENU mutagenesis and the search for deafness genes. *Br J Audiol* **33**, 279-283 (1999).
42. Coghill, E.L., *et al.* A gene-driven approach to the identification of ENU mutants in the mouse. *Nat Genet* **30**, 255-256 (2002).
43. Quwailid, M.M., *et al.* A gene-driven ENU-based approach to generating an allelic series in any gene. *Mamm Genome* **15**, 585-591 (2004).
44. Salinger, A.P. & Justice, M.J. Mouse Mutagenesis Using N-Ethyl-N-Nitrosourea (ENU). *CSH Protoc* **2008**, pdb prot4985 (2008).
45. Weber, J.S., Salinger, A. & Justice, M.J. Optimal N-ethyl-N-nitrosourea (ENU) doses for inbred mouse strains. *Genesis* **26**, 230-233 (2000).
46. Crompton, M., *et al.* A mutation in Nischarin causes otitis media via LIMK1 and NF-kappaB pathways. *PLoS Genet* **13**, e1006969 (2017).
47. Hardisty, R.E., *et al.* The deaf mouse mutant Jeff (Jf) is a single gene model of otitis media. *J Assoc Res Otolaryngol* **4**, 130-138 (2003).
48. Hardisty-Hughes, R.E., *et al.* A mutation in the F-box gene, Fbxo11, causes otitis media in the Jeff mouse. *Hum Mol Genet* **15**, 3273-3279 (2006).
49. Parkinson, N., *et al.* Mutation at the Evi1 locus in Junbo mice causes susceptibility to otitis media. *PLoS Genet* **2**, e149 (2006).
50. Rye, M.S., *et al.* Unraveling the genetics of otitis media: from mouse to human and back again. *Mamm Genome* **22**, 66-82 (2011).
51. Rye, M.S., *et al.* FBXO11, a regulator of the TGFbeta pathway, is associated with severe otitis media in Western Australian children. *Genes Immun* **12**, 352-359 (2011).
52. Segade, F., *et al.* Association of the FBXO11 gene with chronic otitis media with effusion and recurrent otitis media: the Minnesota COME/ROM Family

Study. *Archives of otolaryngology--head & neck surgery* **132**, 729-733 (2006).
53. Tateossian, H.*, et al.* Regulation of TGF-beta signalling by Fbxo11, the gene mutated in the Jeff otitis media mouse mutant. *Pathogenetics* **2**, 5 (2009).
54. Tateossian, H.*, et al.* Otitis media in the Tgif knockout mouse implicates TGFbeta signalling in chronic middle ear inflammatory disease. *Hum Mol Genet* **22**, 2553-2565 (2013).
55. Tateossian, H., Morse, S., Simon, M.M., Dean, C.H. & Brown, S.D. Interactions between the otitis media gene, Fbxo11, and p53 in the mouse embryonic lung. *Dis Model Mech* **8**, 1531-1542 (2015).
56. Zheng, Q.Y., Hardisty-Hughes, R. & Brown, S.D. Mouse models as a tool to unravel the genetic basis for human otitis media. *Brain Res* **1091**, 9-15 (2006).
57. Bhutta, M.F., Cheeseman, M.T. & Brown, S.D. Myringotomy in the Junbo mouse model of chronic otitis media alleviates inflammation and cellular hypoxia. *The Laryngoscope* **124**, E377-383 (2014).
58. Cheeseman, M.T.*, et al.* HIF-VEGF pathways are critical for chronic otitis media in Junbo and Jeff mouse mutants. *PLoS Genet* **7**, e1002336 (2011).
59. Einarsdottir, E.*, et al.* Genome-wide association analysis reveals variants on chromosome 19 that contribute to childhood risk of chronic otitis media with effusion. *Scientific reports* **6**, 33240 (2016).
60. Hafren, L.*, et al.* Predisposition to Childhood Otitis Media and Genetic Polymorphisms within the Toll-Like Receptor 4 (TLR4) Locus. *PLoS One* **10**, e0132551 (2015).
61. Tyrer, H.E., Crompton, M. & Bhutta, M.F. What have we learned from murine models of otitis media? *Curr Allergy Asthma Rep* **13**, 501-511 (2013).
62. Bhutta, M.F. Mouse models of otitis media: strengths and limitations. *Otolaryngology--head and neck surgery : official journal of American Academy of Otolaryngology-Head and Neck Surgery* **147**, 611-614 (2012).
63. Abida, W.M., Nikolaev, A., Zhao, W., Zhang, W. & Gu, W. FBXO11 promotes the Neddylation of p53 and inhibits its transcriptional activity. *J Biol Chem* **282**, 1797-1804 (2007).
64. Abbas, T.*, et al.* CRL1-FBXO11 promotes Cdt2 ubiquitylation and degradation and regulates Pr-Set7/Set8-mediated cellular migration. *Mol Cell* **49**, 1147-1158 (2013).
65. Abbas, T., Keaton, M. & Dutta, A. Regulation of TGF-beta signaling, exit from the cell cycle, and cellular migration through cullin cross-regulation: SCF-FBXO11 turns off CRL4-Cdt2. *Cell Cycle* **12**, 2175-2182 (2013).
66. Duan, S.*, et al.* FBXO11 targets BCL6 for degradation and is inactivated in diffuse large B-cell lymphomas. *Nature* **481**, 90-93 (2012).

67. Ju, U.I., Park, J.W., Park, H.S., Kim, S.J. & Chun, Y.S. FBXO11 represses cellular response to hypoxia by destabilizing hypoxia-inducible factor-1alpha mRNA. *Biochem Biophys Res Commun* **464**, 1008-1015 (2015).
68. Cooter, M.S.*, et al.* Transforming growth factor-beta expression in otitis media with effusion. *The Laryngoscope* **108**, 1066-1070 (1998).
69. Zhao, S.Q.*, et al.* Role of interleukin-10 and transforming growth factor beta 1 in otitis media with effusion. *Chin Med J (Engl)* **122**, 2149-2154 (2009).
70. Bhutta, M.F.*, et al.* A mouse-to-man candidate gene study identifies association of chronic otitis media with the loci TGIF1 and FBXO11. *Scientific reports* **7**, 12496 (2017).
71. Del-Pozo, J.*, et al.* Chronic otitis media is initiated by a bulla cavitation defect in the FBXO11 mouse model. *Dis Model Mech* **12**(2019).
72. Thompson, H. & Tucker, A.S. Dual origin of the epithelium of the mammalian middle ear. *Science* **339**, 1453-1456 (2013).
73. Tos, M. Anatomy and histology of the middle ear. *Clin Rev Allergy* **2**, 267-284 (1984).
74. Fireman, P. Otitis media and eustachian tube dysfunction: connection to allergic rhinitis. *J Allergy Clin Immunol* **99**, S787-797 (1997).
75. Ishii, T., Toriyama, M. & Suzuki, J.I. Histopathological study of otitis media with effusion. *Ann Otol Rhinol Laryngol Suppl* **89**, 83-86 (1980).
76. Karin, M. & Clevers, H. Reparative inflammation takes charge of tissue regeneration. *Nature* **529**, 307-315 (2016).
77. D'Ignazio, L., Bandarra, D. & Rocha, S. NF-kappaB and HIF crosstalk in immune responses. *FEBS J* **283**, 413-424 (2016).
78. Cho, C.G., Pak, K., Webster, N., Kurabi, A. & Ryan, A.F. Both canonical and non-canonical NF-kappaB activation contribute to the proliferative response of the middle ear mucosa during bacterial infection. *Innate Immun* (2016).
79. Ryan, A.F.*, et al.* Recent advances in otitis media. 4C. Interaction between middle ear and inner ear in otitis media. *Ann Otol Rhinol Laryngol Suppl* **194**, 56-59 (2005).
80. Straetemans, M.*, et al.* A comprehensive model for the aetiology of otitis media with effusion. *Med Hypotheses* **57**, 784-791 (2001).
81. Tos, M. Middle ear epithelia in chronic secretory otitis. *Arch Otolaryngol* **106**, 593-597 (1980).
82. Lin, J.*, et al.* Mucin production and mucous cell metaplasia in otitis media. *Int J Otolaryngol* **2012**, 745325 (2012).
83. Val, S., Kwon, H.J., Rose, M.C. & Preciado, D. Middle Ear Response of Muc5ac and Muc5b Mucins to Nontypeable Haemophilus influenzae. *JAMA Otolaryngol Head Neck Surg* **141**, 997-1005 (2015).
84. Hunter, S.E.*, et al.* Mucin production in the middle ear in response to lipopolysaccharides. *Otolaryngol Head Neck Surg* **120**, 884-888 (1999).

85. Paparella, M.M., Sipila, P., Juhn, S.K. & Jung, T.T. Subepithelial space in otitis media. *Laryngoscope* **95**, 414-420 (1985).
86. Lajtha, L.G. Stem cell concepts. *Differentiation* **14**, 23-34 (1979).
87. Blanpain, C. & Fuchs, E. Stem cell plasticity. Plasticity of epithelial stem cells in tissue regeneration. *Science* **344**, 1242281 (2014).
88. Wuidart, A.*, et al.* Quantitative lineage tracing strategies to resolve multipotency in tissue-specific stem cells. *Genes Dev* **30**, 1261-1277 (2016).
89. Lu, C.P.*, et al.* Identification of stem cell populations in sweat glands and ducts reveals roles in homeostasis and wound repair. *Cell* **150**, 136-150 (2012).
90. Mascre, G.*, et al.* Distinct contribution of stem and progenitor cells to epidermal maintenance. *Nature* **489**, 257-262 (2012).
91. Aragona, M.*, et al.* Defining stem cell dynamics and migration during wound healing in mouse skin epidermis. *Nat Commun* **8**, 14684 (2017).
92. Watson, J.K.*, et al.* Clonal Dynamics Reveal Two Distinct Populations of Basal Cells in Slow-Turnover Airway Epithelium. *Cell Rep* **12**, 90-101 (2015).
93. Rock, J.R., Randell, S.H. & Hogan, B.L. Airway basal stem cells: a perspective on their roles in epithelial homeostasis and remodeling. *Dis Model Mech* **3**, 545-556 (2010).
94. Rock, J.R.*, et al.* Basal cells as stem cells of the mouse trachea and human airway epithelium. *Proc Natl Acad Sci U S A* **106**, 12771-12775 (2009).
95. Blanpain, C. & Fuchs, E. p63: revving up epithelial stem-cell potential. *Nat Cell Biol* **9**, 731-733 (2007).
96. Blanpain, C., Lowry, W.E., Geoghegan, A., Polak, L. & Fuchs, E. Self-renewal, multipotency, and the existence of two cell populations within an epithelial stem cell niche. *Cell* **118**, 635-648 (2004).
97. Blanpain, C. & Simons, B.D. Unravelling stem cell dynamics by lineage tracing. *Nat Rev Mol Cell Biol* **14**, 489-502 (2013).
98. Luo, W.*, et al.* Cilia distribution and polarity in the epithelial lining of the mouse middle ear cavity. *Sci Rep* **7**, 45870 (2017).
99. Tucker, A.S.*, et al.* Mapping the distribution of stem/progenitor cells across the mouse middle ear during homeostasis and inflammation. *Development* **145**(2018).
100. Frumm, S.M.*, et al.* A hierarchy of migratory keratinocytes maintains the tympanic membrane. *bioRxiv* (2019).
101. Mulay, A., Akram, K., Bingle, L. & Bingle, C.D. Isolation and Culture of Primary Mouse Middle Ear Epithelial Cells. *Methods Mol Biol* **1940**, 157-168 (2019).
102. Jensen, K.B., Driskell, R.R. & Watt, F.M. Assaying proliferation and differentiation capacity of stem cells using disaggregated adult mouse epidermis. *Nat Protoc* **5**, 898-911 (2010).

103. Suzuki, D., Pinto, F. & Senoo, M. Inhibition of TGF-beta signaling supports high proliferative potential of diverse p63(+) mouse epithelial progenitor cells in vitro. *Scientific reports* **7**, 6089 (2017).
104. Hirsch, T.*, et al.* Regeneration of the entire human epidermis using transgenic stem cells. *Nature* **551**, 327-332 (2017).
105. Yamamoto, K.*, et al.* Middle ear mucosal regeneration by tissue-engineered cell sheet transplantation. *NPJ Regen Med* **2**, 6 (2017).
106. Butler, C.R.*, et al.* Rapid Expansion of Human Epithelial Stem Cells Suitable for Airway Tissue Engineering. *Am J Respir Crit Care Med* **194**, 156-168 (2016).
107. Livet, J.*, et al.* Transgenic strategies for combinatorial expression of fluorescent proteins in the nervous system. *Nature* **450**, 56-62 (2007).
108. Snippert, H.J.*, et al.* Intestinal crypt homeostasis results from neutral competition between symmetrically dividing Lgr5 stem cells. *Cell* **143**, 134-144 (2010).
109. Van Keymeulen, A.*, et al.* Distinct stem cells contribute to mammary gland development and maintenance. *Nature* **479**, 189-193 (2011).
110. Mulay, A.*, et al.* An in vitro model of murine middle ear epithelium. *Dis Model Mech* **9**, 1405-1417 (2016).
111. You, Y. & Brody, S.L. Culture and differentiation of mouse tracheal epithelial cells. *Methods Mol Biol* **945**, 123-143 (2013).
112. You, Y., Richer, E.J., Huang, T. & Brody, S.L. Growth and differentiation of mouse tracheal epithelial cells: selection of a proliferative population. *Am J Physiol Lung Cell Mol Physiol* **283**, L1315-1321 (2002).
113. Moestrup, K.S., Andersen, M.S. & Jensen, K.B. Isolation and In Vitro Characterization of Epidermal Stem Cells. *Methods Mol Biol* **1553**, 67-83 (2017).
114. Schindelin, J.*, et al.* Fiji: an open-source platform for biological-image analysis. *Nat Methods* **9**, 676-682 (2012).
115. Schneider, C.A., Rasband, W.S. & Eliceiri, K.W. NIH Image to ImageJ: 25 years of image analysis. *Nat Methods* **9**, 671-675 (2012).
116. Rueden, C.T.*, et al.* ImageJ2: ImageJ for the next generation of scientific image data. *BMC Bioinformatics* **18**, 529 (2017).
117. Greenbaum, A.*, et al.* Bone CLARITY: Clearing, imaging, and computational analysis of osteoprogenitors within intact bone marrow. *Sci Transl Med* **9**(2017).
118. Wu, D. & Yotnda, P. Induction and testing of hypoxia in cell culture. *J Vis Exp* (2011).
119. Succony, L.*, et al.* S111 Methods To Isolate Basal Cells From The Respiratory Epithelium. *Thorax* **69**, A59-A59 (2014).

120. Hegab, A.E., Ha, V.L., Attiga, Y.S., Nickerson, D.W. & Gomperts, B.N. Isolation of basal cells and submucosal gland duct cells from mouse trachea. *J Vis Exp*, e3731 (2012).
121. Ellerstrom, C., Strehl, R., Noaksson, K., Hyllner, J. & Semb, H. Facilitated expansion of human embryonic stem cells by single-cell enzymatic dissociation. *Stem Cells* **25**, 1690-1696 (2007).
122. Messier, E.M., Mason, R.J. & Kosmider, B. Efficient and rapid isolation and purification of mouse alveolar type II epithelial cells. *Exp Lung Res* **38**, 363-373 (2012).
123. Fujino, N.*, et al.* A novel method for isolating individual cellular components from the adult human distal lung. *Am J Respir Cell Mol Biol* **46**, 422-430 (2012).
124. Franken, N.A., Rodermond, H.M., Stap, J., Haveman, J. & van Bree, C. Clonogenic assay of cells in vitro. *Nat Protoc* **1**, 2315-2319 (2006).
125. Popova, N.V. & Morris, R.J. Genetic regulation of mouse stem cells: identification of two keratinocyte stem cell regulatory loci. *Curr Top Microbiol Immunol* **280**, 111-137 (2004).
126. Rafehi, H.*, et al.* Clonogenic assay: adherent cells. *J Vis Exp* (2011).
127. Hardisty-Hughes, R.E., Parker, A. & Brown, S.D. A hearing and vestibular phenotyping pipeline to identify mouse mutants with hearing impairment. *Nat Protoc* **5**, 177-190 (2010).
128. Liao, J.*, et al.* Full spectrum of malformations in velo-cardio-facial syndrome/DiGeorge syndrome mouse models by altering Tbx1 dosage. *Hum Mol Genet* **13**, 1577-1585 (2004).
129. Fuchs, J.C., Linden, J.F., Baldini, A. & Tucker, A.S. A defect in early myogenesis causes Otitis media in two mouse models of 22q11.2 Deletion Syndrome. *Hum Mol Genet* **24**, 1869-1882 (2015).
130. Wansleeben, C., Bowie, E., Hotten, D.F., Yu, Y.R. & Hogan, B.L. Age-related changes in the cellular composition and epithelial organization of the mouse trachea. *PLoS One* **9**, e93496 (2014).
131. Munoz-Sanchez, J. & Chanez-Cardenas, M.E. The use of cobalt chloride as a chemical hypoxia model. *J Appl Toxicol* **39**, 556-570 (2019).
132. Kretzschmar, K. & Watt, F.M. Lineage tracing. *Cell* **148**, 33-45 (2012).
133. Atik, A.*, et al.* Changes in macular sensitivity after half-dose photodynamic therapy for chronic central serous chorioretinopathy. *BMC ophthalmology* **17**, 140 (2017).
134. van de Moosdijk, A.A., Fu, N.Y., Rios, A.C., Visvader, J.E. & van Amerongen, R. Lineage Tracing of Mammary Stem and Progenitor Cells. *Methods Mol Biol* **1501**, 291-308 (2017).
135. Giangreco, A.*, et al.* Stem cells are dispensable for lung homeostasis but restore airways after injury. *Proceedings of the National Academy of Sciences of the United States of America* **106**, 9286-9291 (2009).

136. Amitai-Lange, A.*, et al.* A Method for Lineage Tracing of Corneal Cells Using Multi-color Fluorescent Reporter Mice. *J Vis Exp*, e53370 (2015).
137. Tomer, R., Ye, L., Hsueh, B. & Deisseroth, K. Advanced CLARITY for rapid and high-resolution imaging of intact tissues. *Nat Protoc* **9**, 1682-1697 (2014).
138. Rheinwald, J.G. Human epidermal keratinocyte cell culture and xenograft systems: applications in the detection of potential chemical carcinogens and the study of epidermal transformation. *Prog Clin Biol Res* **298**, 113-125 (1989).
139. Rheinwald, J.G. & Green, H. Serial cultivation of strains of human epidermal keratinocytes: the formation of keratinizing colonies from single cells. *Cell* **6**, 331-343 (1975).
140. Hegab, A.E.*, et al.* Mimicking the niche of lung epithelial stem cells and characterization of several effectors of their in vitro behavior. *Stem Cell Res* **15**, 109-121 (2015).
141. Hynds, R.E.*, et al.* Cross-talk between human airway epithelial cells and 3T3-J2 feeder cells involves partial activation of human MET by murine HGF. *PLoS One* **13**, e0197129 (2018).
142. Chari, D.A., Frumm, S.M., Akil, O. & Tward, A.D. Cellular Dynamics in Early Healing of Mouse Tympanic Membranes. *Otology & neurotology : official publication of the American Otological Society, American Neurotology Society [and] European Academy of Otology and Neurotology* **40**, e160-e166 (2019).
143. Mulay, A.*, et al.* Loss of the homeostatic protein BPIFA1, leads to exacerbation of otitis media severity in the Junbo mouse model. *Scientific reports* **8**, 3128 (2018).
144. Stenn, K.S., Link, R., Moellmann, G., Madri, J. & Kuklinska, E. Dispase, a neutral protease from Bacillus polymyxa, is a powerful fibronectinase and type IV collagenase. *J Invest Dermatol* **93**, 287-290 (1989).
145. Trosan, P.*, et al.* The enzymatic de-epithelialization technique determines denuded amniotic membrane integrity and viability of harvested epithelial cells. *PLoS One* **13**, e0194820 (2018).
146. Mou, H.*, et al.* Dual SMAD Signaling Inhibition Enables Long-Term Expansion of Diverse Epithelial Basal Cells. *Cell Stem Cell* **19**, 217-231 (2016).
147. Chen, Y.*, et al.* Human primary middle ear epithelial cell culture: A novel in vitro model to study otitis media. *Laryngoscope Investig Otolaryngol* **4**, 663-672 (2019).
148. Vaughan, A.E.*, et al.* Lineage-negative progenitors mobilize to regenerate lung epithelium after major injury. *Nature* **517**, 621-625 (2015).
149. Chambers, R.C. & Mercer, P.F. Mechanisms of alveolar epithelial injury, repair, and fibrosis. *Ann Am Thorac Soc* **12 Suppl 1**, S16-20 (2015).

Presentations and awards arising from this work

1. The Role of KRT5+ Cells in Middle Ear Epithelial Homeostasis
   Shortlisted for prize in the oral presentation session at the Rowena Ryan Prize Awards Day, London, December 2019.

2. The Role of KRT5+ Progenitors in Chronic Otitis Media.
   Awarded second-prize for oral presentation at the Matthew Yung Short Paper Prize, Royal Society of Medicine, London, February 2020.

3. Public Engagement - MRC I'm a Scientist Get Me Out Of Here – National Winner 2019.